EC INV-SARA(99)-D016

SKI Report 99:32

Severe Accident Recriticality Analyses (SARA)

Work Performed under EC Contract No. F14SCT960027

W. Frid
F. Höjerup
I. Lindholm
J. Miettinen
L. Nilsson
E. K. Puska
H. Sjövall

November 1999

ISSN 1104-1374
ISRN SKI-R--99/32--SE

SKi

EC INV-SARA(99)-D016

SKI Report 99:32

Severe Accident Recriticality Analyses (SARA)

Work Performed under EC Contract No. F14SCT960027

W. Frid[1]
F. Höjerup[2]
I. Lindholm[3]
J. Miettinen[3]
L. Nilsson[4]
E. K. Puska[3]
H. Sjövall[5]

[1]Swedish Nuclear Power Inspectorate (SKI), Sweden
[2]Risø National Laboratory, Denmark
[3]VTT Energy, Finland
[4]Studsvik Eco & Safety AB, Sweden
[5]Teoliisuuden Voima Oy, Finland

Co-ordinator
Dr. Wiktor Frid
SKI, SE-106 58 Stockholm, Sweden
Tel. +46 (0)8 698 84 60
Fax +46 (0)8 661 90 86
e-mail wiktor.frid@ski.se

November 1999

SKI Project Number 97130

ABSTRACT

Recriticality in a BWR has been studied for a total loss of electric power accident scenario. In a BWR, the B_4C control rods would melt and relocate from the core before the fuel during core uncovery and heat-up. If electric power returns during this time-window unborated water from ECCS systems will start to reflood the partly control rod free core. Recriticality might take place for which the only mitigating mechanisms are the Doppler effect and void formation. In order to assess the impact of recriticality on reactor safety, including accident management measures, the following issues have been investigated in the SARA project: (1) the energy deposition in the fuel during super-prompt power burst, (2) the quasi steady-state reactor power following the initial power burst and (3) containment response to elevated quasi steady-state reactor power. The approach was to use three computer codes and to further develop and adapt them for the task. The codes were SIMULATE-3K, APROS and RECRIT. Recriticality analyses were carried out for a number of selected reflooding transients for the Oskarshamn 3 plant in Sweden with SIMULATE-3K and for the Olkiluoto 1 plant in Finland with all three codes. The core state initial and boundary conditions prior to recriticality have been studied with the severe accident codes SCDAP/RELAP5, MELCOR and MAAP4.

The results of the analyses show that all three codes predict recriticality – both super-prompt power bursts and quasi steady-state power generation - for the studied range of parameters, i. e. with core uncovery and heat-up to maximum core temperatures around 1800 K and water flow rates of 45 kg/s to 2000 kg/s injected into the downcomer. Since the recriticality takes place in a small fraction of the core the power densities are high which results in large energy deposition in the fuel during power burst in some accident scenarios. The highest value, 418 cal/g, was obtained with SIMULATE-3K for an Oskarshamn 3 case with reflooding rate of 2000 kg/s. In most cases, however, the predicted energy deposition was much smaller, below the regulatory limits for fuel failure, but close or above recently observed thresholds for fragmentation and dispersion of high burn-up fuel. The highest calculated quasi steady-state power following initial power excursion was in most cases about 20 % of the nominal reactor power, according to SIMULATE-3K and APROS. RECRIT predictions were in general different in this respect with either oscillating power or power increase approaching 50 % of nominal power which in both cases resulted in fuel temperatures above the melting point as a result of insufficient cooling. Long-term containment response to recriticality was assessed through MELCOR calculations for Olkiluoto 1 plant. At stabilised reactor power of 19 % of nominal power the containment failure due to overpressurization was predicted to occur 1.3 h after recriticality, if the accident is not mitigated.

The SARA studies have clearly shown the sensitivity of recriticality phenomena to thermal-hydraulic modelling, the specifics of accident scenario, such as distribution of boron-carbide, and importance of multi-dimensional kinetics for determination of local power distribution in the core. The results of the project have pointed out the importance of adequate accident management procedures to be used by reactor operators and emergency staff during recovery actions. Recommendations in this area are given in the report.

ACKNOWLEDGEMENTS

This work was performed under the EC contract No. FI4SCT960027 as a cost-shared project and funded by the European Commission, the Swedish Nuclear Power Inspectorate, VTT Energy, Finland and Risö National Laboratory, Denmark. The authors would like to thank Dr. David Kropaczek of Studsvik Scandpower, Inc. USA for his work with development and testing of the special SIMULATE-3K code version for SARA. The authors would also like to thank Dr. Alejandro Zurita, European Commission, for helpful discussions and his support during the project.

CONTENTS

		Page
ABSTRACT		**i**
ACKNOWLEDGEMENTS		**ii**
EXECUTIVE SUMMARY		**v**
1.	**INTRODUCTION**	**1**
1.1	SARA Work Programme and Organisation	1
1.2	Background	1
1.3	Previous Recriticality Studies	2
1.4	Objective and Scope	4
1.5	Approach	4
2.	**INITIAL CONDITIONS FOR RECRITICALITY ANALYSES**	**6**
2.1	SCDAP/RELAP5 Calculations for Oskarshamn 3 Plant (Task 1)	6
	2.1.1 Oskarshamn 3 plant	6
	2.1.2 Results of SCDAP/RELAP5 analyses	7
2.2	MELCOR and MAAP Calculations for Olkiluoto Plants (Task 2)	10
	2.2.1 Olkiluoto 1 & 2 plants	10
	2.2.2 MELCOR analyses	10
	2.2.3 MAAP analyses	12
	2.2.4 Conclusions	14
3.	**HEAT TRANSFER AND THERMAL-HYDRAULICS ASPECTS OF REFLOODING AND RECRITICALITY (TASK 4)**	**15**
3.1	Basic Phenomena	15
3.2	Void Fraction and Kinetics	17
3.3	Thermal-Hydraulic Modelling Characteristics	18
4.	**DESCRIPTION OF COMPUTER CODES FOR RECRITICALITY CALCULATIONS**	**20**
4.1	SIMULATE-3K Code (Task 1)	20
	4.1.1 Code structure	21
	4.1.2 Code development	22
	4.1.3 Input and output	23
4.2	APROS Code (Task 2)	24
	4.2.1. Code structure	24
	4.2.2 Code development	26
	4.2.3 Input and output	26

4.3 RECRIT Code (Task 3) 27
4.3.1 Code structure 27
4.3.2 Code development 28
4.3.3 Input and output 34

5. RECRITICALITY ANALYSES: INDIVIDUAL STUDIES AND COMMON CASE COMPARISON 35

5.1 SIMULATE-3K Calculations for Oskarshamn 3 (Task 1) 35
5.1.1 Initial conditions and assumptions 35
5.1.2 Specification of calculated cases 36
5.1.3 Results of SIMULATE-3K analysis 37

5.2 APROS Calculations for OL-1 (Task 2) 45
5.2.1 Initial conditions and assumptions 45
5.2.2 Results of APROS analysis 46
5.2.3 Summary of recriticality calculations 54
5.2.4 Energy involved in recriticality power peak 55

5.3. RECRIT Calculations for OL-1 (Task 3) 57
5.3.1 Initial conditions and assumptions 57
5.3.2 Results of RECRIT analysis 58

5.4 Common Case Code Comparison for OL-1 Plant 67
5.4.1 Assumptions and initial conditions 67
5.4.2 Comparison of results 70
5.4.3 Discussion of code comparison results 77

6. CONTAINMENT RESPONSE TO RECRITICALITY: MELCOR ANALYSIS FOR OL-1 PLANT (Task 2) 81

6.1 Assumptions 81

6.2 Containment Response 83

6.3 Discussion 87

7. CONCLUSIONS AND RECOMMENDATIONS 89

REFERENCES 91

EXECUTIVE SUMMARY

The EU project SARA (Severe Accident Recriticality Analyses) comprised four work tasks, each carried out by one of the four participating organisations. These are Studsvik EcoSafe and the Swedish Nuclear Power Inspectorate (SKI) in Sweden, VTT Energy in Finland and Risö National Laboratory in Denmark.

The conditions which facilitate recriticality are based on assumption of total loss of power to all cooling systems as the initiating event. Failure of feed water supply leads to uncovery and heat-up of the reactor core, and eventual degradation of core components due to oxidation and melting. The control rods, which all are inserted at automatic reactor shut down, will start to melt away in the hottest part of the core before the fuel which remains intact for a longer period into the accident. If electric power to the cooling systems is restored, unborated water from emergency core cooling systems starts to reflood the core. Recriticality will then take place if the control rod free part is large enough. The only mitigating mechanisms are the Doppler effect and void formation. The primary arising questions to be answered are:

- Is a super-prompt power burst possible and, if yes, how large is the energy deposition in the fuel?
- Does a long-term reflooding threaten the integrity of the reactor containment?
- What mitigation measures can be used to limit the consequences of a recriticality?

Earlier recriticality studies have shown that recriticality is possible for certain combinations of control rod configurations and reflooding flow rates. These studies have generally been made with one-dimensional or less detailed reactor kinetics codes and the results reveal uncertainties concerning the magnitude of recriticality power and its effect on reactor safety.

The objective of the SARA project was to answer the above questions. The approach was to use three existing reactor kinetics codes and to further develop and adapt them for the task. The codes are SIMULATE-3K (S-3K) of Studsvik, APROS of VTT and RECRIT of Risö. Recriticality calculations were then carried out for a number of selected reflooding transients for the Oskarshamn 3 (O-3) BWR with S-3K and for Olkiluoto 1 (OL-1) BWRs with all three codes. A fourth task, carried out by SKI, comprised a literature survey and an investigation of heat transfer correlations and models which describes the complicated thermal-hydraulic phenomena involved in recooling and quenching of overheated core surfaces during reflood. The aim was to implement such models into the reactor kinetics codes, specifically for the development of the RECRIT code.

Since core damage is not at all, or in less detail, modelled by the kinetics codes, preparatory calculations were performed with the severe accident codes SCDAP/RELAP5, MELCOR and MAAP4. This was done for the O-3 and OL-1 reactors for various accident scenarios in order to determine core state boundary and initial conditions prior to recriticality. Individual recriticality calculations were then carried out with S-3K for O-3 and APROS and RECRIT for OL-1 using, as far as possible, actual fuel and operating data for these reactors. In addition, three common cases were chosen for OL-1, with some simplified fuel data and assumptions, to be calculated with all three codes using the same

boundary conditions, in order to compare the codes and to assess the uncertainties in the predictions.

The results of the recriticality analyses show that all three codes, despite quantitative differences, predict recriticality for the studied range of parameters, i.e. with core uncovery and heat-up to maximum core temperatures above 1800 K, and water flow rates 45 to 2000 kg/s injected into the downcomer. The criticality arrives earlier with high than with low flow rates since the time to reflood the core up to a critical water level then is shorter. Both the first super prompt power peak and the long-term power during continued reflood increase with injection flow rate. A prerequisite for obtaining recriticality is that the control rod free fraction of the core is large enough. Initial core damage calculations showed that the control rod free zone begins in the centre and moves downwards in the core during melt down.

The recriticality takes place in the central control rod free part of the core around and below the quench front, where the void fraction is low enough for moderation. Since only a small fraction of the core becomes critical the power density there can be considerable. All codes gave large values for the maximum nodal power factor, e.g. in the OL-1 common case with 160 kg/s water injection in the range of 13 to 17. Lowest values where obtained from APROS and the highest from S-3K. In one extreme case for the O-3 reactor S-3K calculated maximum nodal power factor of 42. One reason for higher peaking factors in O-3 calculations as compared with OL-1 calculations was that the control rod free zone in the O-3 cases was larger and began at lower elevations in the core.

The first power peak could reach amplitudes several times nominal power but was quickly suppressed by the Doppler effect. The energy of the peak therefore became small, but increased with flow rate and amount of control rod melted away. Within the injection mass flow rate range of 160 kg/s to 1540 kg/s the maximum calculated energy deposition was 70 cal/gUO_2 for the common OL-1 case. The highest value of all, 418 cal/gUO_2, was obtained by S-3K for an O-3 case with 2000 kg/s. The duration of the first power excursion was in the range 1450 ms to 30 ms and was longer for small flow rates while the peak became higher and narrower with increasing reflooding flow. RECRIT turned out to give shorter peaks than S-3K and APROS. All these values were obtained at low system pressures, around 0.5 MPa. APROS calculations with higher pressures, near normal operation, indicated substantially larger energy deposition.

One circumstance that complicated the common case comparison was the different modelling of the core inlet flow used in the three codes. In the APROS calculations the core inlet flow was specified to be constant, and therefore the recriticality power curve was stable in the long-term with only minor initial oscillations. In S-3K and RECRIT the core flow was driven by the gravitational head in the downcomer and controlled by the pressure variations around the recirculation loop consisting of core, upper plenum, steam separator, downcomer, RC pumps and lower plenum with core inlet restrictions. The S-3K calculations for O-3 showed, by varying the loss coefficient in the RC pumps, that the hydraulic damping had a significant effect on the coupled power - flow oscillations. This probably explains the larger power oscillations in the RECRIT calculations since the loop pressure losses there were smaller than in S-3K.

The long-term power at continued reflooding is mainly controlled by the reflooding flow rate, boiling rate and negative void feedback. Various trends were shown by the different codes. S-3K indicated that the power after the first oscillations slowly increased with the rising water level in the core and downcomer until the latter was totally filled. After that, the driving force for the core inlet flow could no longer increase. APROS reached steady-state power sooner since the inlet flow was specified to be constant. With RECRIT, the power after the first prompt peak continued to oscillate showing several power peaks, as mentioned above. However, the average power increased with time leading to fuel temperatures exceeding the melting point and termination of calculations. Due to the short calculation times for the RECRIT cases it is hard to draw any certain conclusions about the long-term effects based on the RECRIT results. The general result of all three codes indicated that the long-term power can be considerably larger than the decay power, e.g. 20% of nominal power at 500 kg/s reflooding flow rate. The long-term steam production exceeds the designed cooling and venting capacity of the containment, which will therefore eventually fail. This was shown through MELCOR calculations carried out for OL-1. The effect of steady core power values of 8, 10, 14 and 19 per cent of nominal power, based on the results from all recriticality calculations, was studied taking into account the real layout of the OL-1 safety systems.

The aim of the code comparison, i.e. to assess the uncertainty in the calculations with the three different codes, was on the whole attained, despite some differences in the simulation and input of the common initial and boundary conditions. All codes employ by necessity simplifications and incomplete modelling of the complicated phenomena involved in a reflooding and recriticality transient. The effect of lack in simulation of certain phenomena has been estimated through parameter studies and code comparison. The inability to simulate e.g. the positive power - pressure feed-back and to describe the negative dependence of injection mass flow rate on pressure in S-3K, was thus compensated by parameter studies. RECRIT, which could simulate both these relations gave supplementary information on these effects. The effect of decoupling the interaction between the core and peripheral systems and specifying input directly as core boundary conditions in the APROS calculations could be evaluated based on results from the two other codes. Some modelling shortcomings in the codes with respect to the interaction between neutronics and thermal-hydraulics phenomena for the whole reactor system remain. This motivates continued development of the codes. However, despite differences in code modelling the main results and conclusions in the SARA project are largely the same independent of which of the three codes they are based on.

Concerning the energy deposition in the fuel during power excursions, the results of SARA analyses differ from other studies. While these studies found that the energy deposition in the fuel due to super-prompt power excursion would be below the threshold for fuel fragmentation and dispersion, the SARA results indicate that for reflooding rates higher than about 500 kg/s these threshold values are approached or exceeded, in some cases with large margin. The threshold values referred to here are in the range 200 – 280 cal/g for low burn-up fuel, and down to about 70 cal/g for high burn-up fuel as observed experimentally. In this context it is important to consider that these threshold values have been obtained in tests with "normal" fuel rods, and are therefore likely to be lower for strongly overheated fuel rods under severe accident conditions. Thus, SARA results

suggest that there might be a risk for fuel fragmentation and dispersal during a reflooding transient. The consequences of such a scenario were not investigated in the SARA project.

In addition, the recriticality can lead to fuel melting due to high power levels and/or repeated power excursions and insufficient cooling, as indicated by some RECRIT results. S-3K and APROS showed recooling to moderate temperatures in the long-term after start of reflooding. Other phenomena which can cause fuel damage are fuel cladding shuttering at fast recooling transients during reflooding of overheated fuel rods. These effects have not been investigated in-depth in SARA.

The first accident management measure to be taken in order to avoid recriticality in the event of a total loss of power accident is of course to restore the reactor coolant supply as soon as possible, before any control rod melting starts. If, however, loss of control rods is suspected, the following measures based on the SARA analyses are proposed:

- Upgrading of the boron shut-down system with the introduction of automatic initiation triggered by e.g. high neutron flux signal after shut down. This will prevent long-term recriticality (except for the first power peak) assuming that the boron concentration will not be diluted by the ECCS water in the containment pool.
- Limitation of the reflooding flow rate whenever control rod melting might be expected:
  - Limitation of the maximum injection mass flow rate to less than 500 kg/s in order to avoid the risk of fuel fragmentation and melting. (This recommendation is based on fuel fragmentation and dispersion thresholds obtained for "normal" fuel).
  - The normal feed water should not be started. The flow rate of the low pressure injection system will be automatically limited, in the short-term due to reactor pressure increase during quenching and in the long-term due to pressure increase from elevated recriticality power. The minimum flow rate will then be equal to that of the high-pressure system (90 kg/s in both O-3 and OL-1), which is sufficient to cool the core if water injection is initiated at maximum core temperatures up to about 1800 K. In this case the recriticality power will be low, thus providing more time for countermeasures.
- Delaying depressurization of the primary system, if possible, in order to limit relocation of control rods.

The SARA studies have clearly shown the sensitivity of recriticality phenomena to thermal-hydraulic modelling, the specifics of accident scenario, such as system pressure and distribution of boron-carbide in the core, and the importance of multi-dimensional neutron kinetics for the determination of local power distributions in the core. With regard to the predicted risk for fuel fragmentation and melting, and prevailing uncertainties, it is recommended that systematic studies of reflooding and recriticality continue. The improved reflooding models should be validated against data from high temperature reflooding experiments. Equally important is the further improvement and testing of the codes capabilities to model the entire BWR primary system as realistically as possible in order to capture the reactor power – primary system behaviour feedback effects.

1. INTRODUCTION

1.1 SARA Work Programme and Organisation

SARA is an acronym for Severe Accident Recriticality Analyses, a cost-shared research project (contract No. FI4SCT960027) carried out within the 1994-1998 European Union Fourth Framework Programme on Nuclear Fission Safety. The SARA project comprised development and improvement of computer codes for simulation of reflooding and recriticality transients in BWRs and analyses of a number of selected severe accident scenarios in Nordic BWRs with these codes. The SARA project comprised four work tasks each carried out by the following participants and with the following content:

Task 1. Studsvik EcoSafe, Sweden. Development and application of the SIMULATE-3K (S-3K) code with support of Scandpower Inc. in the USA.

Task 2. VTT Energy, Finland. Development and application of the APROS code.

Task 3. Risoe National Laboratory, Denmark. Development and application of the RECRIT code.

Task 4. SKI, Sweden. Coordination and literature survey, in particular to investigate heat transfer correlations relevant to the reflooding and recriticality problem.

The BWRs chosen for the recriticality studies were the Olkiluoto 1 (OL-1) plant in Finland, with all three codes, and the Oskarshamn 3 (O-3) plant in Sweden with S-3K alone. Three common cases were selected for OL-1 to facilitate comparison of the results obtained by the three codes in order to compare the simulation capability of these codes and to assess the uncertainty of the predictions.

In addition, TVO (Teollisuuden Voima Oy) in Finland, owner and operator of the OL-1 plants made an in-kind contribution to SARA by carrying out a comprehensive study of reflooding transients for OL-1 by means of MAAP4 calculations.

1.2 Background

Total loss of electric power to the cooling systems of the reactor will cause uncovery and subsequent heat-up of the reactor core due to decay power and insufficient cooling of the fuel. This accident scenario, if unmitigated, will result in overheating, degradation and eventually melt-down of the core. In that case the control rods start to melt first, already at about 1500 K, through an eutectic reaction between the absorber material of boron-carbide and its stainless steel sheath. Early melting of control rod material has been investigated thoroughly in various experiments (Hofmann et al., 1989). Although the fuel claddings of Zircaloy might rupture locally in contact with Inconel spacers at about the same temperature, damage and relocation of fuel take place much later. Metallic Zircaloy fuel cladding starts to melt at about 2100 K, but oxidized Zr can withstand melting up to more than 2900 K, i. e. the same temperature level as for early melting of UO_2 fuel interacting with Zr. Thus, there will be a "time-window" between melting and relocation of the control rod absorber material and damage of the uraniumdioxide fuel.

If the electric power supply is restored, the emergency core cooling systems, and possibly also the feed water system, will be activated and begin to inject unborated water into a core which might be more or less without control rods, but with still intact fuel geometry. (There are also systems with a limited amount of borated water in the studied BWRs, but these must be activated manually). The increasing water level will cause recriticality in the control rod free part of the core, if that part is large enough, which can lead to a substantial burst of power. The only mitigation mechanisms are the Doppler effect, which acts promptly, and void formation. In addition to the power from recriticality, the supply of water to overheated metal surfaces will generate substantial power due to increased oxidation. This is the case especially for the reaction between Zircaloy and water/steam which is strongly exothermic at high temperatures.

Reflooding an overheated core creates strong thermal-hydraulic transients involving complicated phenomena, including thermodynamic non-equilibrium with superheated steam and quenching of hot surfaces with subcooled water. The steam generation due to stored heat in the fuel is considerable and contributes to increase in system pressure that counteracts the injection of cooling water from low pressure emergency cooling systems.

Recriticality could have significant impact on progression and consequences of an accident. One concern is the possibility that the reactor reaches steady-state power well above the decay power thus resulting in steam production and containment loads exceeding those foreseen in accident management strategies. (A related problem connected with reflooding overheated core is the possibility of significantly increased hydrogen production). Another concern is the possibility of the core reaching a state above prompt critical, which could result in very rapid and large power excursion. The worst consequence of this scenario would be melting and disintegration of the fuel, leading to violent fuel-coolant interaction and dynamic loads which could threaten the integrity of reactor pressure vessel and containment.

Recriticality upon reflooding the degraded reactor core is a complex problem involving assessment of core damage progression and core state prior to reflooding and analysis of a transient with strong coupling between neutronics and thermal-hydraulics where the process of quenching very hot fuel rods plays an important role.

1.3 Previous Recriticality Studies

A recriticality study was carried out in the project NKS/RAK-2 within the Nordic Nuclear Safety Programme 1994 -1997 (Höjerup et al., 1997a). The tools were the same as utilised in SARA, but they were then in an earlier stage of development. It was found that reflooding of a partly control rod free core gives a recriticality power peak of a substantial amplitude but with a short duration due to the Doppler feedback. With continued reflooding the fission power stabilises on a level that can be ten per cent or more of the nominal power, the level being higher with higher reflooding flow rate. A scoping study on OL-1 containment response was performed assuming a long-term power level being 20 % of the nominal power. The results showed that containment failure would occur about 3-4 hours after start of core reflooding (the capacity of containment venting system is not sufficient to prevent containment overpressurization). In the case of station blackout with

operating ADS the boron system would be sufficient to terminate the criticality event prior to containment failure. However, in case of feedwater LOCA and boron dilution to the whole containment water pool, boron concentration would not be sufficient to ensure subcriticality in the core.

Scott et al. (1990) performed a bounding analysis and concluded that recriticality is possible if ECCS water is unborated. It was found that the energy deposition in the fuel due to power excursion is probably not sufficient to cause melting and disintegration of the fuel. It was predicted that recriticality is likely to produce steady-state core power levels less than about 20% of nominal power.

The steady-state analyses for a 4-bundle configuration (unit cell) of the Peach Bottom Unit 2 BWR performed by Shamoun and Witt (1994) and Mosteller and Rahn (1991) show the effects of void fractions, temperatures and distribution of the control rod material on recriticality. It was concluded by Shamoun and Witt that recriticality is possible during reflood with unborated water only if at least 95% of the control rod material is lost from a unit cell for void fractions below 20% and when fuel temperatures still are high. Recriticality is not possible under any circumstances during the reflooding phase before fuel quenching, even if 100% of control rod material is lost, if the void fraction exceeds 20%. Reflooding the core with borated water at a boron concentration of 1200 ppm is sufficient to prevent recriticality under short- and long-term recovery conditions corresponding to zero void fraction and high (525 K) and low (325 K) moderator temperature. Mosteller and Rahn found that retention of even a small fraction, 10-20%, of the control rod material in the fuel cell may be sufficient to prevent recriticality. However, three-dimensional effects of core degradation may make these results uncertain.

Bandurski et al. (1994) performed one-dimensional, dynamic analysis on a simplified reactor model (typical 1000 MW thermal power BWR-4 of GE design) using the TRAC/BF1 and ONEDANT codes. They found that a super prompt-critical excursion is possible but of no safety concern for credible reflood rates and that following the power excursion a steady state fission power level of at most about 10% of nominal power is achieved for realistic reflood rates. They pointed out the strong influence of the fuel cooling conditions during the reflooding process on recriticality (e.g. decreasing of Doppler efficiency with increasing reflood rate).

The importance of the two-phase flow and heat transfer regimes for recriticality was discussed by Sandervåg (1988). Okkonen et al. (1993) found that a BWR core can become critical if at least 1 m of the core is without absorber and if the void fraction is less than 60%.

These earlier studies, except NKS/RAK-2, were either made by means of separate, or loose coupled, thermal-hydraulics and reactor kinetics models, or without a more detailed multi-dimensional treatment of the problem. In addition, the problem has not been addressed with realistic plant data for reflooding situations in BWRs.

1.4 Objective and scope

The overall objective of the SARA project was to investigate the recriticality phenomena and to assess the safety implications of recriticality, including accident management aspects. The specific goals were:

- To develop calculation tools which can simulate recriticality during reflood in BWRs in a realistic way, based on state-of the-art knowledge of reactor kinetics and thermal- hydraulics phenomena involved.
- Determine the magnitude of the recriticality power and its spatial and time-wise variation in the core.
- Determine the effects of possible prompt power excursions on the integrity of fuel and primary system.
- Analyse the consequences for the integrity of the containment, in particular at long-term recriticality with elevated power.
- Investigate if and how accident mitigation measures can be modified to avoid or minimise the effects of a recriticality transient.

The scope of the SARA project was as follows:

1. To determine initial and boundary conditions for recriticality through accident progression and reflooding calculations with the SCDAP/RELAP5, MELCOR and MAAP codes.
2. Development and applications of SIMULATE-3K, APROS and RECRIT for recriticality calculations in BWRs.
3. To review the heat transfer and thermal-hydraulics modelling descriptions in the literature applicable to reflooding and quenching phenomena of an overheated core.
4. Analysis of containment response to recriticality.
5. To assess accident management aspects of recriticality.

1.5 Approach

A four-fold approach was utilised to reach the goals of the recriticality analyses through development and application of three computer codes SIMULATE-3K, APROS and RECRIT by Studsvik, VTT and Risö, respectively, within Task 1, 2 and 3. The fourth task was carried out by SKI and comprised support to the code developers through a literature study and a survey of the state-of-the-art of heat transfer physical models related to reflooding and fast power transients.

A preparatory step in SARA was performed calculating initial and boundary conditions prior to recriticality by means of three severe accident codes, especially aimed for analysis of core damage phenomena. Thus, introductory reflooding calculations were made for OL-1 with MAAP4 by TVO in Finland, as an in-kind contribution to SARA, and with MELCOR by VTT. Similar calculations were made by Studsvik for O-3 with

SCDAP/RELAP5. The base scenario was station blackout with successful initiation of the Automatic Depressurization System (ADS) bringing the primary system pressure down to a few bars. In these calculations the effects of recriticality were not taken into account. The results comprise, among others, control rod configuration, core temperature distribution, oxidation effects with hydrogen production, recooling transient and time to complete rewetting of the core. The results of the calculations with the severe accident codes were also utilized for benchmarking of the thermal-hydraulics in the recriticality codes, which in this respect were not so advanced, at least not in the early stage of the SARA project.

First, the recriticality codes were developed separately and applied in individual studies on OL-1 and O-3. Later, a code comparison, using the same (as far as possible) initial and boundary conditions, was made by selecting three common accident sequences for OL-1 for analysis with all three codes. The objective was to assess and to identify the uncertainties and shortcomings of the different codes.

Finally, the containment response to increased power levels due to recriticality was investigated using the MELCOR code. The results of these calculations, together with predictions of fuel response, provided information required to assess the impact of accident management strategies on accident progression.

2. INITIAL CONDITIONS FOR RECRITICALITY ANALYSES

Preparatory calculations for Oskarshamn 3 (O-3) and Olkiluoto 1 (OL-1) were made with the severe accident analysis codes SCDAP/RELAP5, and MELCOR and MAAP, respectively. The aim was to investigate the conditions which can lead to recriticality and to produce initial and boundary condition data as a basis for the S-3K, APROS and RECRIT calculations.

The major results of importance for the recriticality calculations are:

- timing of events, such as for ADS, core uncovery, beginning of control rod melting and fuel rod damage (the time period between the latter two constitutes the "time-window" crucial for recriticality phenomena).
- temperature distribution in the core.
- control rod status before recriticality, i.e. the absorber material mass distribution in the core prior to recriticality.
- reflooding conditions as function of water mass flow injected into downcomer, i.e. core inlet flow rate and water level as function of time.

2.1 SCDAP/RELAP5 Calculations for Oskarshamn 3 Plant (Task 1)

2.1.1 Oskarshamn 3 plant

The BWR chosen for the analysis is the Swedish Oskarshamn 3, which is operated by the OKG AB utility. A schematic of the reactor vessel with internals for a type reactor, ABB-Atom BWR-75, is shown in Figure 2.1.

Oskarshamn 3 is an advanced 3300 MW_{th} BWR with eight internal recirculation pumps. Operating pressure is 7.0 MPa. The core has 700 fuel assemblies and 169 control rods with B_4C as absorber material.

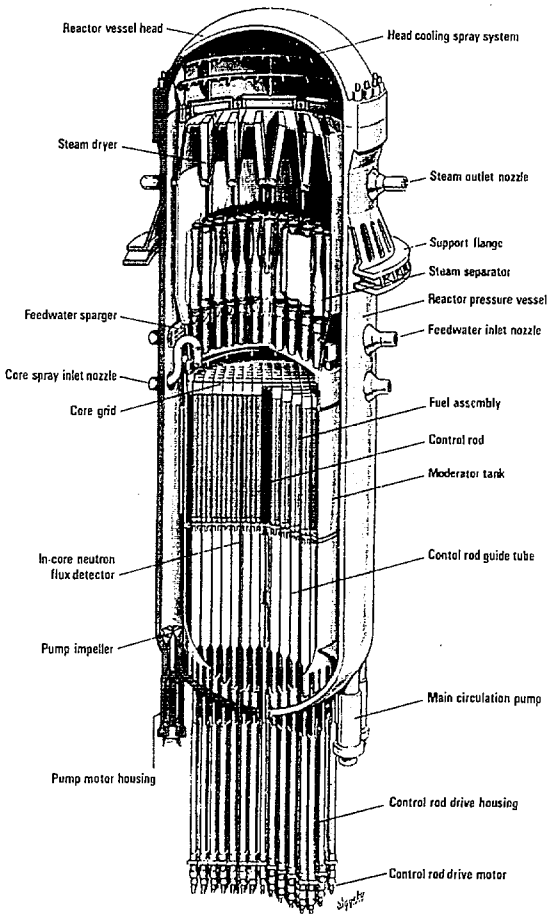

Figure 2.1 Reactor vessel and internals

The Emergency Core Cooling System (ECCS) comprises four high-pressure auxiliary feed water loops and four low-pressure loops. Two loops from each system inject water through spray nozzles above the core. The two other loops feed into the downcomer to facilitate reflooding of the core from the bottom, if the core has been uncovered. The capacity of high-pressure ECCS is 22.5 kg/s per loop, independent of the vessel pressure. The capacity of low-pressure ECCS, which takes water from the condensation pool, is depending on the backpressure, i. e. the pressure difference between primary system and containment. It begins to inject water when the back pressure is below around 1.2 MPa and the flow rate increases to 355 kg/s per loop as the back-pressure goes to zero. The total capacity of all ECCS loops as function of back pressure is shown in Figure 2.2.

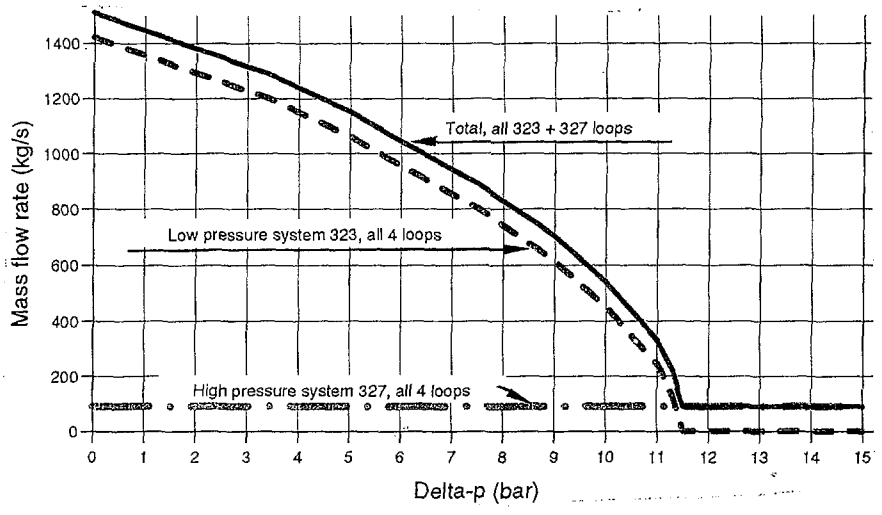

Figure 2.2 ECCS mass flow rate as a function of pressure difference between vessel and containment.

In addition to the flow from the ECCS loops there is a possibility that also the normal feedwater can be taken into operation when the electric power returns. This requires that the isolation valves can be opened. The feedwater flow would then add maximum about 1900 kg/s. The total reflooding mass flow rate at 4 bar back pressure would then amount to 3000 kg/s. Taking into account that the back pressure under these circumstances would be so high that the low pressure injection would cease, the total maximum flow rate will then be limited to about 2000 kg/s.

A detailed plant description with data for the in-vessel components is given in the topical report of the SCDAP/RELAP5 reflooding calculations of initial conditions (Nilsson, 1998).

2.1.2 Results of SCDAP/RELAP5 analyses

Preparatory reflooding calculations for Oskarshamn 3 were made with the severe accident analysis code SCDAP/RELAP5. This work is reported separately in Nilsson (1998). Here, a summary of main results is presented. SCDAP/RELAP5 models the thermal-hydraulics for the whole primary system in more detail than S-3K and calculates core heat-up from decay power as well as core damage progression and oxidation which are not taken

into account in S-3K. The SCDAP/RELAP5 results were used as model for simulation of core heat-up with S-3K. Reactivity effects were not calculated with SCDAP/ RELAP5 since this code has only a point kinetics model which is not detailed enough for recriticality studies.

The reactor model in SCDAP/RELAP5 comprised 140 so called hydrodynamic volumes connected by flow junctions. The core was divided into five concentric rings, each with ten axial nodes. The power distribution and other operating conditions were taken from a SIMULATE-3 output for a specific fuel loading and burnup (mid-cycle), for which the thermal power was 3020 MW.

Studied accident scenarios include station blackout (TB) with depressurisation (ADS) and with returning power to emergency core cooling systems at different times when the fuel had been heated up to temperatures between 1700 K and 2000 K. The ADS was started 10 minutes after the time when the water level in the downcomer had dropped to 0.5 m above the core exit. ADS blowdown was assumed to continue down to a system pressure of 0.5 MPa.

In addition to a base case without reflooding, calculated up to 2 hours after the total loss of AC power, 13 reflooding cases were calculated within the following parameter range:

- Eleven bottom flooding cases with injection of 20 ^{0}C water into the downcomer (DC), with a constant mass flow of 45, 90, 200, 500, 1000, 1500 and 2000 kg/s.
- Two top spray cases, i.e. injection into upper plenum with mass flow rates of 45 and 90 kg/s, started at a core maximum temperature of about 1800 K.

The core uncovery and heat-up is illustrated in Figure 2.3.

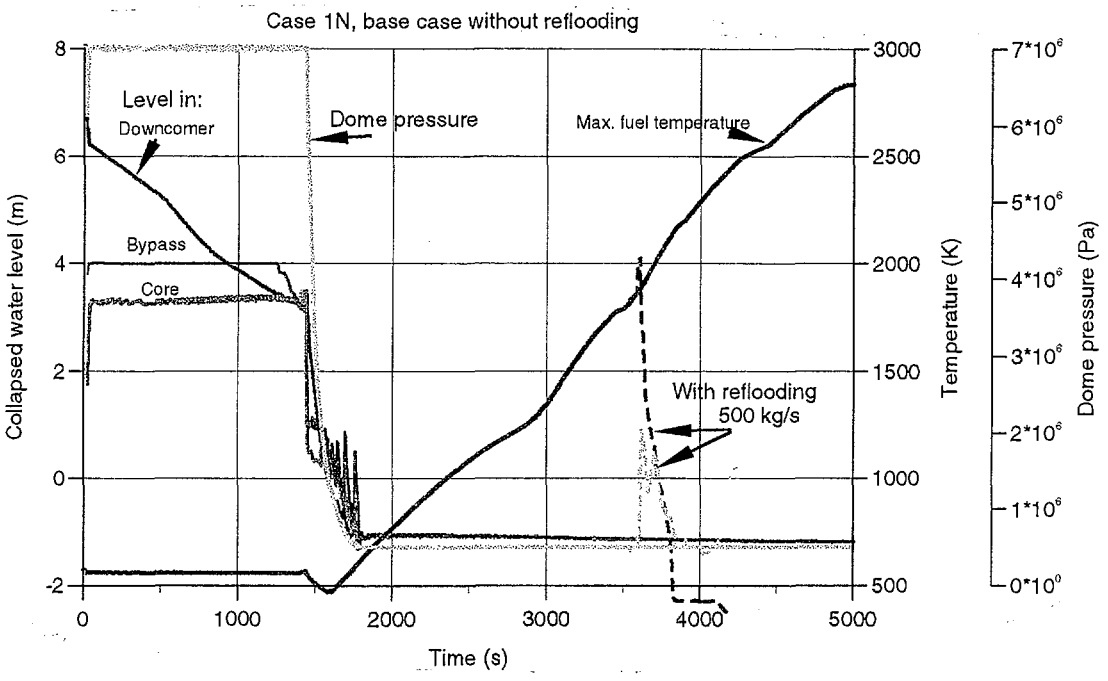

Figure 2.3 Water levels in vessel and maximum core temperatures from SCDAP/RELAP5.

The additional melting of control rods that was obtained during reflood due to increase in power from oxidation processes when water was added to the dry, overheated core is taken into account for the initial conditions in the S-3K calculations.

An example of the temperature distribution in the core before reflooding is shown in Figure 2.4.

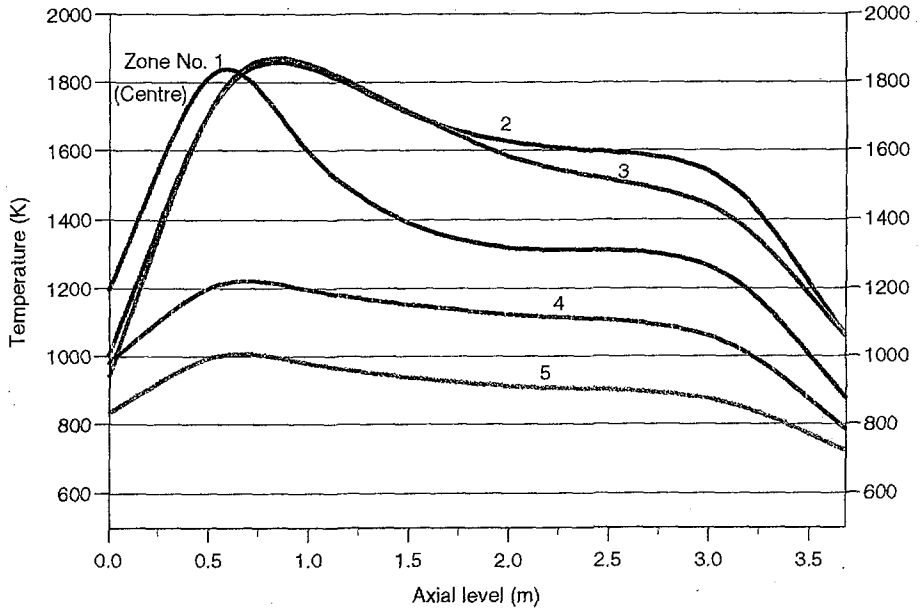

Figure 2.4 Fuel temperature distribution for the five core zones before reflooding.

The state of control rods in the core before recriticality includes the additional melting obtained due to oxidation during reflooding. In most cases melting took place in the three innermost core zones. Melted absorber material was accumulated in the lowermost axial node. It is assumed that control rod material in upper nodes which did not undergo melting, according to SCDAP/RELAP5, could not be supported by lower, empty nodes but was relocated into the bottom nodes.

The water level in the vessel was more than 1 m below the core inlet after blowdown according to SCDAP/RELAP5. Different times were then needed to reach the core lower boundary for different reflooding rates. The resulting reflooding velocity , i.e. the speed with which the water level increases in the core, is a function of the injection mass flow rate and the boiling rate in the core. A substantial fraction of the water is boiled off in the core which reduces the net reflooding velocity. The additional pressure drop in the core from increased two-phase flow counteracts the reflooding as well. Varying pressure drops in the parallel core channels makes the water surfaces oscillate between different channels.

2.2 MELCOR and MAAP Calculations for Olkiluoto Plants (Task 2)

2.2.1 Olkiluoto 1 & 2 plants

The Olkiluoto power station comprises two twin BWR units, OL-1 and OL-2, operated by the Finnish TVO consortium (Teollisuuden Voima Oy). The reactor is of the same type as the Oskarshamn 3 plant, of ABB Atoms design (see Figure 2.1), but somewhat smaller. Originally the thermal power was 2000 MW but after upgrading is now 2500 MW. The reactor has 500 fuel assemblies (about 86 000 kg UO_2), 121 control rods and 6 internal recirculation pumps. The reactor fuel modelled in these calculations is ABB Atoms SVEA-100. The emergency core cooling systems are similar to those in O-3, but the individual top spray nozzles above the core have been replaced by GE-designed spargers around the periphery. In addition, the boron system has been modified so that it will start automatically at high power signal if the downcomer level falls below a certain value.

2.2.2 MELCOR analyses

The calculations were performed for Olkiluoto 1&2 BWR plants with MELCOR 1.8.3 code (Lindholm, 1997). The selected accident scenario was a total station blackout with successful depressurization of primary system initiated 900 seconds after the downcomer water level had dropped to 0.5 m from the core top. The axial and radial power peaking factors were provided by TVO for fuel burnup of 19.7 MWd/kgU. Two different core nodalizations were used for testing the sensitivity of the MELCOR model. In the first nodalization the core was divided into 5 radial rings with equal flow areas and 10 axial equally long segments. In the second finer nodalization the core was divided axially into 25 segments with 5 radial rings.

The core input model parameters were selected so that no particulate debris formation was allowed in the core region. The candling heat transfer coefficients for steel, steel oxide and B_4C were set to 500 W/m^2K (default value is 1000 W/m^2K). These input parameter selections were made to find a conservative initial state in respect of possible recriticality. The early and intermediate phases of core degradation are probably more realistically simulated by precluding the particulate debris formation and allowing fuel and cladding to reach higher temperatures (up to 2500 K) in intact geometry than by using the code default values resulting in early particulate debris formation (typically at temperatures around 2100 K).

In the two variations of core nodalization, the reflooding start criteria was that about 60 % of the control rods had melted in the core. This stage was achieved in the coarser core nodalization case at 4200 s and at 4800 s with finer axial nodalization. This sensitivity is caused partially by the more accurately defined power distribution of the core in the latter case, resulting in lower power generation in the upper and lower ends of the core.

MELCOR 1.8.3 predicts, if early formation of particulate debris is precluded by model parameter selection, that a BWR core can reach a state where large fraction (>60 %) of the control rods have melted and the intact fuel geometry is still preserved. The core heatup and melting pattern follows largely the initial power distribution of the core,

forming an "U-shape" surface in the core which is without control rods, leaving the periphery of the core less damaged than the central parts of the core.

The eutectic reaction between B_4C and steel control blades leads to early melting and relocation of control rods around the temperature of 1520 K. The core material temperature histories in the centre core node is shown in Figure 2.5.

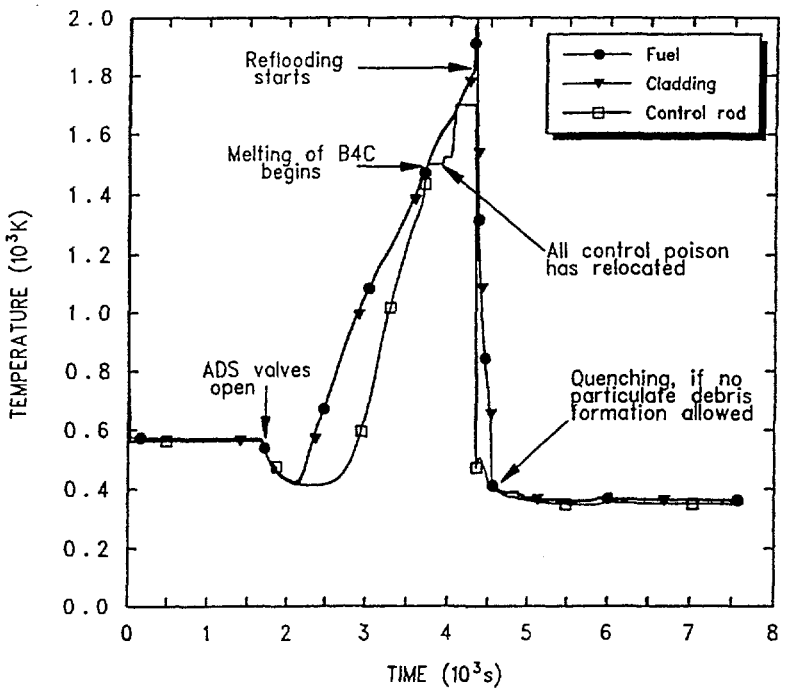

Figure 2.5 Core material temperature histories. Core reflooding rate is 540 kg/s (2.8 cm/s), injected on top of the core.

In the case of coarse core nodalisation (5x10) about 56 % of the control rods have melted at the onset of reflooding and the maximum core temperature was 1837 K. Most of the control rods have relocated on the lowest core node and on the core support plate node. Fuel in these calculations remained in the intact geometry. Some cladding oxidation had taken place during the core heatup.

The finer axial discretisation of the core (5 x 25 nodes) resulted in augmentation of control rods melting. In this case about 69 % of the control rods had melted and relocated prior to the start of reflooding. The maximum core temperature was 1970 K and it was reached in the centre ring at the elevation of one third from the top of the core. The difference in the location of the hottest core node in the calculations with different nodalisations is directly related to the power peaking factors, as mentioned above. The B_4C mass distribution in the core before start of reflooding is illustrated in Table 2.1.

The variation of reflooding capacity revealed that quenching of a core at an average temperature of about 2000 K takes a few hundred seconds. Relatively efficient cooling was achieved with reflood rates larger than 540 kg/s. In the case with the lowest reflood rate, i.e. 45 kg/s, the cooling of the core took a significantly longer time than in the other studied cases.

Table 2.1 Mass fraction of boron carbide left in a core node at the start of reflooding.

Fraction of B_4C from original inventory left in a node at the start of core reflooding (at 80 min from start of accident)

center line of core/axial node	Radial ring					
	1	**2**	**3**	**4**	**5**	
25	0	0	0	0	1.0	
24	0	0	0	0	1.0	
23	0	0	0	0	1.0	
22	0	0	0	0	1.0	
21	0	0	0	0	0.92	
20	0	0	0	0	0	
19	0	0	0	0	0	
18	0	0	0	0	0	
17	0	0	0	0	0	
16	0	0	0	0	0	
15	0	0	0	0	0	
14	0	0	0	0	0	
13	0	0	0	0	0	
12	0	0	0	0	0	
11	0	0	0	0	0	
10	0	0	0	0	0	
9	0	0	0	0	0.12	
8	0	0	0	0	0.68	
7	0	0	0	0.	1.02	
6	0	0.01	0.	0.	1.53	
5	0	0.02	0.	0.	1.88	
4	0	0.04	0.	0.	2.13	
3	0	0.03	0.	0.	2.40	
2	0	0.10	0.	0.	2.29	
1	1	1.54	2.0	3.0	5.46	
0	2	23.10	2.0	2.0	2,56	*

* Mass fractions larger than unity refer to mass addition due to melt relocation during heatup.

In all cases significant additional heatup due to oxidation and subsequent further melting of control rods was recognized after the start of reflooding. This phenomenon should be considered in recriticality analyses.

2.2.3 MAAP analyses

Reflooding of a degraded BWR core was also studied with the MAAP 4.0.2 computer code for Olkiluoto 1 and 2 nuclear power plant units (Sjövall, 1997). The initial conditions were the same as for the MELCOR calculations described in the preceding section. The active core was divided into 20 axial and 7 radial nodes.

According to MAAP 4 predictions, the core is fully cooled as long as it is covered by two-phase mixture. After the top of fuel is uncovered at 25 minutes into the accident, the core temperature begins to increase.

The default parameters for core degradation were used, which led to core collapse after start of reflooding, if reflooding was started when the maximum core node temperature had exceeded 1750° C. Consequently, the maximum core node temperature at start of reflooding had to be lower than this value.

The following five sequences were calculated:

1. No reflooding.
2. Reflooding with 2 auxiliary feedwater system pumps to downcomer when the hottest core node had reached 1230° C at 40 minutes into the accident. Reflooding capacity was 45 kg/s, corresponding to the water level rise velocity in the core of 0.23 cm/s. After reflooding, top part of core collapsed but there was a time period with intact fuel geometry and relocated control material.
3. Reflooding with 2 auxiliary feedwater system pumps to downcomer, 2 auxiliary feedwater system pumps into upper plenum and 4 core spray system pumps into upper plenum when the hottest node had reached 1530° C at 45 minutes into the accident. All water supplied to upper plenum was diverted directly into lower plenum through core by-pass. The auxiliary feedwater system capacity was 22.5 kg/s per pump. The core spray system flow is pressure dependent. The maximum reflooding capacity in this sequence was 550 kg/s, corresponding to the water level rise velocity of 2.8 cm/s.
4. Reflooding with 3 feedwater system pumps to downcomer when the hottest node had reached 1530° C at 45 minutes into the accident. Reflooding capacity was 1350 kg/s, corresponding to the water level rise velocity of 6.8 cm/s.
5. Reflooding with hypothetical feedwater capacity to downcomer when the hottest node had reached 1530 °C at 45 min into the accident. Reflooding capacity was 2000 kg/s, corresponding to the water level rise velocity of 10 cm/s.

The results of the MAAP calculations can be summarized as follows:

1. In the peripheral radial ring (comprising 192 fuel assemblies and 44 control rods), all control rod material was in place at the time of reflooding. In other radial nodes control rods were relocated to about half of the core.
2. After reflooding only with auxiliary feedwater system, the upper part of core collapsed but there was a time period with intact fuel geometry and relocated control material. In the other cases fuel geometry remained intact.
3. The amount of hydrogen generated, predicted peak primary system pressure and maximum fuel temperature are shown in Table 2.2.

Table 2.2 Hydrogen generation, system pressure and maximum fuel temperatures from MAAP

Case	Reflooding capacity	Hydrogen generation	Primary system pressure peak during reflooding	Maximum fuel temperature
1	0 kg/s	120 kg	No reflooding	No reflooding
2	45 kg/s	170 kg	0.8 MPa	2450 °C
3	550 kg/s	30 kg	3.5 MPa	1350 °C
4	1350 kg/s	80 kg	4.5 MPa	1750 °C
5	2000 kg/s	60 kg	4.5 MPa	1700 °C

In all cases reflooding accelerated hydrogen generation and core heat-up. In the case where the core was reflooded only with the auxiliary feedwater system this was the reason for the collapse of the core.

2.2.4 Conclusions

The accident progression calculations with SCDAP/RELAP5, MELCOR and MAAP have shown that extensive melting and relocation of control rods takes place in the central part of the core before there is any severe damage of the fuel when the reflooding is started before the fuel temperature have reached about 2100 K. The duration of this "time-window" was predicted to be in the range of a few minutes to about 40 minutes. It should be noted, that core degradation is rather sensitive to certain modelling parameters, especially in the integral codes like MELCOR and MAAP. The differences in predicted core-end states before recriticality reflect the modelling differences and uncertainties. It was decided to use the MELCOR results as principal basis for recriticality calculations for the OL-1 reactor plant.

3. HEAT TRANSFER AND THERMAL-HYDRAULICS ASPECTS OF REFLOODING AND RECRITICALITY (TASK 4)

Since reflooding plays a very important role in large-break loss-of-coolant accident (LOCA) safety analysis of core thermal limits, it has been the subject of extensive experimental and analytical studies. The physics of reflooding, i.e. the two-phase flow and heat transfer, is very complex, which is reflected in the fact that advanced thermal-hydraulics codes, such as RELAP5 and TRAC, still have problems in accurately predicting experimental results in spite of recent improvements of these codes (Analytis, 1996, Hochreiter, 1997, Elias et al., 1998). The situation is even more complicated in a severe accident situation due to high initial fuel temperatures, significant oxidation of the fuel cladding as well as strong thermal-hydraulic transients should the core become critical.

3.1 Basic Phenomena

The reflooding phenomena can briefly be summarised as follows for the bottom-up quench front progression; see Figure 3.1. When the water level, after the lower plenum refill phase, reaches the lower parts of the overheated core an intense evaporation of the cooling water will occur. This results in an increase of the local pressure which will to some extent push back the incoming water. Due to the intense evaporation process the steam phase will contain substantial water entrainment which will contribute to the cooling of the fuel cladding in these zones to temperatures which allow quenching (precursory cooling). After a few oscillations a continuous progressing quench front will be established. The stable reflood process is characterised by a quench front moving up through the core. The region below the quench front contains mostly single phase liquid while the region above can be dispersed with the water existing as droplets and/or slugs at moderate reflooding rates and as a more or less continuous water core (inverted annular film boiling) at higher reflooding rates and subcooled conditions.

The flow and heat transfer in the vicinity of the quench front is very complex. The heat transfer can typically be characterised as nucleate or transition boiling. The flow regime in this region is mostly churn-turbulent with an average void fraction in the associated zone between 0.4 and 0.6. Observations indicate that the void fraction increases sharply downstream of the quench front and reaches a fairly constant level around 0.8. Superheated steam exists downstream of the churn-turbulent region thus resulting in a region of thermodynamic nonequilibrium.

The existence of the two-phase region above the quench front may have an impact on the approach to criticality and on the magnitude of the power burst. Thus, the power excursion is dependent on the initial reactor power and the thermal-hydraulic behaviour during reflooding. The reactor may have been subcritical for some time and the neutron flux may therefore have decreased to low levels. The fuel heat-up and the Doppler feedback as well as the void formation due to nuclear heating may therefore be significantly delayed as a result of the long reactor period as compared to the reactivity addition rate. The existence of a churn-turbulent region above the quench front may to

some extent dampen this effect. Local two-phase levels will vary stochastically with time over the radial cross-section. The reactivity will thus fluctuate significantly and the configuration will intermittently be critical before the quench front reaches the critical elevation. It is therefore possible that the neutron flux has reached levels which are sufficient to produce immediate fuel heat-up thus limiting the power excursion.

The thermal response of the fuel, and thus the possibility of fuel failure, depends on the rate of reactivity insertion and the heat transfer from the fuel to the coolant which to great extent is determined by the time constant of the fuel (approximately 5 seconds). Under conditions with relatively low reflooding rate and therefore low reactivity insertion rates there may be sufficient time to conduct the generated power to the coolant. The water would be heated up to saturation and voiding would start. The heat would be generated below the water surface and pool boiling would occur. Voiding has two effects: level swell occurs and increases the volume of the critical configuration and thereby increases the reactivity but, on the other hand, the increasing moderator temperature and increasing void generally tend to decrease the reactivity.

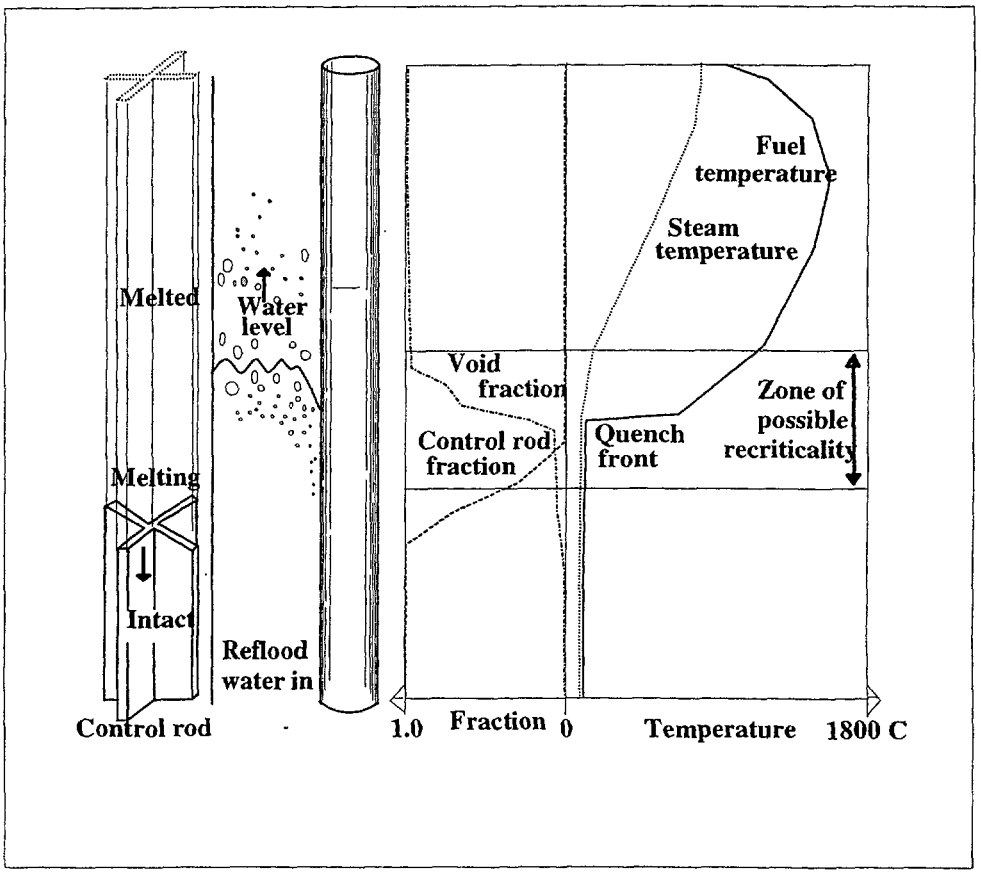

Figure 3.1 Reflood of degraded core: schematic illustration of axial profiles.

3.2 Void Fraction and Kinetics

Some basic features of recriticality during reflooding are illustrated in Figure 3.2 and Figure 3.3 where the infinite multiplication factor is shown as a function of void fraction with fuel temperature and control rod concentration as parameters (Miettinen and Höjerup, 1999a). The multiplication factors were calculated assuming that the void fraction in the bypass area is the same as in the fuel channels.

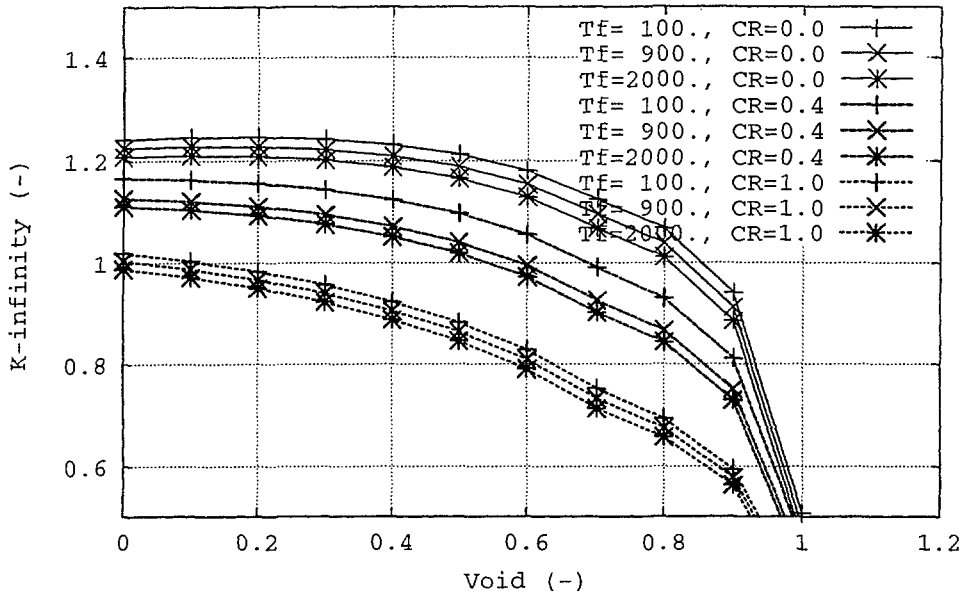

Figure 3.2 Infinite multiplication factor calculated from the CASMO data for 10 MWd/kgU fuel (BOC) and void history of 0.45.

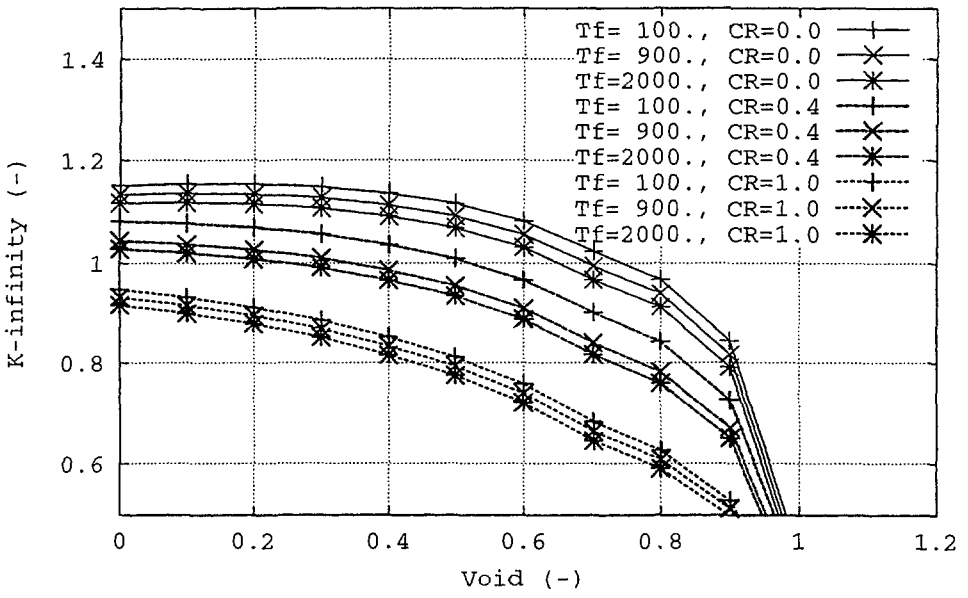

Figure 3.3 Infinite multiplication factor calculated from the CASMO data for 20 MWd/kgU fuel (MOC) and void history of 0.45.

As can be seen, the relation between reactivity and changes in void fraction depends strongly on the void fraction range. No criticality is possible in the void fraction range of 0.85 -1.00 for burnup of 10 MWd/kgU (Beginning of cycle, BOC), Figure 3.2, and in the void fraction range of 0.70 - 1.00 for burnup of 20 MWd/kgU (Middle of cycle, MOC) Figure 3.3. For burnup of 30 MWd/kgU (End of cycle, EOC) the corresponding void fraction range is 0.50 to 1.00 (not shown). It is also seen that in the BOC core the criticality is possible in the cold conditions with any control rod concentration, i.e. 0 - 100 %, when the infinite multiplication factor is used as the criterion. The criticality is possible with control rod concentrations of 0 – 50 % for MOC data and 0 –35 % for EOC data.

The above results show that recriticality is unlikely downstream of the quench front where the void fraction exceeds about 0.8. It should also be noted that the multiplication factor is only weakly dependent on the fuel temperature.

3.3 Thermal-Hydraulic Modelling Characteristics

The modelling of heat transfer and thermal-hydraulic phenomena in S-3K, RECRIT and APROS is different which of course has impact on reflooding and recriticality. A comparison of some important thermal-hydraulic features of the three codes is shown in Table 3.1.

Table 3.1 Comparison of thermal-hydraulic modelling characteristics

Thermal-hydraulics	RECRIT	APROS	SIMULATE-3K
Pressure calculation in the common case comparison	By artificial control valves	Boundary condition	Boundary condition
Core inlet flow in the common case comparison	Injection into downcomer, gravity feed into the core	Flow boundary condition at the core inlet	Injection into downcomer, gravity feed into the core
Momentum equation solution	Integral momentum	Full momentum equation	Integral momentum equation
Phase separation	Drift-flux model for bubbly and droplet flow	Drift-flux models for bubbly and droplet flow	Drift flux model
Wetted wall heat transfer	Forced convection and nucleate boiling	Forced convection and nucleate boiling	Forced convection and nucleate boiling
Quench front model	Discrete moving boundary between wetted and dry wall, analytical correlation for quench front velocity	Quenching results from the heat transfer transition from post-dryout heat transfer to wetted wall heat transfer	Quenching results from the heat transfer transition from post-dryout heat transfer to wetted wall heat transfer
Post-dryout heat transfer	Wall-to-vapour heat transfer, inverted annular film boiling, transition boiling, radiation absorption to droplets	Wall-to-vapour heat transfer, inverted annular film boiling, transition boiling, radiation absorption to droplets	Wall-to-vapour heat transfer, interfacial heat exchange
Radiation between multidimensional core nodes	Calculated both in radial and axial direction	No calculation	No radiation model
Simulation of control rod melting	Simulation possible	No calculation	No calculation

Only RECRIT has a model for quench front movement. However, the current version of RECRIT does not model the so-called Inverted Annular Film Boiling (IAFB) region, which can exist during reflooding with subcooled water and high flow rates (Analytis and Yadigaroglu, 1987). In addition, the analysis of QUENCH single rod experiments suggests that at very high fuel temperatures a new flow region, called Droplets-Splashes region, where the heat transfer is very intensive can exist downstream from the IAFB region

(Hofmann et al., 1997). Also, it seems that the heat transfer coefficient in the IAFB region in the QUENCH tests is much higher than in experiments with lower surface temperatures. This is attributed to very intensive disturbances at the water-steam interface and more pronounced radiation effects in the QUENCH experiments. These effects, as well as heat transfer in the dispersed flow film boiling region, should be evaluated when more information become available from the QUENCH experiments.

The approach used in RECRIT to adequately simulate the cooling and rewetting of the core fuel rods during reflooding has been to implement a simplified but yet accurate model, which also has proven to be computational effective. It seems that this approach is reasonable considering the limited amount of available data. More detailed description of thermal-hydraulic modelling in RECRIT is presented in section 4.3.

4. DESCRIPTION OF COMPUTER CODES FOR RECRITICALITY CALCULATIONS

4.1 SIMULATE-3K Code (Task 1)

SIMULATE-3K is a transient version of the steady-state core analysis computer code SIMULATE-3. The latter is part of the Studsvik Core Management System (CMS) code package for BWR and PWR applications which consists of two principal codes; CASMO and SIMULATE. The relation between the different codes is illustrated in Figure 4.1.

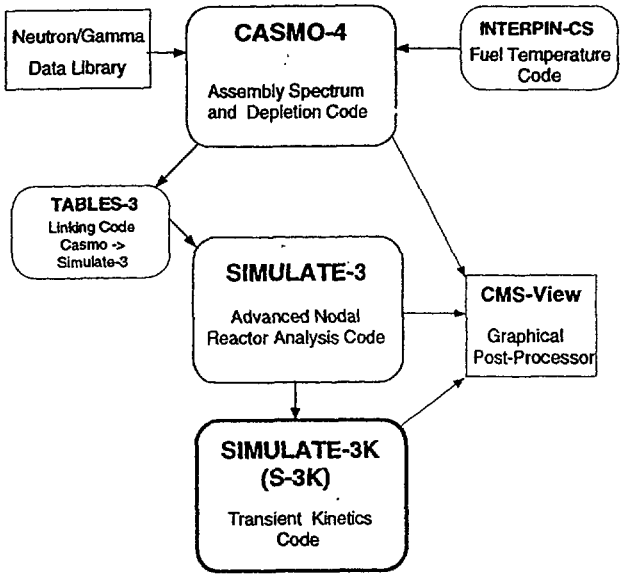

Figure 4.1 Studsvik's Core Management System, CMS.

CASMO-4 is the latest version of the CASMO transport theory assembly, spectrum and depletion code. CASMO-4 is widely used by utilities in many countries. SIMULATE-3 is a three-dimensional two-group reactor analysis steady-state core simulator used for in-core fuel management studies, core design calculations, and calculations of safety parameters. The first version was produced in 1985. One of the original goals in the development of SIMULATE was to introduce an accurate advanced nodal method which required no normalisation to fine-mesh calculations or to measured data. A description of the SIMULATE-3 modelling and methodology is given in Cronin et al. (1995).

With SIMULATE-3K (S-3K) the transient analysis capabilities were incorporated into SIMULATE-3 (Borkowski et al., 1994). This work has resulted in the addition of a neutron kinetics model and a transient fuel pin heat conduction model coupled to a hydraulic channel model. This has required incorporation of extra numerical features to ensure the stability and accuracy of the numerical solution. The latest version S-3K/2.00 incorporates a 5-equation thermal-hydraulics model with one flow channel per assembly. S-3K has been successfully applied on and validated against various full-plant transients such as control rod drop and ejection events, as well as BWR stability measurements. The code is under continuous development in order to extend its range of applicability.

4.1.1 Code structure

S-3K comprises coupled three-dimensional kinetics and parallel channel thermal-hydraulics models for the core region. The core boundary conditions can in turn be coupled to an outer one-dimensional peripheral system to form a closed recirculation loop including also upper plenum, steam separator, downcomer, recirculation pumps and lower plenum for BWRs.

The major physical modelling capabilities comprises:

- **Full two-group, three-dimensional transient neutronic solution.**

The nodal solution in S-3K is the same as in the steady-state method, QPANDA. The time-dependent version of these equations is solved in the full three-dimensional form. The delayed neutron precursor equations are solved in six groups.

- **Transient channel thermal-hydraulic model.**

Transient mass, energy and momentum transport are modelled. Each channel is modelled explicitly, which is an important distinction from many other transient nodal codes with lump channels. The five equation formulation employs a drift flux model. A donor cell differentiating scheme uses an integral (nodal) formulation on an edge-centred mesh (rather than staggered mesh) to obtain rapid spatial convergence with decreasing mesh size. Boiling is treated with the EPRI void/quality model (Zuber-Findlay slip representation), which is the same as in the steady-state SIMULATE-3. The hydraulics models are the same for PWRs and BWRs.

- **Transient pin conduction.**

A pin conduction solution is performed in each node. Average fuel temperature is calculated for each node. Peak fuel temperature is also calculated. Likewise, fuel enthalpy (cal/g) is calculated in both cases. The pin conduction properties are all functions of temperature and exposure. Heat transfer coefficients is flow-regime dependent and a function of local (node-average) coolant conditions.

The calculational sequence for the neutronics/thermal-hydraulics is depicted in Figure 4.2. The connection between the core model and the peripheral systems model is shown in Figure 4.3.

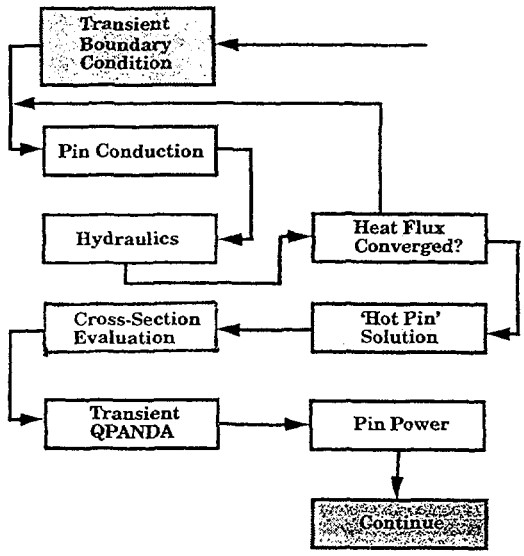

Figure 4.2 S-3K Neutronics-T/H Calculation Sequence

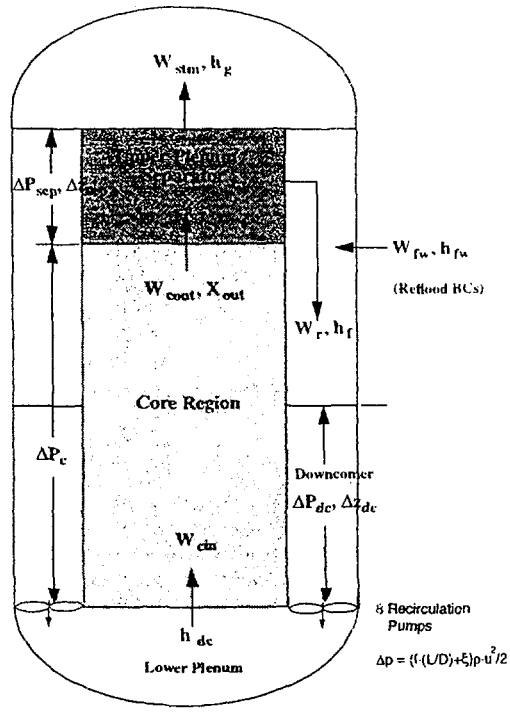

Figure 4.3 SARA Peripheral Systems Model

4.1.2 Code development

To make simulation of the special conditions prevailing under reflooding and fast recooling transients possible, some modifications and upgrading of the S-3K code were needed, especially of the thermal-hydraulic system models. The code development for SARA applications is described in Kropaczek (1999).

Two major areas for improvement were identified:

1. Improvement of the code's capability to simulate core heat-up following loss of power with core uncovery.
2. Improvement of the code's capability to calculate the rising water level in the core during reflood.

For Task 1, several minor coding changes were needed. The released version of S-3K had some coding checks that prohibited the inlet flow from being reduced below 0.1% of rated flow, regardless of input. This limitation was necessary for most standard applications. Coding changes were implemented which now allows the flow to be reduced to 0% of rated core flow, and this gives a more realistic heat-up simulation.

For Task 2, the problem with the rate of rising water level stems from the lack of coupling between the peripheral systems model and the core model in the standard version of the S-3K code. The core inlet flow rate depends directly on core pressure drop which is

dictated by integral loop momentum balance over the core, upper plenum, steam separator, downcomer and lower plenum. Core inlet enthalpy requires accounting for the liquid recirculation rate from the steam separator. Therefore, simply knowing the downcomer reflood flow rate and temperature is insufficient to determine the core flow. To properly model the reflood rate requires a direct calculation of loop energy, momentum and mass balance. This was achieved through modelling upgrading with the following assumptions:

1. Coupled lower plenum and downcomer.
2. Coupled upper plenum and separator.
3. Coupled lower plenum/downcomer are comprised of single phase liquid and are perfectly mixed.
4. Coupled upper plenum and separator assumes a homogeneous equilibrium mixture (HEM).
5. Recirculated liquid from separator is saturated with zero carryover to the steam dome.
6. No modelling of the steamline and no pressurization calculation.
7. Linearization of frictional pressure drop as a function of core inlet flow.

The governing equations to be solved are the equations for conservation of mass and energy for the two phases (water and steam) and momentum equation for the two-phase mixture. A detailed description can be found in Kropaczek et al. (1997).

However, there are some limitations in the code that might be of importance for the thermal-hydraulic calculations. It was thus outside the scope and time frame of the present project to include special quench heat transfer models, oxidation models and a steam dome component. Lack of modelling of axial heat conduction in fuel pins, and radiation between assemblies at high temperatures are some other limitations of present code version in its application to the reflooding transients.

4.1.3 Input and output

Execution of S-3K requires a library file with CASMO cross section data for the fuel segments in the actual core loading, and a restart file from a steady-state regular SIMULATE-3 run up to the burn-up step of the fuel cycle before the transient to be calculated in S-3K. Since most of the plant system description and the initial boundary conditions are transferred from the restart file, rather few input data are required for S-3K. Except data for computing control, time-step, etc. the following major blocks of input data were used in SARA calculations:

- Control rod configuration, initial rod positions and tables specifying rod movements (e.g. for simulation of rod melting).
- Core inlet mass flow before reflooding as a function of time.
- Pressure in core exit as a function of time.
- Temperature of core inlet flow as a function of time.
- Loss coefficients and component data for steam separators and recirculation pumps.

- Volumes and other dimensions for upper plenum, downcomer and lower plenum.
- Feed water (ECCS) mass flow rate to downcomer as a function of time for recriticality transient.
- Feed water temperature as a function of time.

The output comprises an explicit output file, a binary plot file and a number of additional files with special information. The plot file can be processed by the CMS-View graphics programme to produce plots of various output parameters. These are scalars, "global" parameters like total core power, core flow, average values of reactivity, burnup, pressures, temperatures, void etc. in the core. In addition, three-dimensional, nodal average values can be displayed for a number of parameters for which e.g. core maps can be produced. The scalars chosen are set by default, but the three-dimensional variables can be selected by specification in the input. In the modification of S-3K made for the SARA some output scalars were added for the peripheral system and a special "SARA" edit group was included for:

1. Core inlet flow
2. Core outlet flow
3. Core exit quality
4. Core mass inventory
5. Downcomer mass inventory
6. Downcomer level
7. System pressure
8. System saturation temperature
9. Core pressure drop
10. Core loss coefficient
11. Feedwater flow
12. Feedwater temperature
13. Steam flow
14. Recirculation flow
15. Steam enthalpy
16. Recirculation enthalpy
17. Feedwater enthalpy
18. Downcomer enthalpy

4.2 APROS Code (Task 2)

APROS (Advanced PROcess Simulator) is a multifunctional simulation computer tool for the dynamic simulation of nuclear and conventional power plant processes and for the simulation of industrial process dynamics (Silvennoinen et al., 1989, Puska et al., 1995a). It has been developed by Technical Research Centre of Finland (VTT) and IVO Power Engineering Ltd (IVO PE) (from 1.1.1999 Fortum Engineering Ltd.). APROS simulation environment consists of an executive system, model packages, equation solvers, a real-time database and interface models.

Nuclear applications of APROS include at present engineering simulators or plant analysers, training simulators, plant safety analysis and severe accident research.

4.2.1 Code structure

APROS software consists of physical models that are grouped into general and application specific packages. The packages required for nuclear applications are the nuclear reactors, thermal-hydraulics, automation and electrical systems.

The essential models in the recriticality calculations performed within the SARA-project have been the core three-dimensional neutronics model and the five- and six-equation thermal-hydraulic models.

APROS code has one-dimensional and three-dimensional core neutronics models (Puska et al., 1995b). Both models have two energy groups and six delayed neutron groups. The finite-difference type three-dimensional neutronics model is able to describe both hexagonal and quadrilateral fuel assembly geometry. Reactivity feedback effects due to fuel temperature, coolant density and temperature, coolant void fraction, coolant boron content and control and scram rods are taken into account in the models.

The one- and three-dimensional core neutronics models can be connected with the homogeneous, the five-equation or the six-equation thermal-hydraulic model of APROS. The five-equation model is based on the conservation equations of mass and energy for liquid and gas phases and momentum equation for mixture of gas and liquid. In the five-equation model the gas and liquid interface friction is not calculated, but the differential phase velocities are obtained through the drift flux correlations.

The six-equation model describes the behaviour of one-dimensional two-phase flow. The model is based on the conservation equations of mass, momentum and energy for the gas and liquid phases separately. The equations are coupled with empirical correlations describing various two-phase phenomena. The pressures and velocities, volume fractions and enthalpies of each phase are solved from the discretized equations using an iterative procedure. A moving mesh model for axial heat conduction can be used, if the heat flows have to be calculated with great accuracy. At present, axial heat conduction in the fuel rod can also be taken into account.

The thermal-hydraulic part of APROS contains also calculation of fuel enthalpy and oxide layer thickness on cladding surface and power production by cladding oxidation according to Baker-Just model, as required for the hot channel calculations.

In APROS the thermal-hydraulic model convergence is required to be reached first during each time step. Calculation of fuel temperatures, coolant densities and temperatures, void fractions and boric acid concentrations is performed in the thermal-hydraulic part. This information is transferred to the neutronics model for use in the calculation of feedback corrections of nodal cross sections. The feedback correction calculation requires also information on the positions of control rods in core which is obtained from the automation models of APROS. Then the fast and thermal flux values and the six delayed neutron precursor group concentrations are calculated. The calculation is repeated until the flux values converge or maximum number of iteration rounds is reached. Based on the fast and thermal neutron flux values calculated for each neutronics node in the core and the decay heat model, the power produced in each node is calculated. The power produced is then converted into relative power of each heat structure and transferred back to the heat structures of the reactor channels that are a part of the thermal-hydraulic model. It is possible to direct part of the power produced directly to the thermal-hydraulic node representing the coolant.

There is also an automatic time step control in APROS. If convergence is not reached with the user-specified or default convergence criteria in thermal-hydraulic part with the allowable number of iterations, the time step size is halved and a new calculation starting from the values of the previous time step is initiated. The process is continued until convergence is reached or until the minimum allowable time step size is reached. In the same manner, after a few steps with the shortened time step size, the model starts to increase the step by doubling until the maximum time step length is reached.

The time step control in APROS was initially mastered solely on the basis of the convergence of the thermal-hydraulic model. However, in nuclear applications there are also several situations, like reactivity peaks, that require shortened time step due to the power increase even though the thermal-hydraulic model would not indicate a need for time step reduction. If the relative fast flux change per time step is greater than allowed, the simulation time step will be reduced in the same manner as with the thermal-hydraulic model.

4.2.2 Code development

The analyses of the SARA-project recriticality cases were started with APROS code version 4.05 and the last calculations were performed with code version 4.08. As an extension to the original project plan, part of the calculations were performed using the six-equation thermal-hydraulic model in the reactor core channels. The particular needs of the SARA-project required some model development, especially of cladding oxidation, and the further development of the materials properties description in APROS.

The model development for the RECRIT code in Task 3 could not be utilised in APROS in the manner assumed at the beginning of the project.

4.2.3 Input and output

The communication interfaces of APROS cover both the design interface that is used in process creation, modification and simulation and the presentation interface for the presentation of simulation results. For the design interface there are at present two alternatives, the old UNIX-based configuration tool GRINAP and a new Pentium/NT-based configuration tool GRADES.

In APROS the user operates the graphical user interface using components at the process component level. These correspond typically to components that can be found in power plants, like pumps or pipes. The data required is similar to that found in the data sheets of the real plant components. The user can specify the connections of the process component into other process components, too. On the basis of the information given at the process component level, the system then creates the calculational level of nodes and branches. During the simulation the user can change the process component data or change the connections of the process component to other process components without the need of recompilation of the code.

In the three-dimensional core model the process components are the fuel assemblies, the control assemblies, the reflector assemblies and the one-dimensional thermal-hydraulic flow channels. For each fuel assembly the user must specify a name, a x-y position in the core model, division of assembly in axial sections, as well as burn-up, enrichment, and for BWR also void and control rod history in each axial section. Similar information, plus indication of control rod position, is given for each control assembly. Additionally, for each fuel assembly and control assembly the name of the thermal-hydraulic channel where it belongs must be specified. For each thermal-hydraulic channel a name must be specified along with the type of thermal-hydraulic model (five- or six-equation model), fuel rod geometry data, number of fuel rods, flow area of channel, hydraulic diameter, nominal power and division of the channel in the axial direction, etc.

In addition, the three-dimensional model requires some general information like indication of reactor type (BWR, PWR or VVER) and assembly geometry (hexagonal or quadratic) plus cross section data file. This data is typically created by codes like CASMO or CASMO-HEX.

For the presentation of process displays and simulation results there are various tools in UNIX and NT environments. The calculation results can be stored into files and plotted with various plotting routines. The GNUPLOT program is used for the presentation of APROS three-dimensional core model simulation results either on screen during the simulation or as plotted pictures from specified time points during simulation.

4.3 RECRIT Code (Task 3)

The development of the RECRIT code was initiated during the Nordic cooperative project NKS RAK-2 (Höjerup et al., 1997a) and has been continued in the SARA project. RECRIT is a stand-alone code capable of simulating a loss-of-coolant accident, with melting and relocation of control rods and subsequent recriticality upon start of ECCS pumps. During the whole development of the RECRIT code the overall objective was to create a fast running computer code using simple but adequate and robust methods. The neutronic part of the code was developed at Risö National Laboratory in Danmark and the thermal-hydraulic part was developed at VTT in Finland.

4.3.1 Code structure

The neutron flux distributions, reactivities, etc. are calculated by the subroutine TWODIM, which is a two-dimensional, standard diffusion theory, multi-group, difference approximation code (Lindström, 1970). The RECRIT core is described by a two-dimensional, cylindrically symmetric geometry model. The number of radial and axial nodes, as well as the number of energy groups, are specified by input data. Typically 10 radial by 25 axial nodes are used. In calculations two energy groups have been used.

Tables of group diffusion cross sections are given for a range of fuel types, fuel histories, burnups, fuel and water temperatures, coolant void fractions, and control rod status (rodded/unrodded). Such data may be provided by any suitable lattice code,

e.g. CASMO. The RECRIT code will then calculate the actual data by linear interpolations in these 7-dimensional tables.

The RECRIT code follows the accident in time steps, the lengths of which depend on the instantaneous reactivity. When the reactor is subcritical, the time steps may be long (~ 10-1 seconds), when the reactor is approaching criticality, the time steps get gradually shorter (~1-0.1 seconds), and when the reactor becomes supercritical, the timesteps must be even shorter (~ 0.1-0.001 seconds). If super-prompt criticality occurs, it requires timesteps in the 0.0001 seconds range.

The calculational procedure consists of a data flow between the thermal-hydraulic subroutine, THYDTR, and the neutronic subrotine NFLUX. The former supplies void, temperatures, etc. on the basis of the power-distributions calculated and delivered by the latter.

4.3.2 Code development

Neutronics

The original version of TWODIM was aimed for stationary solutions, but during the project the code was modified to allow the dynamical solutions (Höjerup, 1997b). The original capabilities of TWODIM with respect to multi-group treatment have been preserved in the new kinetic version. The kinetic model can accommodate time steps of varying lengths; long time steps at negative or small positive reactivities, while shorter time steps at super-prompt criticality.

In addition, the following new features have been implemented in the code:

1. The possibility of reading in an initial distribution of reactor power, which defines the decay heat distribution during the accident. Either a detailed (node by node) distribution may be read, or a "standard" distribution, which is a cosine in axial direction and a cosine with an extrapolated radius in radial direction, is generated by the code.
2. A calculation of "effective" void has been implemented. In normal power operation use, it is implicit in the cross section calculation, that void is only present inside the assembly shroud (fuel box), and that the space between the boxes is filled with full density water. In the transients experienced during recriticality, however, the water levels inside and outside the boxes may be quite different. This is taken into account in the "effective void" calculation, which assumes that only the total amount of water counts, not whether it is inside or outside the box. This is considered to be a reasonably good approximation. It requires, however, that the cross section tables are produced under the assumption that the void is the same inside and outside the fuel box.
3. Some effort has been devoted to the improved presentation of the results.

During the late phase of the project, some investigations were made into the rate with which void is being generated due to the slowing down of fast neutrons (Höjerup, 1998a, 1998b). This part of the energy liberated in the fission process is only about 2.5% of the

total energy, but during super-prompt power peaks this energy may be large enough to generate a significant mass of steam. As this takes place in about one micro-second after the fission, it may constitute a void-reactivity feedback almost as "prompt" as the Doppler effect from the heating of the fuel.

At the end of the project, however, it is still unclear, whether the significant mass of steam may develop into a significant volume of steam on this short time scale. If it does not, the reactivity feedback will not be so large. If it does, however, in addition to the (beneficial) effect of void-feedback, there may also be a risk of pressure waves from the expanding steam.

Thermal-Hydraulics

The basic equations for the thermal-hydraulic solution are written for liquid and steam mass conservation, mixture momentum conservation and liquid and steam energy conservation. In the solution procedure the mass conservation equations of liquid and vapour are added together for giving the mixture mass equation.

The phase separation for all flow regimes is solved by the drift flux model:

$$u_g = C_0 u_m + V_{gj} \qquad (1)$$

where V_{gj} is the drift flux velocity, which is a function of pressure, diameter and flow pattern, C_0 is the distribution parameter, describing the effect of the non-uniform distribution of phases over the flow area, u_m is the average mixture velocity, and u_g is the gas phase velocity. The correlation was originally developed for the bubbly flow but has been expanded to other flow regimes such as churn-turbulent flow, droplet dispersed flow and counter-current flow. The resulting correlation includes drift flux velocity and distribution parameter which are also functions of void fraction.

The considered heat transfer regimes are depicted in Figure 4.3. These heat transfer regimes are typically defined for the reflooding phase when the core cooling water is provided through the bottom of the core, as has been investigated in many studies of reactor core cooling after a large break LOCA accident. Below the quench front the wall surface is wetted and the heat transfer includes single phase convection to liquid and boiling heat transfer. As long as the liquid is subcooled, a part of the heat is used for the liquid heatup.

In the post-dryout regime downstream of the quench front the heat transfer surface is not wetted and five heat transfer mechanisms may be distinguished: transition boiling heat transfer, film boiling heat transfer, steam heating by convection, interfacial heat transfer from superheated steam to water droplets and radiation heat transfer to liquid droplets. Above the quench front the liquid exists as droplets due to vigorous steam generation at the quench front.

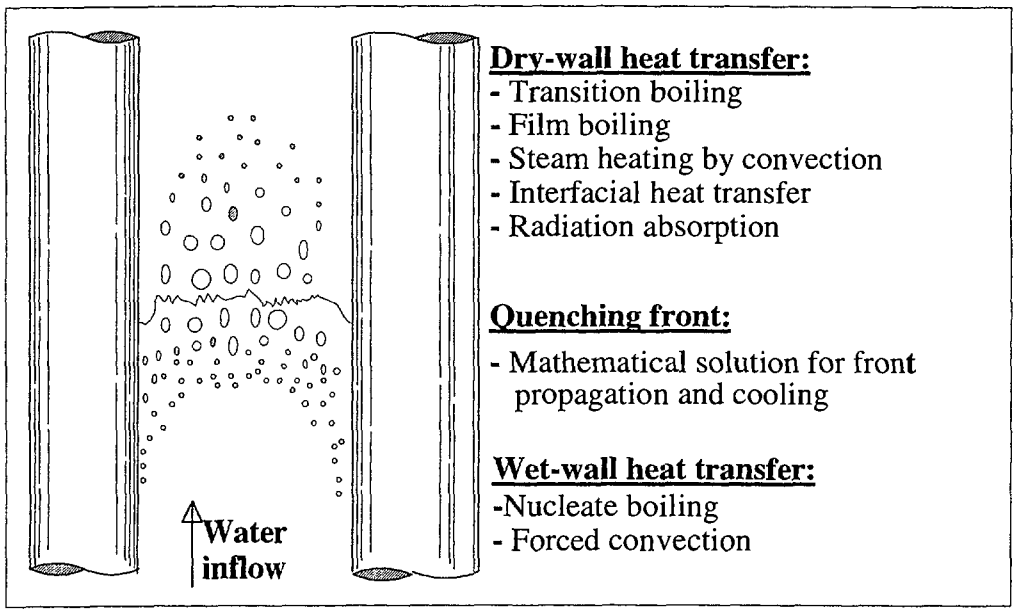

Figure 4.3 Reflooding heat transfer modes considered in RECRIT model.

The post-dryout heat transfer and quench front velocity modelling are the most important processes in reflooding analysis. It has to be pointed out, that no general correlation exists for the post-dryout regime at reflooding. In RECRIT the quench front movement is described by an analytical model and the different heat transfer mechanisms above the quench front are considered simultaneously. However, instead of using the heat flux values as given by the RECRIT heat transfer models, a user tuning parameter is applied to account for the efficiency of each heat transfer mechanism. In the code validation against experiments the combination of different "efficiency" coefficients was searched for the optimal result, as described in section 4.3.2.

Below the quench front the heat transfer is modelled by the modified Chen correlation which includes nucleate boiling and convection heat transfer. The heat transfer coefficient decreases across the quench front by more than two orders of magnitude from that of nucleate boiling to that of film boiling. The quench front propagation is calculated using an analytical model with two basic parameters, the Leidenfrost temperature and the wet-side heat transfer coefficient. The heat transfer on the dry-side is assumed to be zero.

The Leidenfrost temperature may be expressed for the reflooding pressure range as $T_L = T_{sat} + \Delta T_L$, where T_L is the Leidenfrost temperature, T_{sat} is the saturation temperature and ΔT_L is the temperature difference, currently assumed to be constant and equal to 170 K.

As mentioned earlier, five different heat transfer mechanisms are distinguished downstream of the quench front, and efficiency coefficients have been applied to four of these.

The expression corresponding to the film boiling heat flux is defined as:

$$q_{FB} = Ch_{Br}(1-\alpha)(T_w - T_s) \qquad (2)$$

where h_{Br} = 200 W/m^2/K, is the heat transfer coefficient predicted by the Bromley correlation for the inverted annular flow at 2 bar, α is the local void fraction, T_w is the surface temperature, and T_s is the saturation temperature. Since the heat transfer coefficient is a weak function of pressure no pressure dependency is included. The void fraction term accounts for the limited area for water existing in the vicinity of the wall. The coefficient C ranges from 0.08 to 0.20, when the pressure varies from 20 bar to 1 bar.

The expression corresponding to the transition boiling is defined as:

$$q_{TB} = Aq_{CHF}\frac{\Delta T_L(T_w - T_s)}{[\max(T_w - T_s, \Delta T_L)]^2} \qquad (3)$$

where q_{CHF} is the critical heat flux calculated by a correlation based on the Zuber pool boiling model, T_w is the surface temperature, and T_s is the saturation temperature. The coefficient A is used for the relative efficiency of the transition boiling process and is varying between 0.10 to 0.25 when the pressure varies from 20 bar to 1 bar. In principle, the transition boiling model is a heat flux decay function taking into account the reduced wall surface contact area that can be expected in the vicinity of the quench front.

Forced convection from the fuel cladding to the steam and interfacial heat transfer between superheated steam and water droplets are calculated in single phase steam and dispersed liquid regions. Forced convection heat transfer coefficient in the steam region is based on the Dittus-Boelter equation for pure steam.

The interfacial heat transfer between overheated steam and water droplets is calculated by:

$$q_{IF} = DC_{IF}\alpha(1-\alpha)\rho_l(T_g - T_s) \qquad (4)$$

where q_{IF} is the heat flux per unit volume, C_{IF} = 1500 W/kg/K, α is the local void fraction, T_g is the gas temperature, T_s is the saturation temperature, and ρ_l is the liquid density. The above value of the coefficient C_{IF} has been found to be a good estimate for the heat transfer between gas and 1 mm size droplets with a typical relative velocity of about 3 m/s. The coefficient D is a user tuning parameter which ranges from 0.40 to 0.70 when the pressure varies from 20 bar to 1 bar.

The radiation absorption in the liquid is assumed to be proportional to the liquid content:

$$q_{RAD} = B\sigma\varepsilon(1-\alpha)(T_w^4 - T_s^4) \qquad (5)$$

where σ is the Stefan-Boltzman constant, ε is the emissivity of the wall, and α is the local void fraction. B is the user parameter taking into account the transmissivity of the fluid; its values range from 0.15 to 0.20 when the pressure is varying from 20 to 1 bar.

Validation of reflooding modelling

The reflooding model of RECRIT has been validated against several experiments (Miettinen, 1999b). Related to earlier design base accident studies, much data is available from experiments where the initial temperature before reflooding ranges from 600 to 1000 °C. The reflooding experiments in ERSEC-7, FLECHT, GÖTA, ACHILLES and REWET-II facilities were selected for validating the reflooding capabilities under these conditions. In addition, validation against very recent high temperature QUENCH tests at FZKA in Germany is underway. In Table 4.1 the parameter ranges of the used experiments are summarized.

Table 4.1 Reflooding experiments used for validation of RECRIT.

Facility	No. of rods/ Length (m)	T_{max} (°C)	Pressure (bar)	Quench Time (s)	Rise velocity (m/s)
ERSEC -7, France (2 tests)	1 / 3.3	870	1, 3	1300, 750	0.055
ACHILLES, UK (1 test)	69 / 3.6	1050	3	370	Gravity fed
REWET-II, Finland (5 tests)	19 / 2.4	910	1, 3	250-500	0.02 - 0.10
GÖTA, Sweden (16 tests)	64 / 3.6	950	1, 3	600-900	0.008- 0.024
FLECHT, USA (4 tests)	49 / 3.6	790	1, 4, 6.7, 20	50 – 150	0.076
QUENCH, Germany (3 tests)	21 / 1.0	1600	2	200 < 700° C	0.015

The validation results were used for tuning the rewetting and post-dryout heat transfer parameters. The tuning process is discussed in detail in the RECRIT validation report (Miettinen, 1999b). The parameters in Table 4.2 have been selected for reflooding and recriticality calculations.

Table 4.2 Selected heat transfer parameters based on experimental validation.

Parameter	Selected value
Wet side heat transfer coefficient [$W/m^2/K$]	$2.0*10^5$
ΔT_L [K]	170.0
C in Equation 2 for film boiling	0.14
A in Equation 3 for transition boiling	0.18
D in Equation 4 for interphasial heat transfer	0.55
B in Equation 5 for radiation	0.17

In Figure 4.4 and 4.5 the validation results for one of the GÖTA tests, at 1 bar, are shown. The GÖTA tests were designed for studies of the emergency core cooling behavior of a ASEA-ATOM BWR fuel rod bundle.

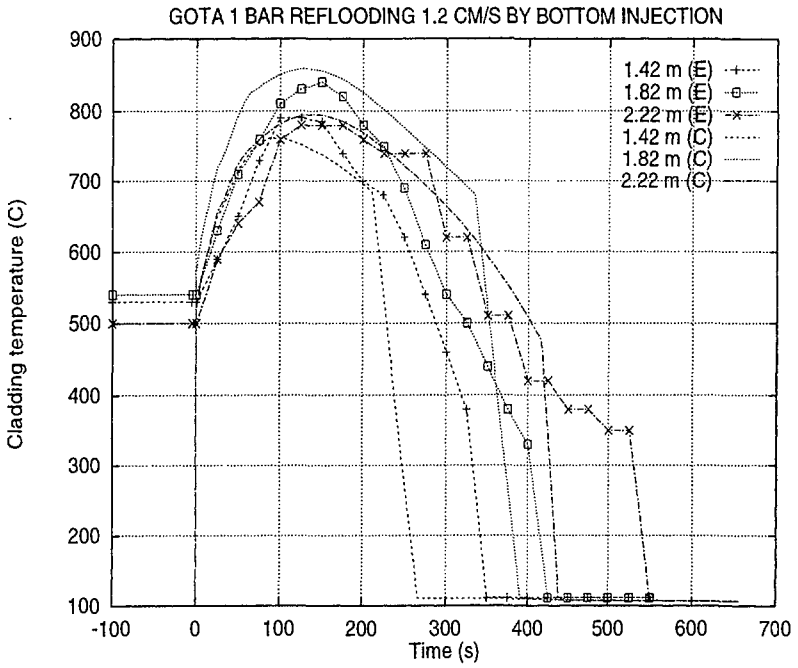

Figure 4.4. RECRIT validation against GÖTA emergency cooling test with bottom reflooding. Cladding temperature as a function of time.

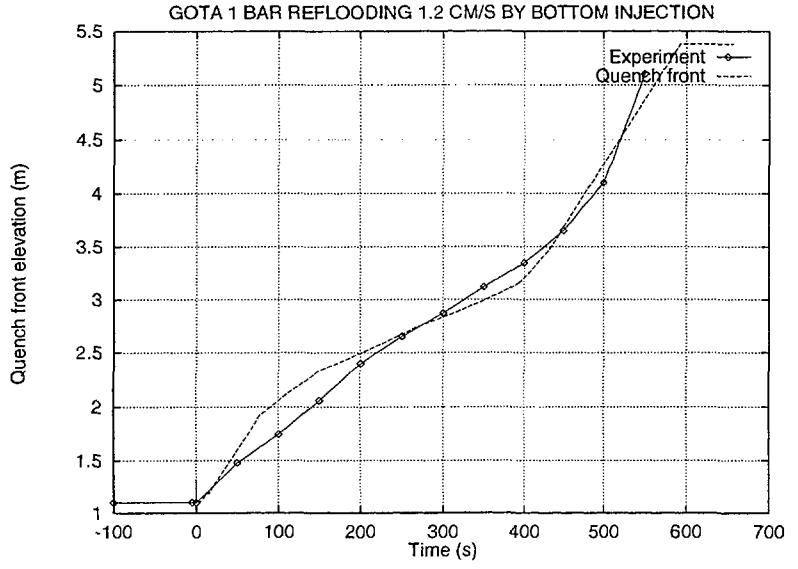

Figure 4.5 RECRIT validation against GÖTA emergency cooling test with bottom reflooding. Quench front elevation as a function of time.

4.3.3 Input and output

The input for the RECRIT code is kept at a minimum by using default values wherever practical. Even so, the necessary amount of data to define the primary system and the boundary conditions are quite extensive (Miettinen and Höjerup, 1999c).

5. RECRITICALITY ANALYSES: INDIVIDUAL STUDIES AND COMMON CASE COMPARISON

Individual recriticality calculations were carried out with S-3K for O-3, and with APROS and RECRIT for OL-1. The goal was to use realistic reactor operating data, as far as possible. In addition, three common cases were chosen for the OL-1 reactor to be calculated with all three codes using simplified assumptions and boundary conditions. The aim was here to provide information on various modelling effects and uncertainties in the analyses by comparing the results from the codes.

5.1 S-3K Calculations for Oskarshamn 3 (Task 1)

5.1.1 Initial conditions and assumptions

All calculations presented here were carried out with the latest S-3K code version in which the so-called "peripheral systems" were activated (Nilsson, 1999).

In order to simulate realistic conditions in the transient S-3K calculations, operating data for Oskarshamn 3 were taken from SIMULATE-3 steady-state core-follow calculation results provided by the utility. The middle of cycle 3 was chosen where the cycle burn-up was 3.59 MWd/kgU (for new fuel), and the average burn-up 16.1 MWd/kgU for all assemblies. At this point the reactivity was quite high since much of the burnable poison was gone. The power was 3020 MW_{th}, i.e. 100 %, with the recirculation flow reduced to 79 % of its nominal value. Because minor modifications were made for the S-3K model, among others replacing eight SVEA-100 assemblies by the same number of type 7 SVEA-64 assemblies, new steady-state SIMULATE-3 runs were performed.

The plant boundary conditions were the same as in the preparatory SCDAP/ RELAP5 reflooding calculations, but due to modelling differences the initial conditions before reflooding, after the heat-up phase, differ. Among other things, the core model is more detailed in S-3K with each fuel assembly described as a separate flow channel and the fuel modelled down to pin level, while in SCDAP/RELAP5 the assemblies were grouped into five parallel radial rings. In S-3K 25 axial nodes were used but only 10 nodes were used in SCDAP/RELAP5. On the other hand S-3K did not take into account oxidation heat generation, only decay power after scram.

The following initial conditions prior to recriticality were assumed:

- Restart from SIMULATE-3 steady-state at 100 % power and 79% RC flow.
- Station blackout at 3 seconds simulated by insertion of all control rods starting at 1 second and fully inserted at 3 seconds.
- Simulation of RCP pump stop by reduction of core inlet flow to 3 % from 1 to 3 seconds, then to 1% during 1430 to 1750 seconds and to 0 after 1777 seconds. Retaining a small flow before pressure reduction at 1777 seconds (see below) gave better agreement with SCDAP/RELAP5 results for the initial boil-off with core uncovery and heat-up of the fuel.

- Simulation of depressurization (ADS) was done by reduction of the pressure to 0.5 MPa during 1430 to 1777 seconds, and then keeping the pressure constant in accordance with the SCDAP/RELAP5 calculations.
- Control rod melt-down in inner positions was simulated by withdrawal of the rods in groups 1 to 3 from 100 to 10 % inserted during 2000 to 2800 seconds. (Corresponding to 36 outer control rods remaining fully inserted and the rest 133 rods inserted only up to 0.37 m from bottom of the core).
- Start of feed water injection into the downcomer, gradually increasing the flow to full value from 2908 to 2912 seconds. Various constant flow rates were then chosen for different cases.

5.1.2 Specification of calculated cases

First, a number of scoping calculations were made, among other things to investigate the sensitivity for some input variables in the new S-3K code version. It was seen that setting the pressure loss coefficients to zero in the pump connection between downcomer and core inlet caused rather large flow oscillations due to flow-power feedback after recriticality. The only flow restrictions were then the core inlet orifices. Since no measured values of the loss coefficients for the internal RCPs were available, best estimate, guessed values were applied in order to obtain a reasonable damping of the flow oscillations. A parameter study was then carried out in order to investigate the sensitivity for variations in the loss coefficients.

A base case (Case No. 1) was then calculated with the following conditions:

- ECCS water mass flow rate to downcomer = 500 kg/s
- Initial core maximum temperature = 2093 K
- Initial water level = 0.0 m (core inlet level)
- System pressure = 0.5 MPa, constant
- Control rod status: 133 innermost rods withdrawn to 90% in group Nos. 1-3, outer 36 fully inserted, according to SCDAP/RELAP5 predictions.
- Temperature of ECCS water at injection point = 293 K
- Flow restriction in RCP loop: D=0.2 m, L=1.0 m, ξ =10.0 (Loss coefficient in pump, velocity heads). No. of RCPs = 8 (See Figure 4.3)
- Hydraulic time step at recriticality point = 0.01 s

The parameter study was then carried out with variations from the base case No.1, as shown in Table 5.1.

Table 5.1 Case matrix for S-3K calculations

Case No	Parameter	Value (Variation from base case)
2	ECCS flow rate to DC	90 kg/s
3	"	200 "
4	"	1000 "
5	"	1500 "
6	"	2000 "
7	Control rod melt down	Less melt down, 70, 60 & 50% in group 1, 2 & 3
8	Initial max. core temperature	Lower (1800 K)
9	ECCS water temperature	Increased to 353 K
10	System pressure	From SCDAP/RELAP5, ramp to 1.75 MPa
11	Recirculation loop pressure loss	Reduced, D=0.6, L=0.0 m, ξ =10.0
12	"	Increased, D=0.1, L=1.0 m, ξ =10.0
13	Calculation time step	Reduced to 0.001 s

5.1.3 Results of S-3K analysis

Prompt recriticality was predicted in all cases when the water level at reflooding had increased into a certain height in the control rod free part of the core. The amplitude of the peak increased with feed water flow rate, but the duration of the first recriticality became short, a few tenths of a second, due to Doppler feedback. Increased void formation kept the power at a low level until the continued increase in water level gave rise to new power peaks, however, with lower amplitudes than the first one. The power continued to increase as long as the effective reactivity was slightly above unity. It is reasonable to assume that, at the end, the core power balanced the ECCS water flow, since the water level in the core seemed to reach an asymptotic upper value. The calculations were stopped when the down-comer was completely filled. The core inlet flow had then reached its maximum value and after that the calculations arrived into unstable conditions with unrealistic code response.

The recriticality was very local to its nature and the fission power was developed in few nodes in the core centre and in the lowermost part, which became reflooded. This is illustrated in Figure 5.1 which shows the nodal power factors for a longitudinal section of the core at the first recriticality peak in the base case. The power distribution was, on the whole, rotational symmetric in the cross section plane.

The maximum power factors were obtained at axial level 5, i. e. about 0.7 m above core inlet. The distribution of nodal power factors in axial plane 5 is depicted in Figure 5.2.

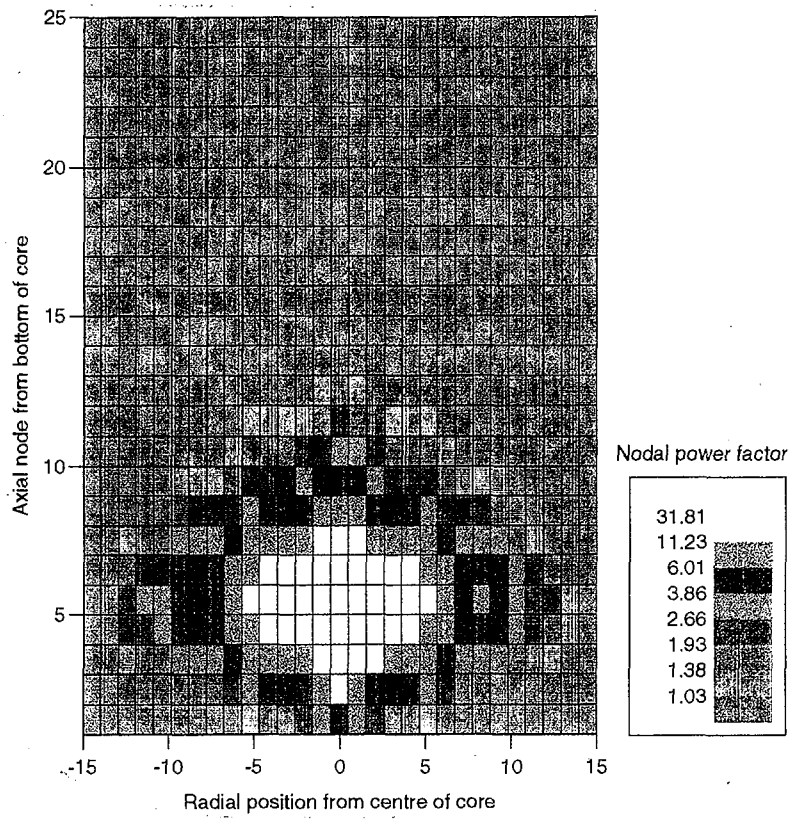

Figure 5.1 Nodal power factors at first recriticality in Case 1 (Base case) in axial plane through core centre.

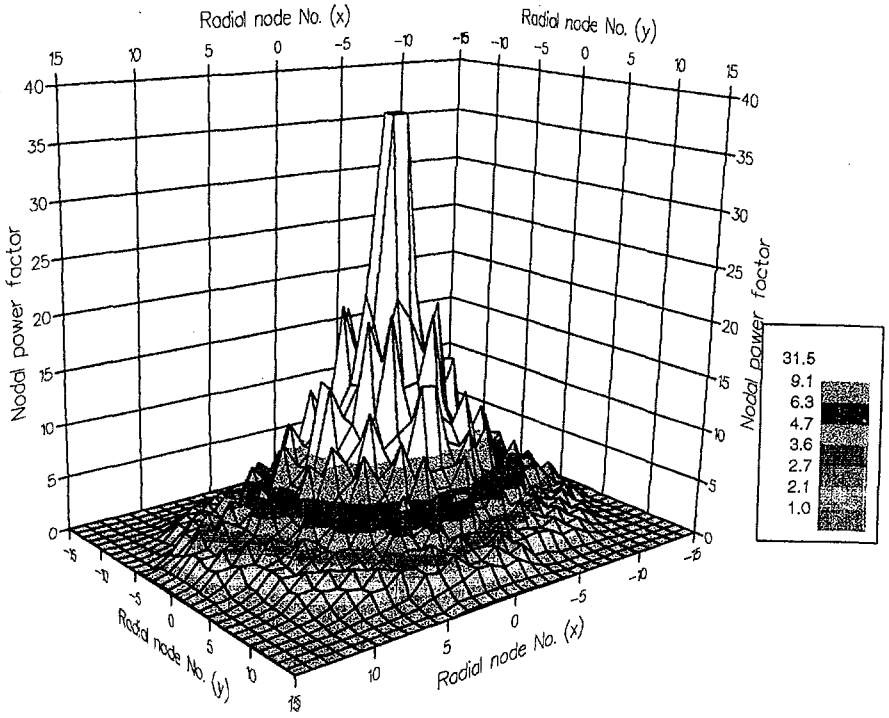

Figure 5.2 Nodal power factors at first recriticality in Case 1 in cross sectional plane at axial level 5.

The effect of injection mass flow rate on peak power is illustrated in Figure 5.3.

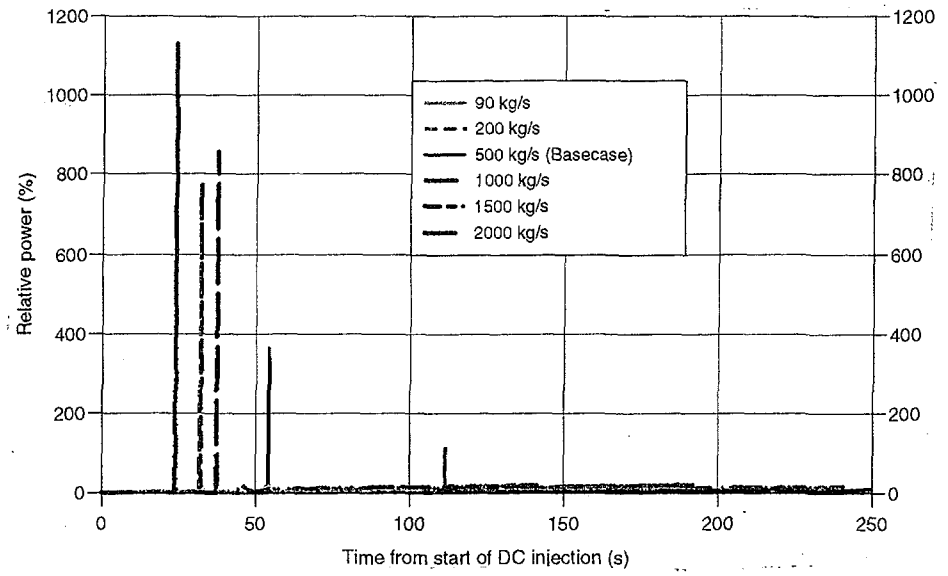

Figure 5.3 Total core power versus time after start of ECCS flow for various injection flow rates to downcomer. Cases 1 to 6.

The total power reached more than 11 times nominal power with 2000 kg/s. The peak arrived earlier with increasing flow rate due to the shorter time needed to reach the critical water level. The shape of the prompt recriticality peak is shown in Figure 5.4. In order to improve the resolution around the peak, short time steps had to be used. Missing data points explains why the peak in the plot is lower in Case 5, with 1500 kg/s, than in Case 4, with 1000 kg/s. The reduced maximum hydraulic time step used in Case 13, 0.001 s instead of 0.01 s as in the other cases, had the effect of giving a narrower but higher power peak as shown in Figure 5.4.

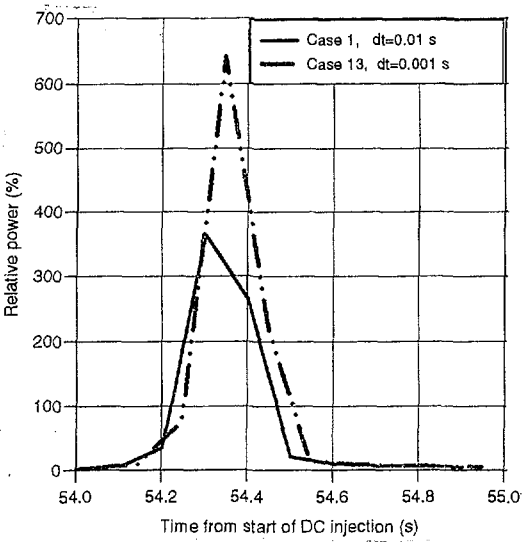

Figure 5.4 Shape of first power peak in case 1 and 13.

The power in the long-term after the first recriticality peaks increased slowly, and as mentioned above it seemed to approach some asymptotic value. Also here the power level became higher with higher reflooding flow rate and reached 15% of nominal power for the 2000 kg/s case. All power values corresponds to total power, i.e. includes power from decay of fission products. The decay power, which before recriticality amounts to about 1.3% of nominal power, is slightly increased to about 1.7% as new short- lived isotopes are created at restarted fission. Figure 5.5 shows the long-term power.

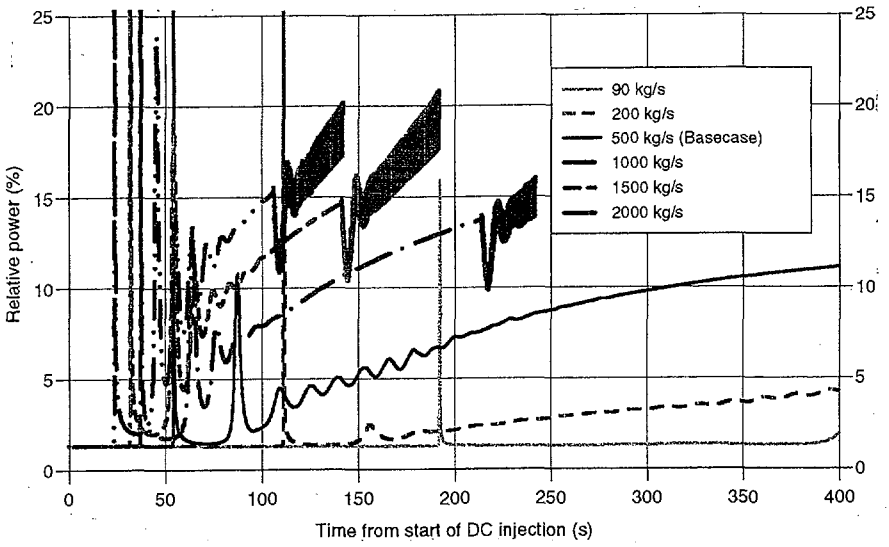

Figure 5.5 Total reactor power in the long-term after first prompt recriticality for different ECCS flow rates. Cases 1 to 6.

The relation between some crucial parameters are shown in Fig. 5.6 for the 500 kg/s base case.

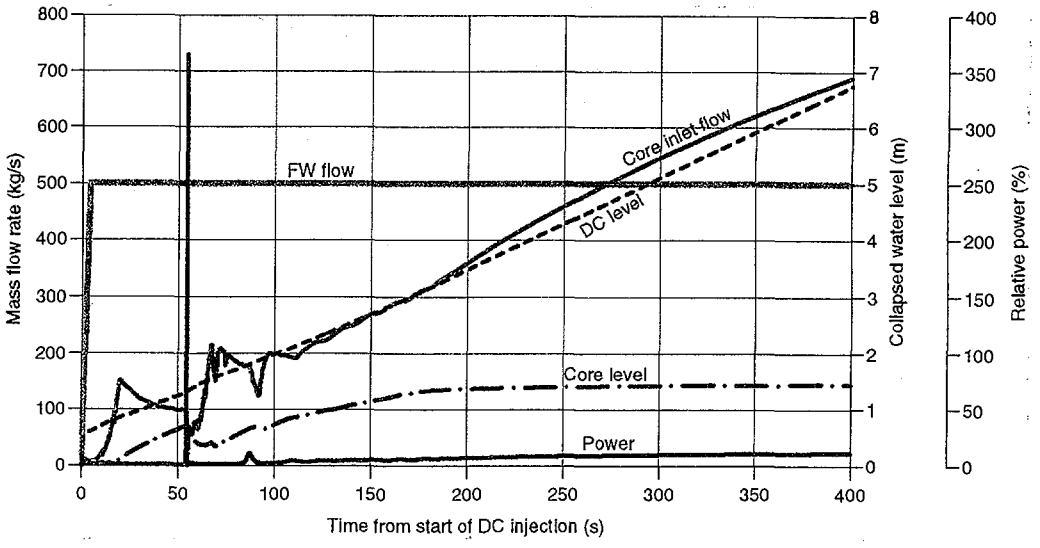

Figure 5.6 Flow rates, water levels and core power as functions of time in the base case.

After start of water injection into the downcomer, the inlet flow starts from zero with some delay needed to fill the downcomer to a certain level and create a driving pressure head. Since the injection flow rate is constant, the downcomer level increases and so the inlet flow rate. At a certain water level in the core critical conditions are reached which leads to the first prompt recriticality. The added power increases boiling and thus the two-phase flow pressure drop in the core which counteracts the core inlet flow. This kinetic - hydraulic coupling leads to flow - power oscillations the amplitude of which is a function of the downcomer injection flow rate and the hydraulic damping.

The effect of hydraulic damping in the recirculation loop was studied by varying the pump loss coefficients in Cases 11 and 12. These and the core inlet orifices determine the hydraulic damping in the recirculation loop consisting of downcomer, pumps, lower plenum, core and steam separators. Low values of the loss coefficients resulted in significant oscillations in the inlet mass flow rate. The initial prompt power peak increases also with reduced damping. After the first peak the inlet flow and the power oscillates in phase with a frequency of about 0.2 Hz. The amplitudes, as well as the mean value of the power, increase with decreased loss coefficients as shown in Figure 5.7.

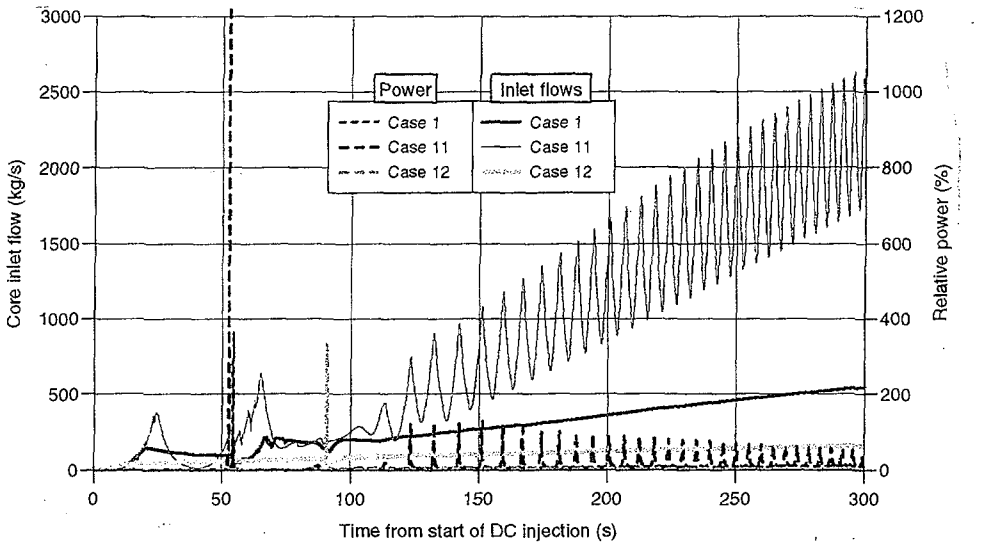

Figure 5.7 Effect of hydraulic damping in the recirculation loop. Cases 1, 11 & 12.

The exact values of the pump loss coefficients are uncertain, but the values used in the base case are judged to be reasonable and give flow oscillations closer to the SCDAP/RELAP5 results. The low values used in Case 11 and the high values in Case 12 are probably outside the real range.

The amount of control rods left in the core (control rod melting) at start of reflooding was naturally a crucial factor for the timing of the first recriticality and for the magnitude of the core power afterwards. With a smaller control rod free fraction of the core and more absorber material up to a higher axial level, the recriticality was delayed and the peak power decreased as shown in Figure 5.8.

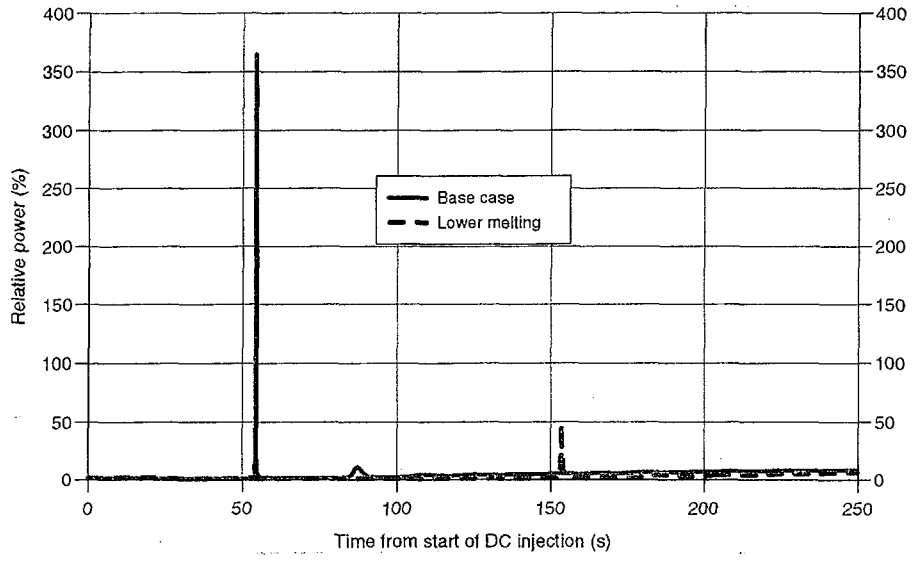

Figure 5.8 Effect of control rod melt down before reflooding. Cases 1 and 7.

The initial maximum core temperature had only a minor effect on recriticality power. Decrease of maximum initial core temperature before reflooding from 2093 K to 1800 K increased the power by about 3 per cent.

The effect of ECCS water temperature was studied in Case 9, in which it was raised to 80 °C from being 20 °C in all other cases. The reference value 20 °C is low and might be valid only initially before the containment pool, from where the low pressure ECCS water is taken, is heated by steam blowdown. However, the increase from 20 to 80 °C had a minor effect on recriticality power and the power decreased only by 3 per cent.

All cases were run at constant **steam dome pressure**, 0.5 MPa, except in Case 10 where a pressure transient was applied, taken from SCDAP/RELAP5 results for a reflooding case with 500 kg/s. The pressure increase was caused by intensified vaporisation during rewetting, and by hydrogen production due metal-water reaction, primarily oxidation of Zirconium. A simplified pressure curve was given as input to S-3K as shown in Figure 5.9.

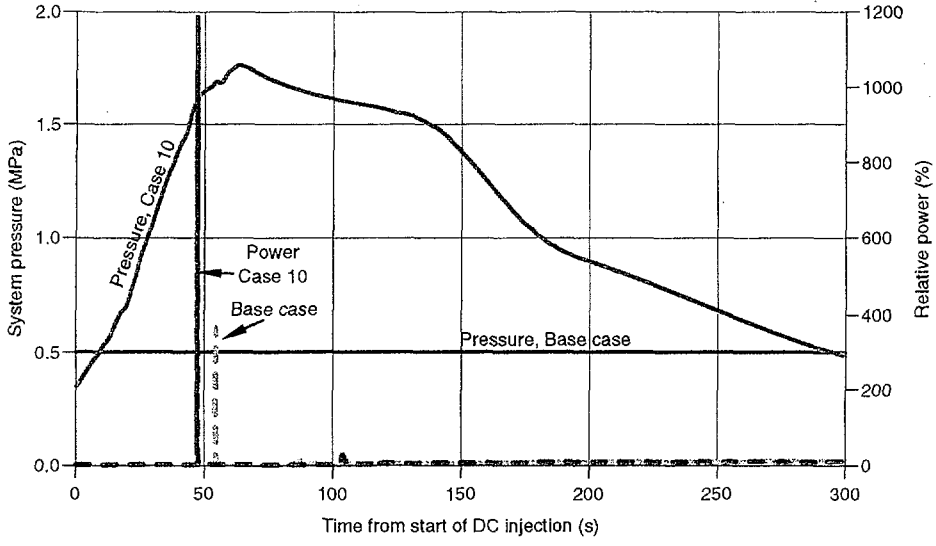

Figure 5.9 System pressure transient applied in Case 10 and its effect on recriticality power.

The increase in pressure during the first part of the reflooding phase lead to a substantial increase in recriticality power compared to the base case. The additional power increase was caused by reduced void fraction at increasing pressure (void collapse). The recriticality power will increase the pressure further, but since the energy in the first power peak is rather small this positive feedback will probably be minor.

A reduction of the thermal-hydraulic **calculation time** step around the time of the first recriticality peak gave improved resolution. The peak value became higher but the width, or duration, of the peak shorter, i.e. the total energy remained about the same. The effect of time-step is illustrated in Figure 5.4.

Calculations of **temperature development and heat-up during reflooding** showed that S-3K predicted rewetting and recooling by the reflooding water in all cases. Only for the larger feedwater flowrates, above 500 kg/s, did the recriticality peak contribute to increase the maximum fuel temperature, as shown in Figure 5.10. However, in the nodes with the highest nodal power factor, which did not have to coincide with the location of the maximum core temperature, the heat-up could be more noticeable.

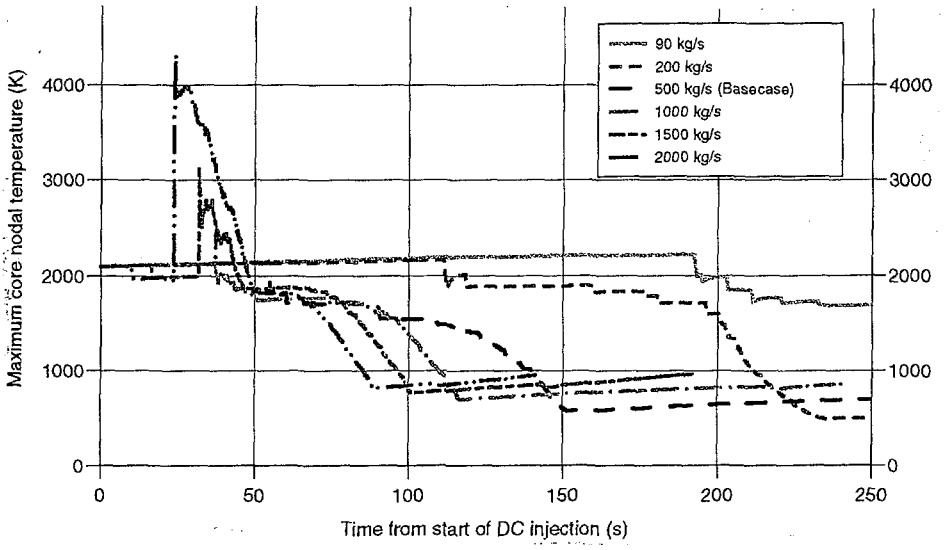

Figure 5.10. Maximum nodal fuel temperatures for various feed water flow rates.

The energy deposited in the fuel during the super prompt recriticality peak was evaluated since it might be so large that it can threaten the integrity of the fuel. Since prompt recriticality was developed very locally in the core the power factor in some nodes there could be very high, as illustrated in Figure 5.1 and Figure 5.2.

Calculation of maximum energy deposition was made based on the maximum nodal power factor, a rough integration of the plotted power curve and the mass of the UO_2 in the core. These values are presented in Table 5.2 together with some other crucial results from the S-3K calculations for O-3.

Table 5.2 Summary of main results of S-3K calculations for O-3

Case no:	1	2	3	4	5	6	7	8	9	10	11	12	13
Time* at first power peak (s)	54.3	192	111	37,3	32,0	23.9	153	82,1	53,0	47,2	52.6	90.6	54.3
Peak amplitude, relative (Times nominal power)	3.65	0.16	1.11	8.56	7.78	11,3	0.47	5.35	3.26	11.8	12.7	3.30	6.42
Max. nodal power factor (-)	37.2	41.8	42.1	36.5	36,2	36.9	30.9	38.5	37.5	23.4	39.2	39.1	37.6
Duration of 1:st peak (s)	0.45	1.13	0.49	0.38	0.38	0.31	1.45	0.35	0.46	0.39	0.36	0.42	0.35
Energy deposition in fuel during first peak (cal/g)	134	14	59	237	354	418	44	176	126	222	397	130	192
Energy deposition during 100 ms of the peak (cal/g)	36	2	17	104	110	136	5	59	37	80	140	38	69
Maximum fuel temperature (K)	2147	2212	2167	2438	3148	4328	2138	2432	2145	2065	4430	2181	2698
Power at end of simulation, % of nominal	11.4	4.6	7.5	13.8	14.6	15.5	11.4	11.,8	7.6	11.4	17.4	10.0	11.4
Time at end of simulation (s) **	423	2592	1079	214	141	106	499	450	399	453	550	466	432

*)The time is counted from start of injection to downcomer **)Time to fill the downcomer completely

The energy deposition in the fuel where the largest power density occurred during the recriticality peak became considerable at the higher reflooding rates. Since the power is developed within a short time, fuel damage could occur. If a large energy is generated in the fuel pellet in a short time so that the heat losses through the gap and cladding to the coolant are small, most of the energy goes to heat-up of the fuel which then can be fragmented. Much research has been carried out to determine the upper limit of energy deposition (cal/gUO_2) which the fuel can withstand before fragmentation takes place. The figures vary, and are among other things depending on fuel composition and burnup. Normally, the regulatory limit for BWR fuel is in the range 200-280 cal/gUO_2 (OECD, 1996, MacDonald, 1980), but lower values, down to about 70 cal/gUO_2, have been measured for high burnup fuel (Fuketa, 1995). The excess energy deposition is reflected in the calculated maximum fuel temperature, which exceeded the fuel melting temperature in three cases (Case 5, 6 and 11).

All cases above were calculated for middle of fuel cycle 3 where the average cycle burnup was 3.59 MWd/kgU. The average burnup for the whole core, including fuel retained from the two previous cycles, was then 16.1 MWd/kgU. In order to see the effect of cycle burnup, Case 1 was also calculated with restart from a low burnup of 0.4 MWd/kgU, i.e. at beginning of cycle. The results indicate only minor difference in peak recriticality power. The only noticeable effect was that the first power peak arrived somewhat earlier with lower burnup. No run was made for higher burnup at the end of cycle, but it is assumed that this would result in smaller recriticality power, since the fuel then has less excess reactivity.

5.2 APROS Calculations for OL-1 (Task 2)

The recriticality calculations were performed using three-dimensional neutronics and both the 5-equation and 6-equation thermal-hydraulic model with user defined boundary conditions for core inlet and outlet (Puska, 1998a). Four different reflooding rates were used: 45 kg/s, 540 kg/s, 1350 kg/s and 1900 kg/s. The initial conditions for these calculations were selected on the basis of the MELCOR results. The main objective of APROS calculations presented in this section was to determine the magnitude of prompt power peaks. Therefore, the calculated transients were intentionally short. For the highest reflooding rates the calculation were stopped even earlier due to numerical problems.

5.2.1 Initial conditions and assumptions

The calculations were started from a normal full power steady-state operation. Core decay heat according to the ANSI standard was assumed. First a reactor scram was produced. Then the core coolant flow was gradually stopped, and the core was allowed to heat up as a consequence of the continuous decay heat buildup until the maximum nodal average fuel temperature of 1670 °C was reached. This was the temperature when the control rods started to melt. The melting of the control rods was then described with sudden withdrawal of part of the central control rods to form approximately an U-shaped control rod pattern, in accord with MELCOR predictions. The assumed melted control rod configuration is shown in Figure 5.11. Thereafter, the reflooding was started. The reflood rates were those used in the MELCOR calculations, i.e. 45, 540, 1350 and 1900 kg/s. In all cases the reflooding rate was assumed to remain at the constant level throughout the calculation. Since the calculations were performed with the core model only, the core inlet flow was also constant and equal to assumed reflooding rates. In addition, the temperature of the core inlet water remained constant throughout the calculations. The system pressure was 6.5 MPa, i.e. close to normal operating pressure, in all calculations.

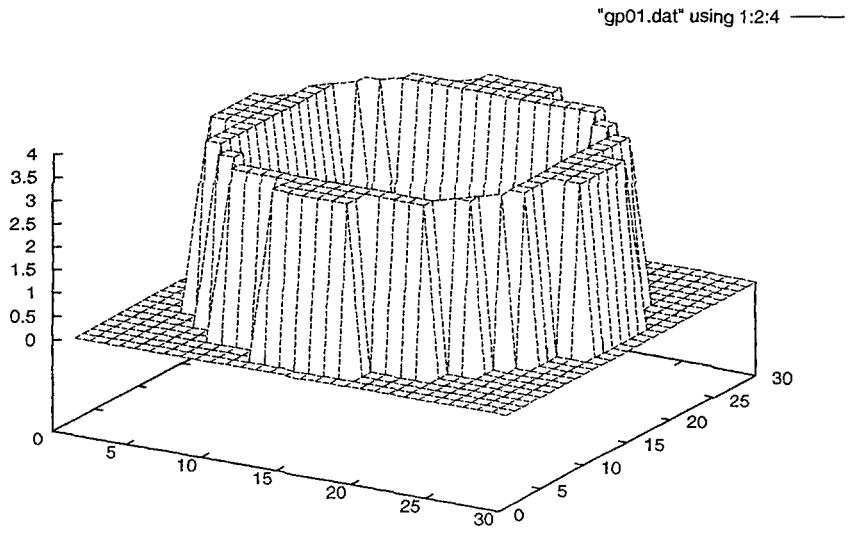

Figure 5.11 *Assumed control rod pattern after the melting of control rods in APROS calculations.*

5.2.2 Results of APROS analysis

The core total power, average fuel temperature, average coolant density, average coolant temperature, average coolant void fraction, maximum nodal power peaking factor and maximum nodal fuel temperature were calculated with the APROS code using the three-dimensional neutronics with the five-equation thermal hydraulic model.

The core total power and average fuel temperature for reflooding rate of 45 kg/s are shown in Figures 5.12 and 5.13. As can be seen, a small and narrow recriticality power peak is reached after some 200 seconds of reflooding. The maximum recriticality power predicted is 45 % of nominal power, and the power level is then stabilised at 8 % of nominal power with the continued reflooding.

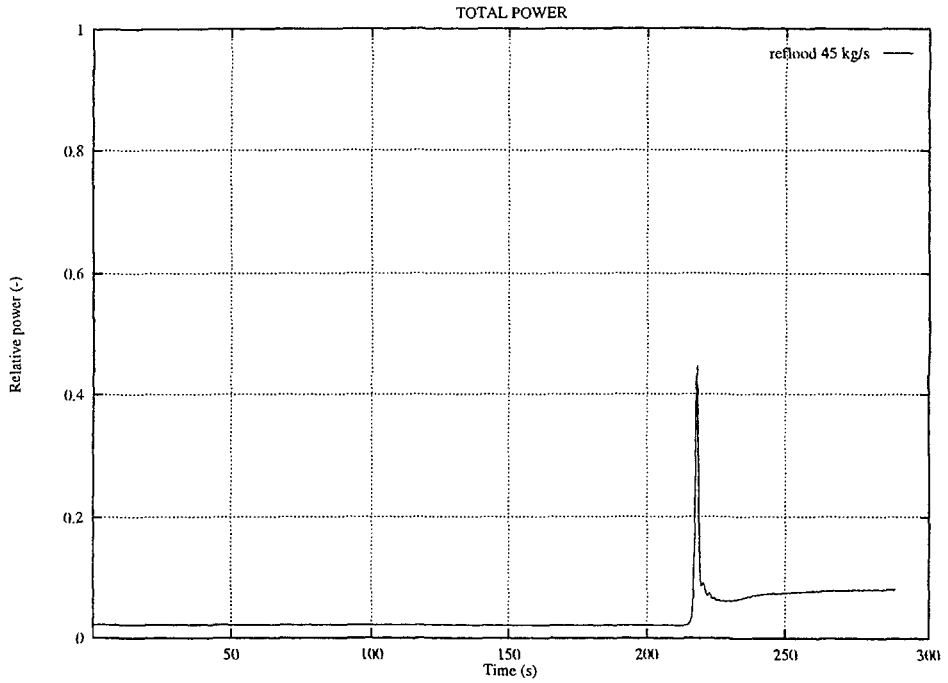

Figure 5.12 Total power with reflooding rate 45 kg/s.

Due to reflooding the core coolant temperature decreases. The average core coolant density increases and void fraction decreases. The decrease of core coolant temperature leads to decrease of average fuel temperature. The recriticality peak has only a very minor effect on the core temperature and density behaviour. The stabilisation of the temperatures, densities and void fractions after the recriticality power peak results in the stabilised power level. The fuel temperature at 45 kg/s reflooding is shown in Figure 5.13.

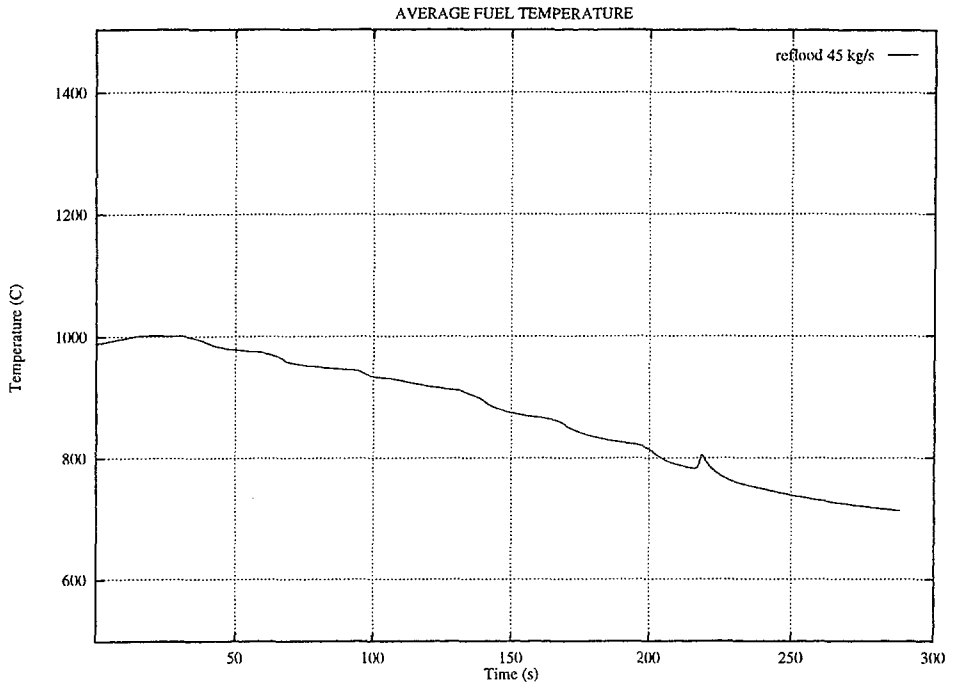

Figure 5.13 Average fuel temperature with reflooding rate 45 kg/s.

Some examples of the results obtained with the reflooding rates of 540 and 1350 kg/s are presented in Figures 5.14 through 5.18. Figure 5.14 shows the total power behaviour. The relative power peak values predicted for the reflooding rates of 540 kg/s and 1350 kg/s were 17.2 and 47.9 times nominal full power level, respectively. After the first power peak the power oscillates for a few seconds. In the 540 kg/s case the power stabilises at about 60 % of nominal power. In the 1350 kg/s case the calculations were stopped at 10 seconds due to numerical problems, but it seems as if the total power stabilises at about 120 % of nominal power.

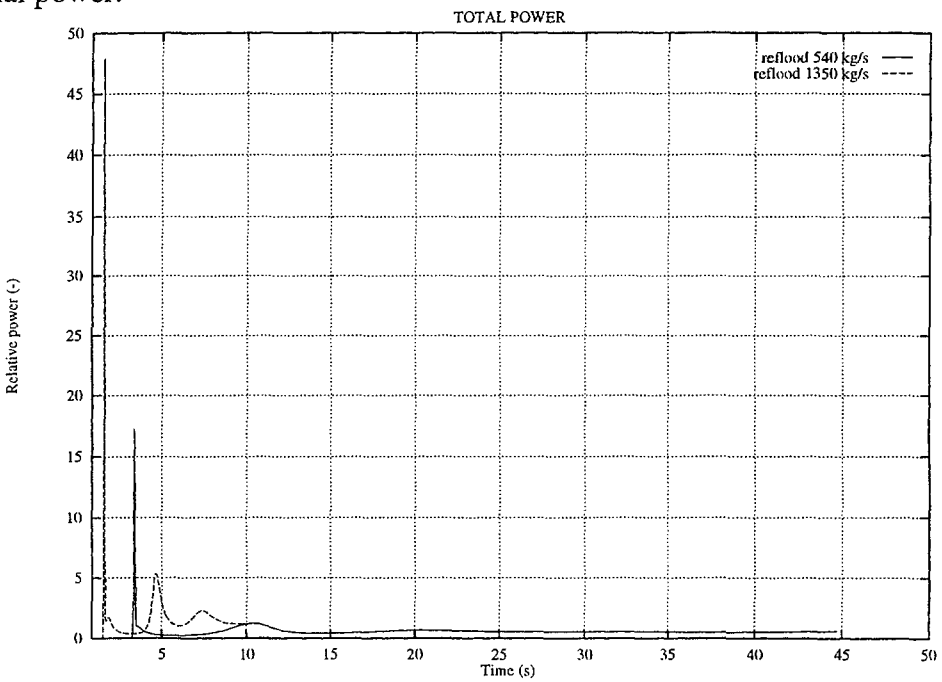

Figure 5.14 Total power at reflooding rates 540 and 1350 kg/s.

Average fuel temperature behaviour is shown in Figure 5.15. Due to the higher power peak and due to the higher stabilised power level after the recriticality peak, the fuel temperature calculated for the reflooding rate 1350 kg/s is significantly higher than with reflooding rate 540 kg/s.

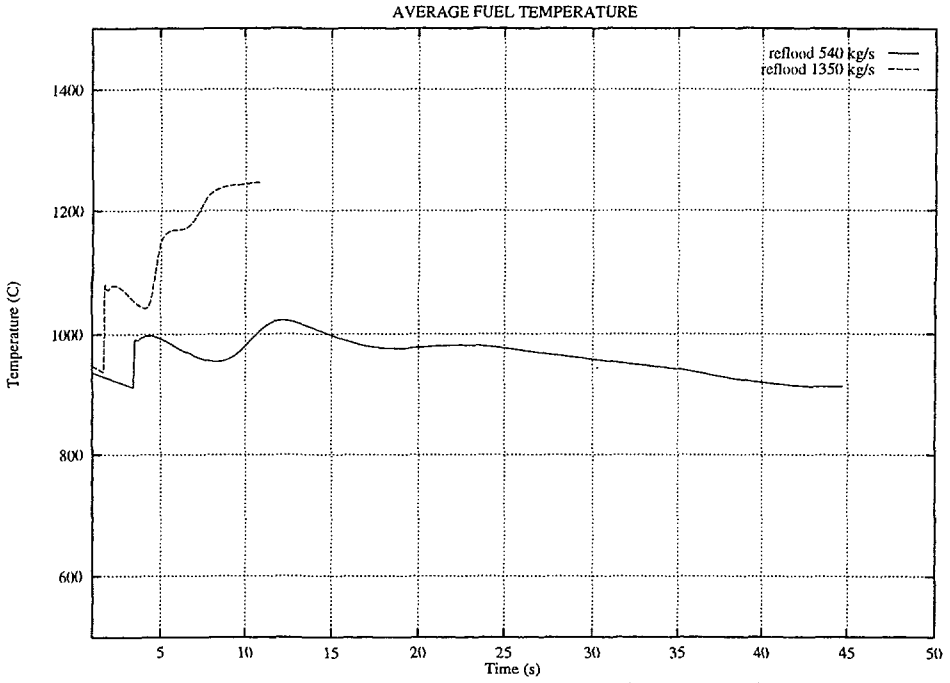

Figure 5.15 Average fuel temperature at reflooding rates 540 and 1350 kg/s.

Core average void fraction is shown in Figure 5.16. The higher reflooding rates leads to lower core average coolant temperature and to lower core average void fraction. Both of these factors contribute to the higher stabilised power level with the reflooding rate 1300 kg/s in comparison with the reflooding rate 540 kg/s.

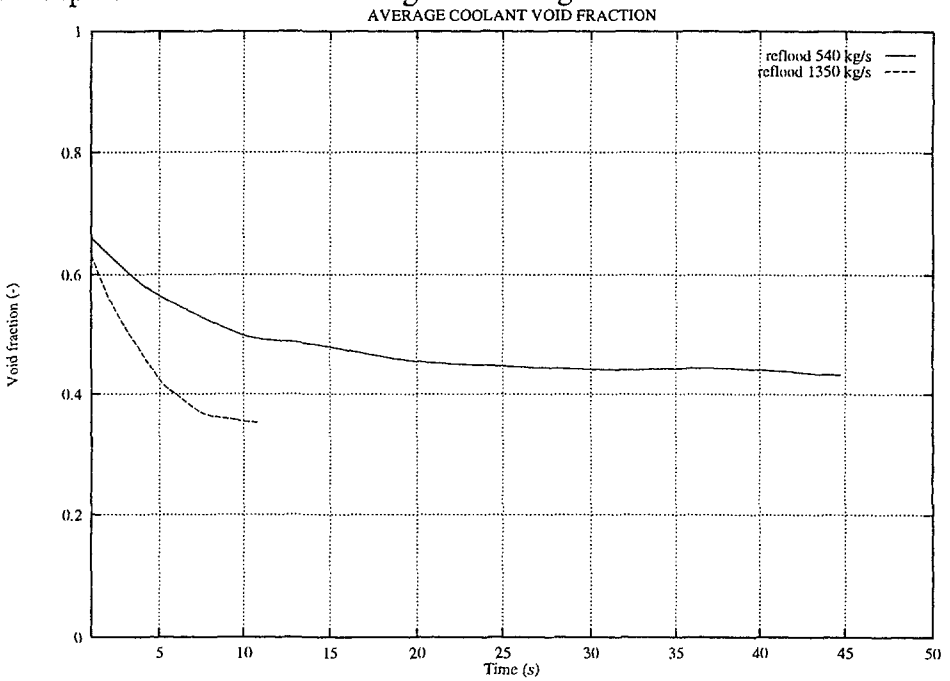

Figure 5.16 Average coolant void fraction at reflooding rates 540 and 1350 kg/s.

Maximum nodal power peaking factor for the reflooding rates of 540 kg/s and 1300 kg/s is shown in Figure 5.17. It can be seen that for both reflooding rates fairly similar maximum power peaking during the recriticality peak was predicted.

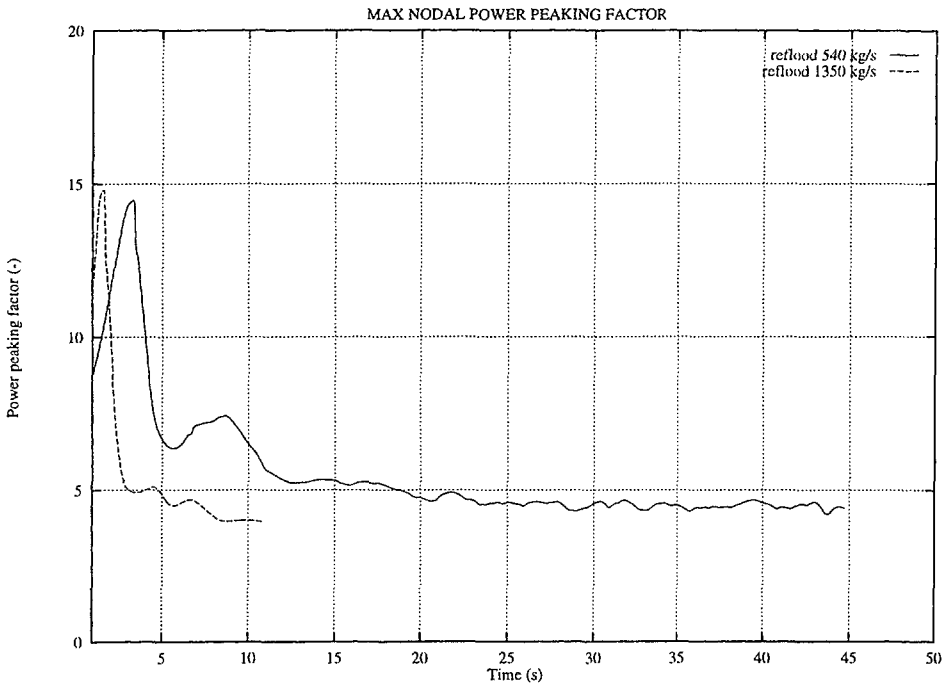

Figure 5.17 Maximum nodal power peaking factor at reflooding rates 540 and 1350 kg/s.

Maximum nodal fuel temperatures predicted with the reflooding rates 540 kg/s and 1300 kg/s are presented in Figure 5.18. Due to the higher recriticality power peak reached with the reflooding rate of 1300 kg/s the maximum nodal temperature reached with this reflooding rate is also higher than that reached with the reflooding rate of 540 kg/s. It can be observed that with both reflooding rates the maximum nodal fuel temperature is predicted to exceed the fuel melting temperature.

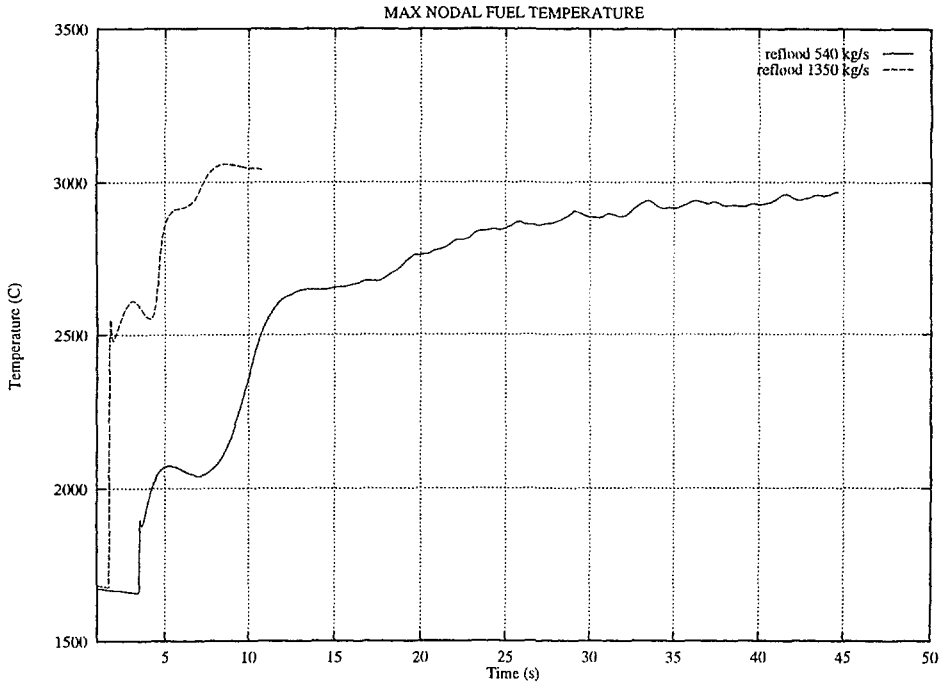

Figure 5.18 Maximum nodal fuel temperature at reflooding rates 540 and 1350 kg/s.

Selected APROS results for the highest studied reflooding rate of 1900 kg/s are shown in Figures 5.19 through 5.22. In these figures the time scale is different from the previous results due to the fact that the time was not reset to zero at the beginning of the reflooding.

The total power behaviour during the transient is presented in Figure 5.19. The first power peak is very high, approximately 1448 times the nominal full power level. After this first power peak the power first oscillates at very high levels and then stabilises at the level of 3.2 times the nominal power.

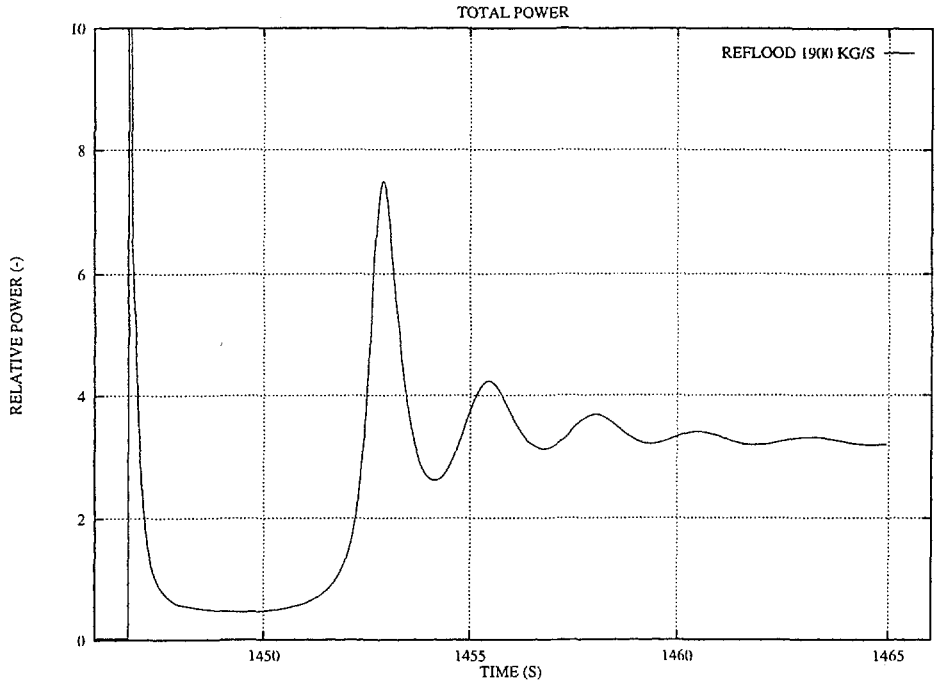

Figure 5.19 Total power at reflooding rate 1900 kg/s.

Average fuel temperature is shown in Figure 5.20. It can be noticed that in spite of the very high power levels obtained, the average fuel temperature remains well below the fuel melting temperature.

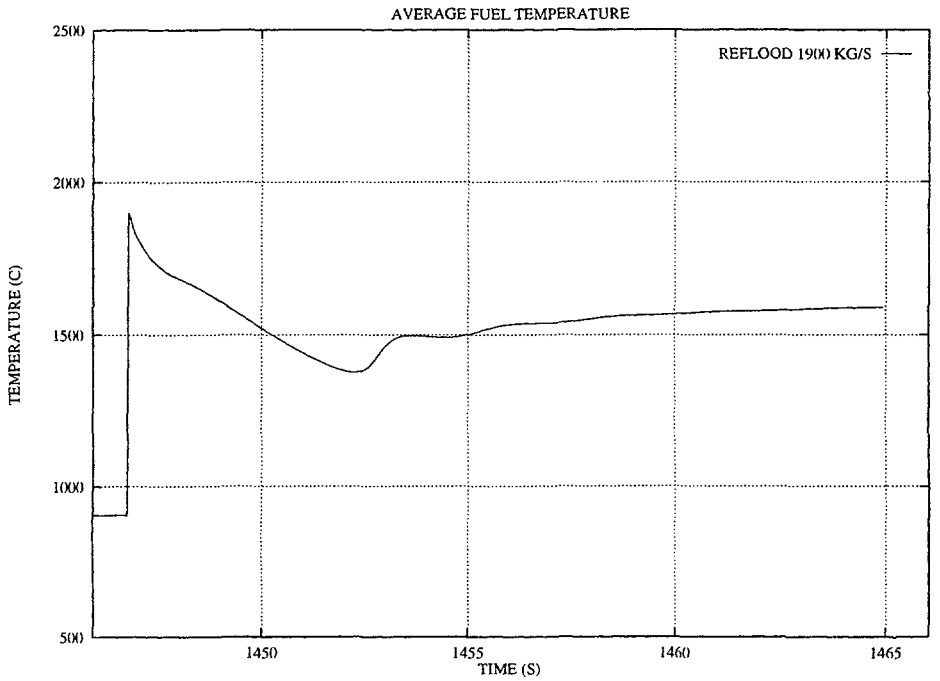

Figure 5.20 Average fuel temperature at reflooding rate 1900 kg/s.

Due to the very high reflooding rate, the coolant temperature and core average void fraction were predicted to be clearly lower than for the lower reflooding rates, which contributed via positive reactivity effect to high power level after the initial power peak.

The maximum nodal power peaking factor is shown in Figure 5.21. It can be seen that the maximum nodal power peaking factor is comparable with the power peaking factor predicted with the reflooding rates 540 kg/s and 1300 kg/s.

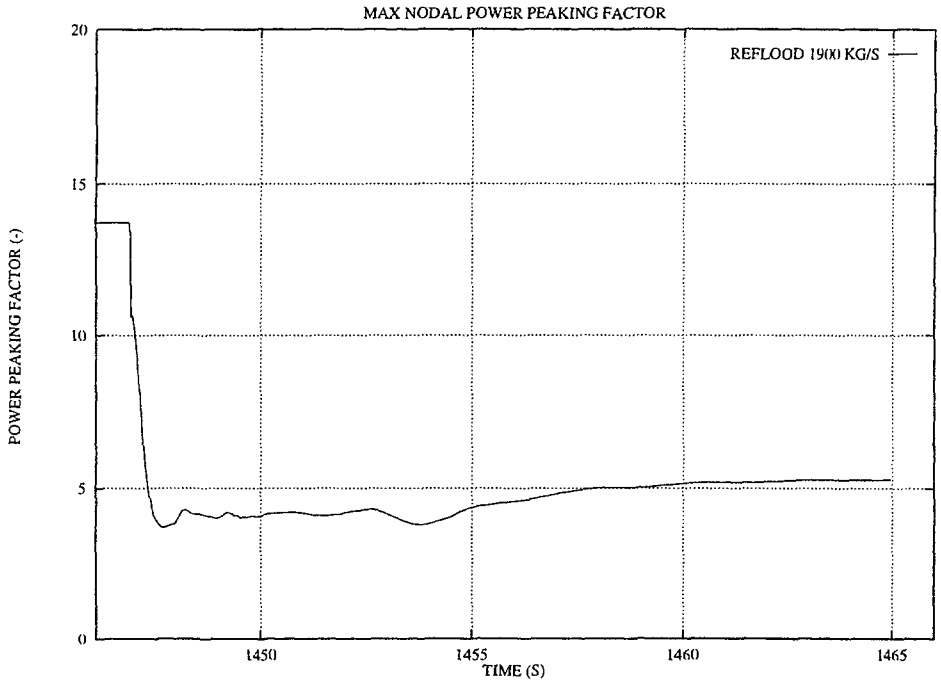

Figure 5.21 Maximum nodal power peaking at reflooding rate 1900 kg/s.

The maximum nodal fuel temperature is presented in Figure 5.22. This result indicates that the fuel melting temperature is clearly exceeded due to the energy created in the first recriticality power peak. The maximum fuel temperature is predicted to remain well over fuel melting temperature during the transient. The numerical values obtained for fuel temperatures in this transient were not considered to be realistic and reliable due to the fact that the materials properties and correlations used in APROS were developed for normal transients assuming only some minor melting at the centre of the UO_2 pellet.

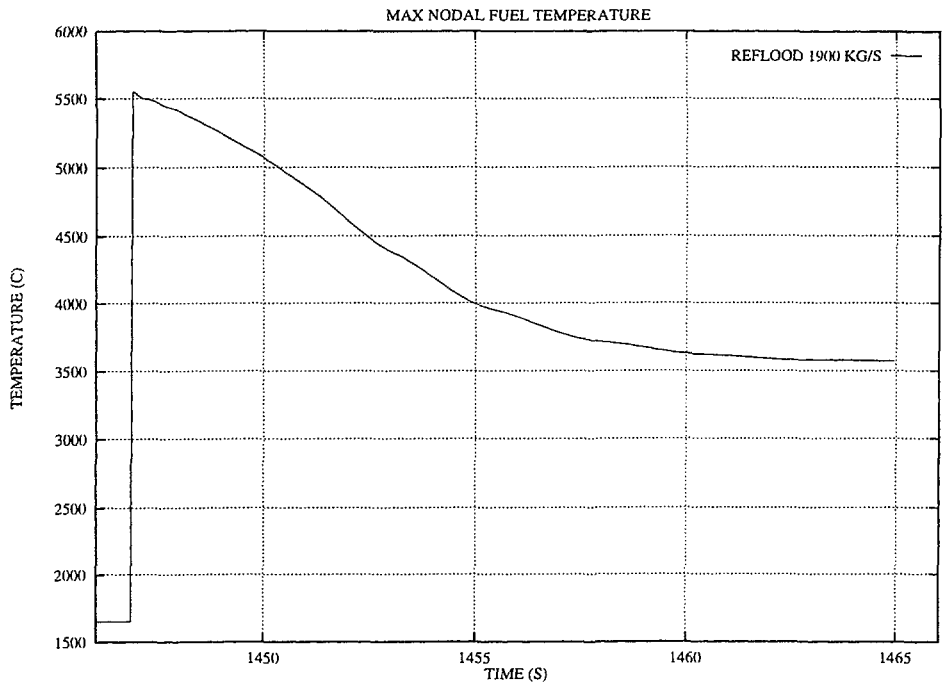

Figure 5.22 Maximum nodal fuel temperature at reflooding rate 1900 kg/s.

The results of the APROS calculation with the reflooding rate 1900 kg/s indicate that due to the very high power peak and very high fuel maximum temperature a large part of the fuel rods would melt or break into pieces. Thus, further study of this reflooding case was not considered realistic since both the capabilities of the physical models used and materials properties assumed were clearly exceeded.

The power and temperature distribution in the core during and after the recriticality peak give valuable information when trying to assess whether the fuel will be damaged due to the recriticality peak and following operation at elevated power. Figure 5.23 shows the calculated fast neutron flux, nodal fuel temperature and void fraction at three elevations in the core at the time of recriticality peak with reflooding rate of 540 kg/s with the five-equation thermal-hydraulic model. According to the APROS results, the power production during and after reactivity peak is concentrated to approximately one third of the core.

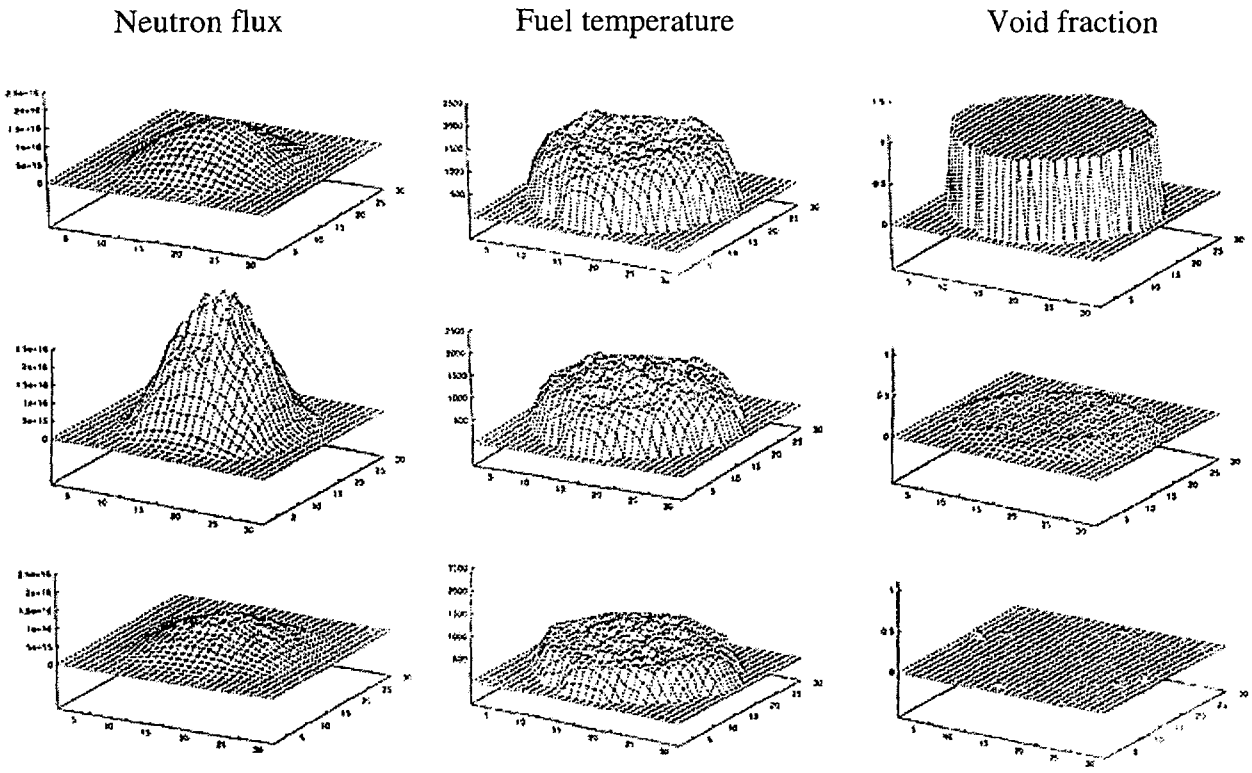

Figure 5.23 Calculated fast neutron flux, nodal fuel temperature and void fraction at three elevations in the core at the time of recriticality peak with reflooding rate of 540 kg/s with the five-equation thermal-hydraulic model.

5.2.3 Summary of recriticality calculations

The results of recriticality calculations performed with the five-equation thermal-hydraulic model are presented in Table 5.3. The corresponding results using the six-equation thermal hydraulic model are shown in Table 5.4. With the six-equation model numerical problems with mass error criteria were met after the power peaks and therefore the stabilized power levels were not calculated. The power peaking factors obtained with the six-equation model were somewhat lower than those obtained with the five-equation model.

Table 5.3. Results of APROS recriticality analysis for Olkiluoto BWR core with various reflooding rates. Core total relative power versus steady state full power. 3-D core neutronics and 5-equation thermal-hydraulics.

Reflooding rate (kg/s)	Peak Power (relative)	"Stabilised" power (relative)
45	0.45	0.08
540	17.2	0.60
1350	47.9	1.17
1900	1448	3.19

Table 5.4 Results of APROS recriticality analysis for Olkiluoto BWR core with various reflooding rates. Core total relative power versus steady state full power. 3-D core neutronics and 6-equation thermal hydraulics.

Reflooding rate (kg/s)	Peak Power (relative)
45	0.51
540	14.03
1350	35.22
1900	N. A.

The calculations performed with both the five- and the six-equation thermal-hydraulic models have shown that the higher the reflooding rate, the sooner the recriticality power peak occurs. The height of the power peak and the power level after the peak depends on the reflooding rate.

The analyses have also shown that similar power peaks were obtained with five- and six-equation thermal-hydraulic models. For the 45 kg/s reflooding rate the recriticality peak was reached considerably faster (after 120 seconds) with the six-equation model than with the five-equation model (after 220 seconds). With the larger reflooding rates no significant differences in peak timing between the five- and six-equation alternatives was observed.

The main purpose of the calculations was to find out the timing and height of the recriticality power peak, and to compare the results of the five- and six-equation models. Due to the assumptions used in the calculations, as well as short transients, one has to be careful when applying the results to real plant situation. Further, when the average node fuel temperature reaches melting point, analysis with APROS, which assumes intact fuel geometry, will no longer be realistic.

The numerical problems encountered in the 1350 kg/s case, which stopped calculations after only 10 seconds into the transient, were absent in the common case code comparison calculations described in section 5.4. The main difference between these two calculations was the primary system pressure which in the code comparison analysis was 0.5 MPa.

5.2.4 Energy involved in recriticality power peak

In the recriticality calculations with APROS using the five-equation model and high initial pressure level (i.e. 6.5 MPa) the recriticality peak of Figure 5.24 was obtained for the case with 540 kg/s reflooding mass flow rate.

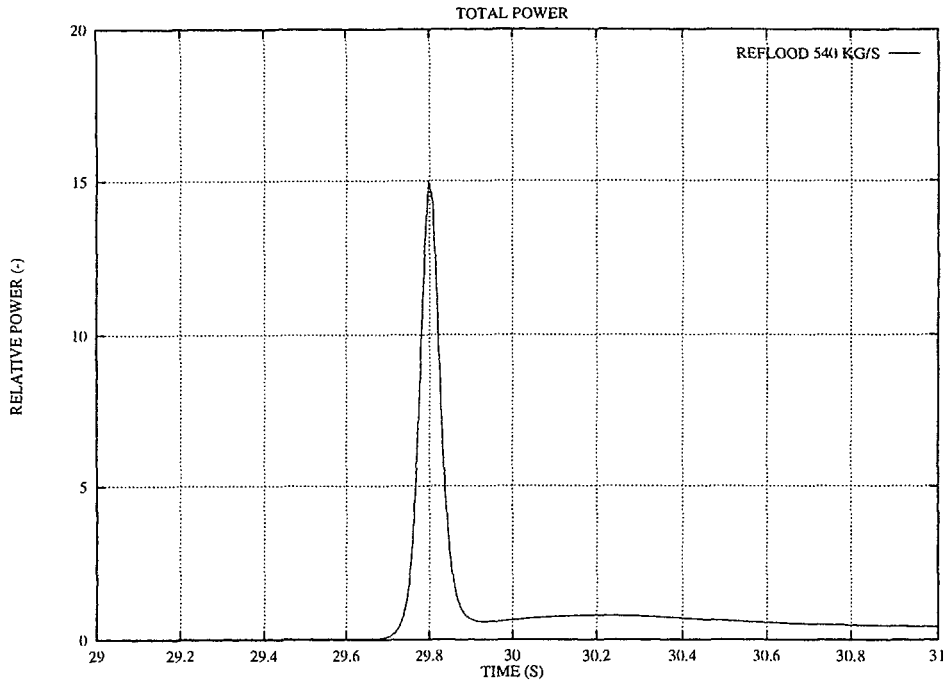

Figure 5.24 Power peak with reflooding rate 540 kg/s.

According to Figure 5.24, the peak duration was approximately 0.2 seconds. The peak can be approximated as a triangle. With these assumptions we obtain for the total energy in the peak: 15x2500 MWx0.2s / 2 = 3750 MJ

According to data given by TVO, the fuel mass in one assembly is 172 kg. Since there are 500 assemblies, the total fuel mass is estimated as 500 x 172 kg = 86000 kg. APROS results indicate, according to Figure 5.25, that the maximum nodal power peaking factor in the 540 kg/s case is approximately 14.

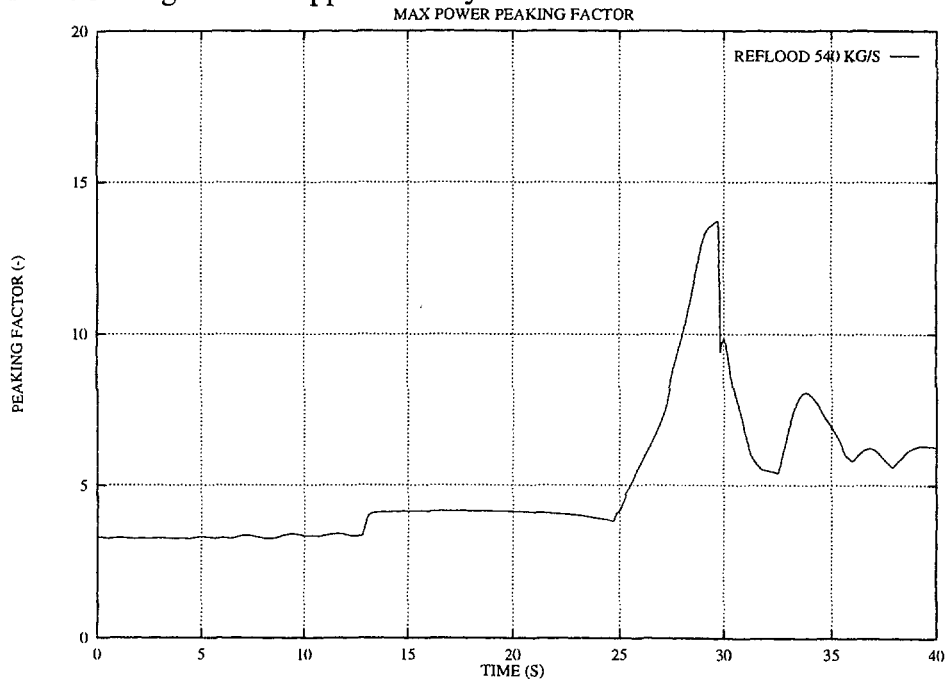

Figure 5.25 Maximum nodal power peaking factor with reflooding rate 540 kg/s.

With the fuel mass of 86 000 kg we obtain an energy deposition of 145 cal/gUO_2, which is of the same order as the cladding failure criterion of 140 cal/g, but less than the conventional RIA criterion of 230 cal/g for fuel under normal operating conditions.

Since in the present APROS calculations the recriticality power peak height has been correlating quite strongly with reflooding rate (higher peaks with higher reflooding) whereas the peak duration has been of the order of 0.1 s, it is likely that the 45 kg/s reflooding would not pose a threat to fuel integrity and that the 1350 kg/s reflooding would cause more fuel failure than the studied 540 kg/s case.

5.3. RECRIT Calculations for OL-1 (Task 3)

Three cases for OL-1 have been analysed with the RECRIT code (see also note on page 66):

Case 1: Calculation from the beginning of the accident with **normal** ADS and reflooding rate of 160 kg/s.

Case 2: Calculation from the beginning of the accident with **delayed** ADS and pressure dependent reflooding rate.

Case 3: Calculations showing the effect of void from neutron slowing down.

5.3.1 Initial conditions and assumptions

Case 1 is a pendant to the first case of the comparative studies (see Section 5.4), i.e. with a constant injection rate of 160 kg/sec starting at the time when the maximum fuel temperature reaches 2100 K.

The automatic depressurisation system (ADS) will start when the water level in the downcomer falls below a certain value (1 m above the top of the core). The ADS will take the reactor pressure down to the vicinity of the containment pressure by conducting steam to the condensation pool. When the water level in the core decreases, the temperature in the "above water level" part of the core begins to increase. The control rods are assumed to melt and disappear (no relocation is modelled in RECRIT) at 1000° C.

In order to get conditions for recriticality, water injection has to start when either the maximum fuel temperature is above a certain input value, or the average control rod presence is below a certain input value. Both these criteria were used in the first case. Water injection may also be started at a certain input time. The water level in the reactor will then start to increase until eventually a critical state is reached.

The results until the start of the injection may be compared to the MELCOR calculation. In Table 5.5 the times for core uncovery and injection start are compared.

The results of two RECRIT runs are given. In one run, the injection was started at the signal of control rod presence being below 0.5 (CR=0.5), which was the value MELCOR gave. In the other run, the injection was started when the maximum fuel temperature

reached 2100 K. This maximum fuel temperature was reached by MELCOR simultaneously with the control rod presence of 0.5.

Table 5.5 Comparison of RECRIT and MELCOR.

Code/Case	Core uncovery (seconds)	Injection start (seconds)	CR presence At inject. Start	T_{fuel} At inject. start (K)
MELCOR	2600	4200	0.5	2100
RECRIT/ (CR= 0.5)	2769	3037	0.5	1924
RECRIT/ (T_{fuel}= 2100K)	2769	3454	0.22	2100

Case 2 aimed at showing the advantages if the ADS was not started until either electricity was back, or the water level in the downcomer decreased to about 1 m above core bottom. The activation of the ADS is done to make it possible for the low pressure ECCS to operate. However, in a station black-out scenario the low pressure ECCS is not operating, so it seems unnecessary to start the ADS too early and thereby loose the coolant. Thus, in Case 2 the ADS was started later, 5000 seconds after the accident initiation to compare with 1900 seconds in the first case, which equals the actual plant ADS-setpoint.

In Case 2, the high pressure injection (50 kg/s) starts at the same time as the ADS, i.e. when electricity has come back. When the pressure falls below 10 bar, the low pressure ECCS will inject an amount of water, which varies from 0 kg/sec at 10 bar to 440 kg/s at 1.5 bar. This is close to actual conditions at the plant.

5.3.2 Results of RECRIT analysis

Case 1 and Case 2

Time period before criticality

The RECRIT predictions are shown in Figures 5.26 and 5.27 for Case 1 with normal ADS, and in Figures 5.28 and 5.29 for Case 2 with delayed ADS.

The power, which is the decay heat of the radioactive fuel, falls steadily from some 325 MW to some 35 MW. The water levels in the core (which is the space inside the fuel boxes), the bypass channel (which is the space inside the moderator tank and outside the fuel boxes), the lower plenum, and the downcomer are shown. They are measured from the bottom of the core. In the core and the bypass channel the levels are constant in the beginning (equal to the core height). In the first case the levels fall rapidly until core uncovery, when the ADS starts. In the second case the levels first fall slowly down to about 1 m above core bottom and then rapidly as the ADS starts.

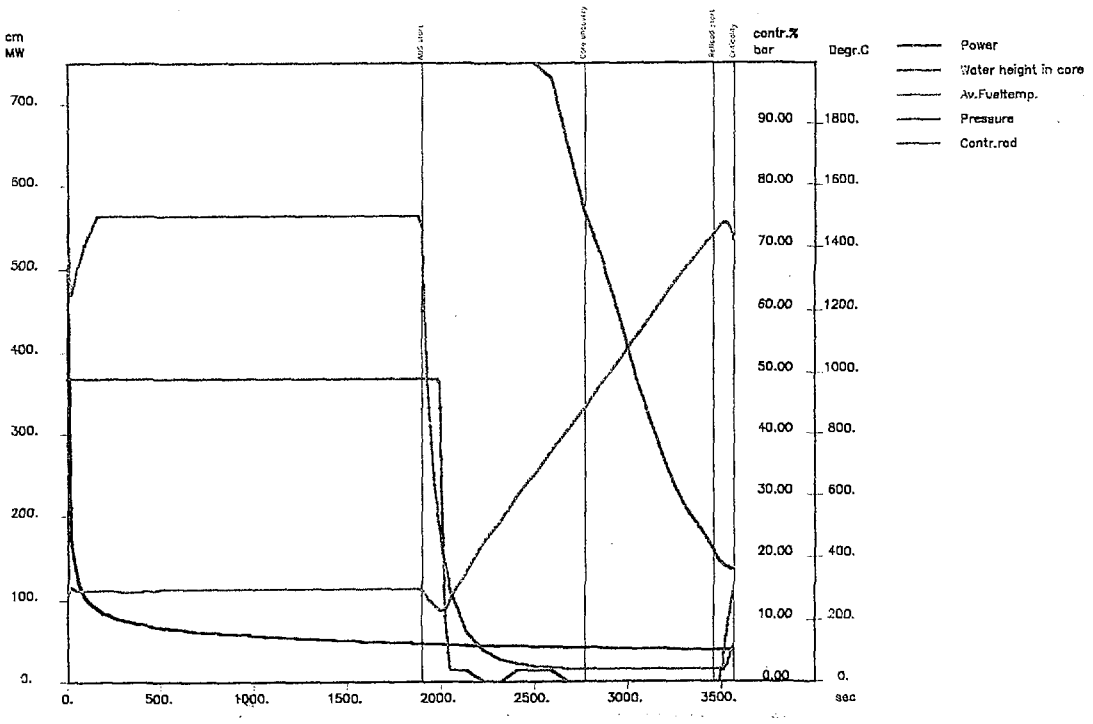

Figure 5.26 OL-1 parameters before recriticality as functions of time. Reflood rate 160 kg/s. Case 1. Normal ADS, reflooding due to high T_{fuel}.

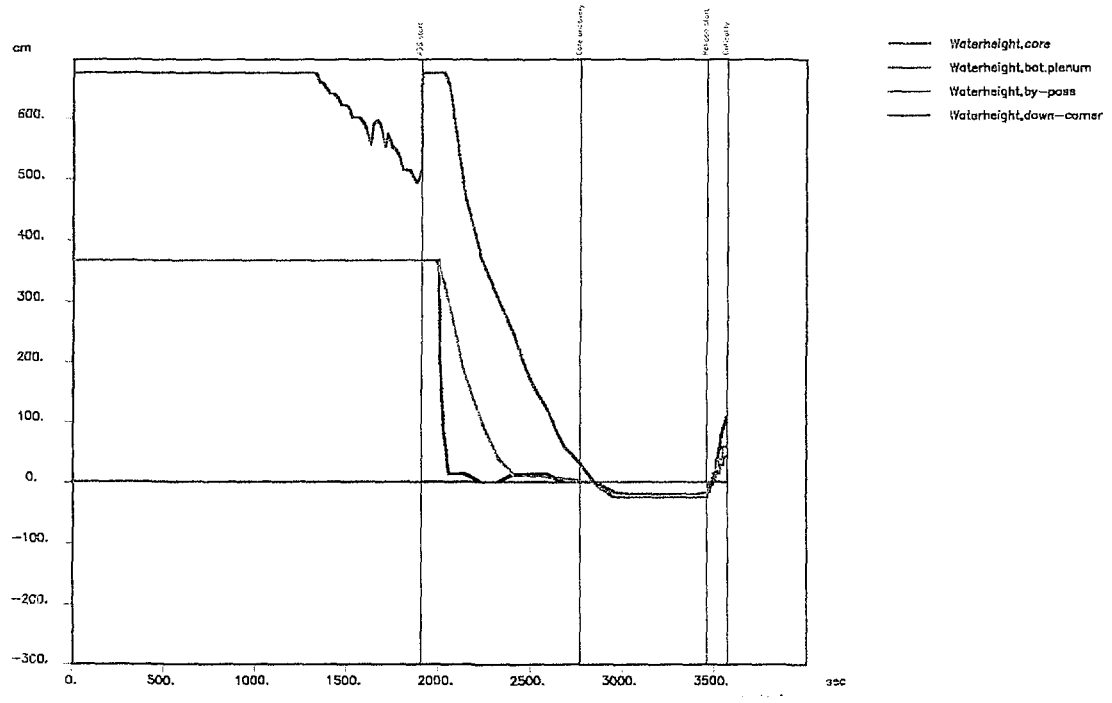

Figure 5.27 OL-1 water levels before recriticality as functions of time. Reflood rate 160 kg/s. Case 1. Normal ADS, reflooding due to high T_{fuel}.

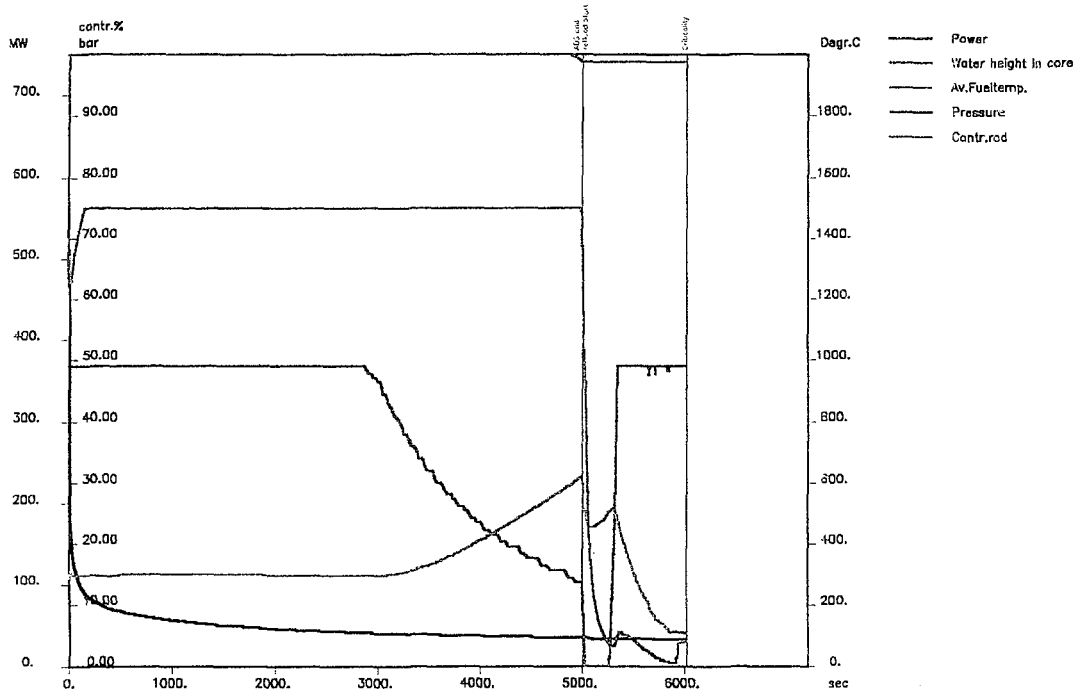

Figure 5.28 OL-1 parameters before recriticality as functions of time. Pressure dependent reflood rate. Case 2. Delayed ADS, reflooding due to time = 5000 s.

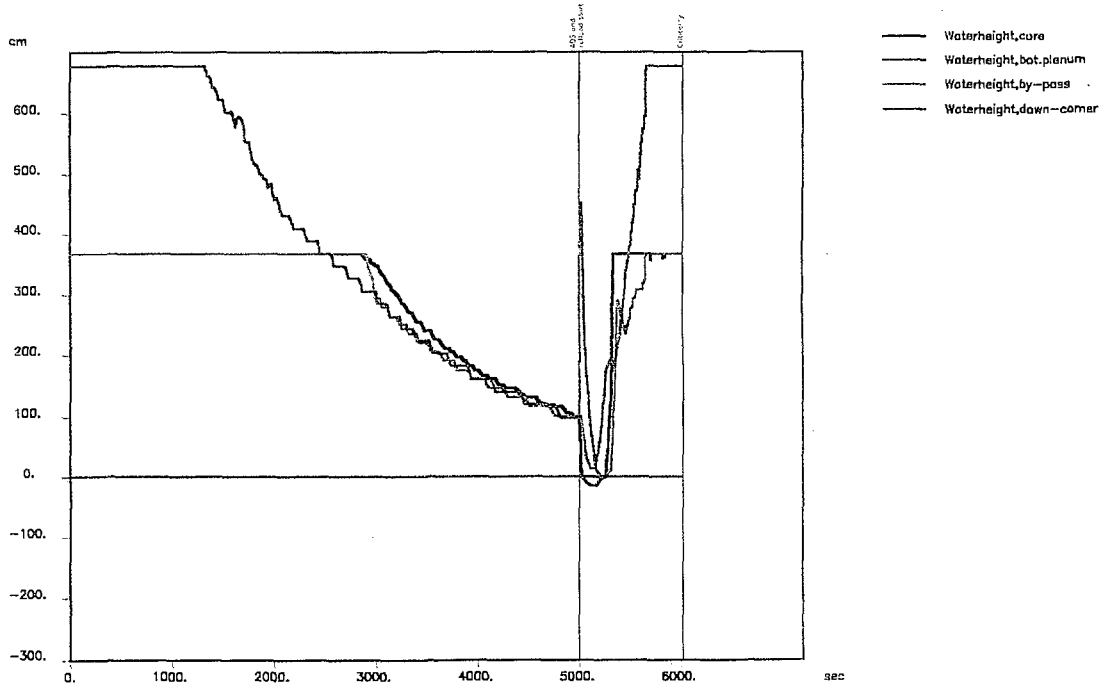

Figure 5.29 OL-1 water levels before recriticality as functions of time. Pressure dependent reflood rate. Case 2. Delayed ADS, reflooding due to time = 5000 s.

The level in the downcomer falls below its maximum value after some 1500 seconds. However, when the ADS starts, the water level will raise as a result of flashing.

The system pressure is almost constant until ADS-start. It then falls rapidly towards containment pressure. When injected water begins to rewet hot, uncovered fuel, the pressure may increase a little again, but is kept below 5 bar by valve regulation.

Finally, the melt-away of the control rods is shown. It starts when the maximum fuel temperature reaches 1000° C and proceeds until the cooling effect of the reflooding becomes effective. In the second case only a very small fraction of the control rods is melted.

Time period after criticality

The transient is very fast in this period, as the reactor system will usually attain a state of super prompt criticality.

Some interesting parameters are shown in Figure 5.30 (Case 1, normal ADS) and in Figure 5.31 (Case 2, delayed ADS). The two cases are quite different due to the different control rod distributions. In fact, the configuration in the second case can only become critical when the core is fully covered by water, and then not until the water has been cooled by mixing with the cold injected water.

The reactivity increases due to the water injection and reaches almost 1% (1.3$) after ~2 seconds in the first case. This brings the power up from almost zero to a peak value of ~700 MW.

In the second case the rate of increase of reactivity is very much slower, as it is not due to the increase in water height (the core is fully covered), but to a steadily falling water (and fuel) temperature. The accompanying power-peak is lower in this case, some 250 MW.

(The power is composed of the **fission** power and the **decay** power. While the decay power is ~35 MW at the time of criticality, the fission power starts really low, in micro-watt range, because of an extremely low neutron density. The number of neutrons in the beginning is determined by the very weak source of spontaneous fission neutrons from U^{238}).

The power-accompanying increase in fuel temperature and an increased steam production from neutron slowing down make the reactivity go negative and end the power excursion. In the first case the continued water injection steadily increases the water level and makes the reactor critical again. The consequences of these subsequent criticalities may in general be anything, from an increase in void contents balancing a slowly increasing power level to violent power bursts. After some time the fuel temperature will exceed the melting point.

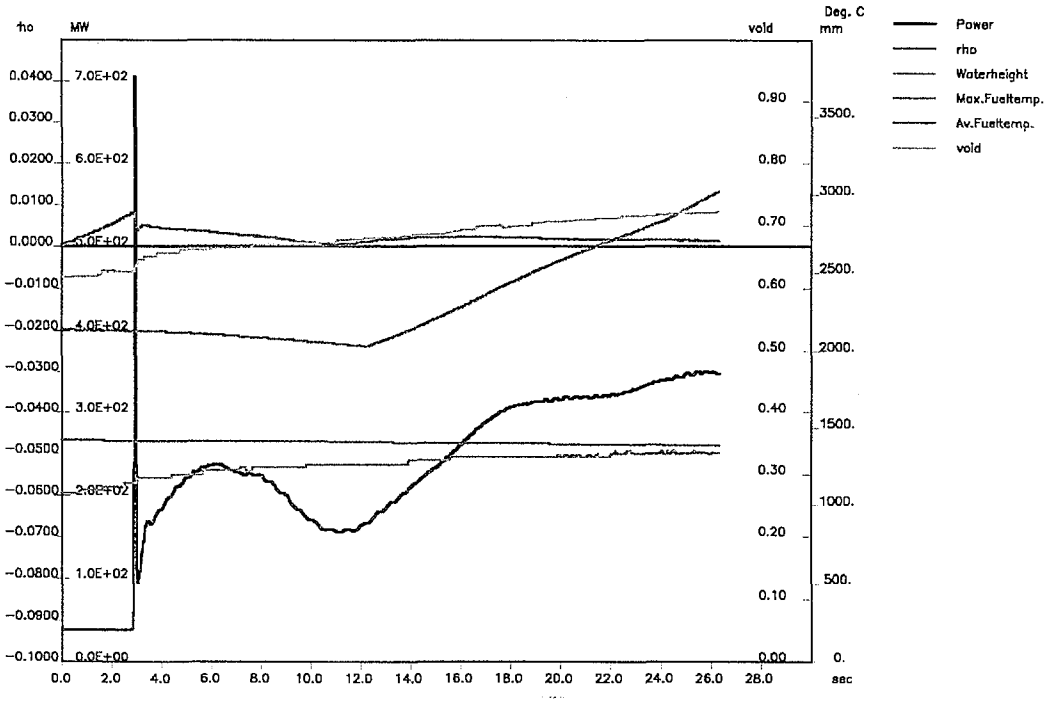

Figure 5.30 OL-1 parameters after recriticality as functions of time. Reflood rate 160 kg/s. Case 1. Normal ADS, reflooding due to high T_{fuel}.

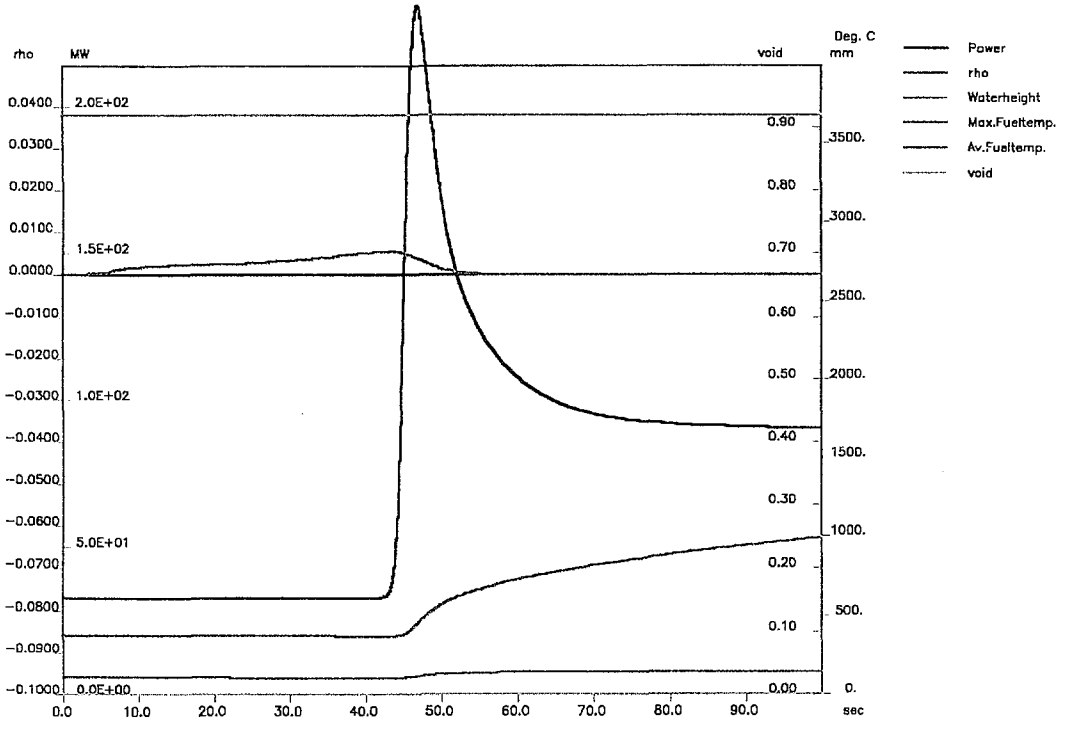

Figure 5.31 OL-1 parameters after recriticality as functions of time. Pressure dependent reflood rate. Case 2. Delayed ADS, reflooding due to time = 5000 s.

In Figure 5.32 (normal ADS) and Figure 5.33 (delayed ADS) some examples of spatial distributions are shown. The distributions refer to the time of the first power peak.

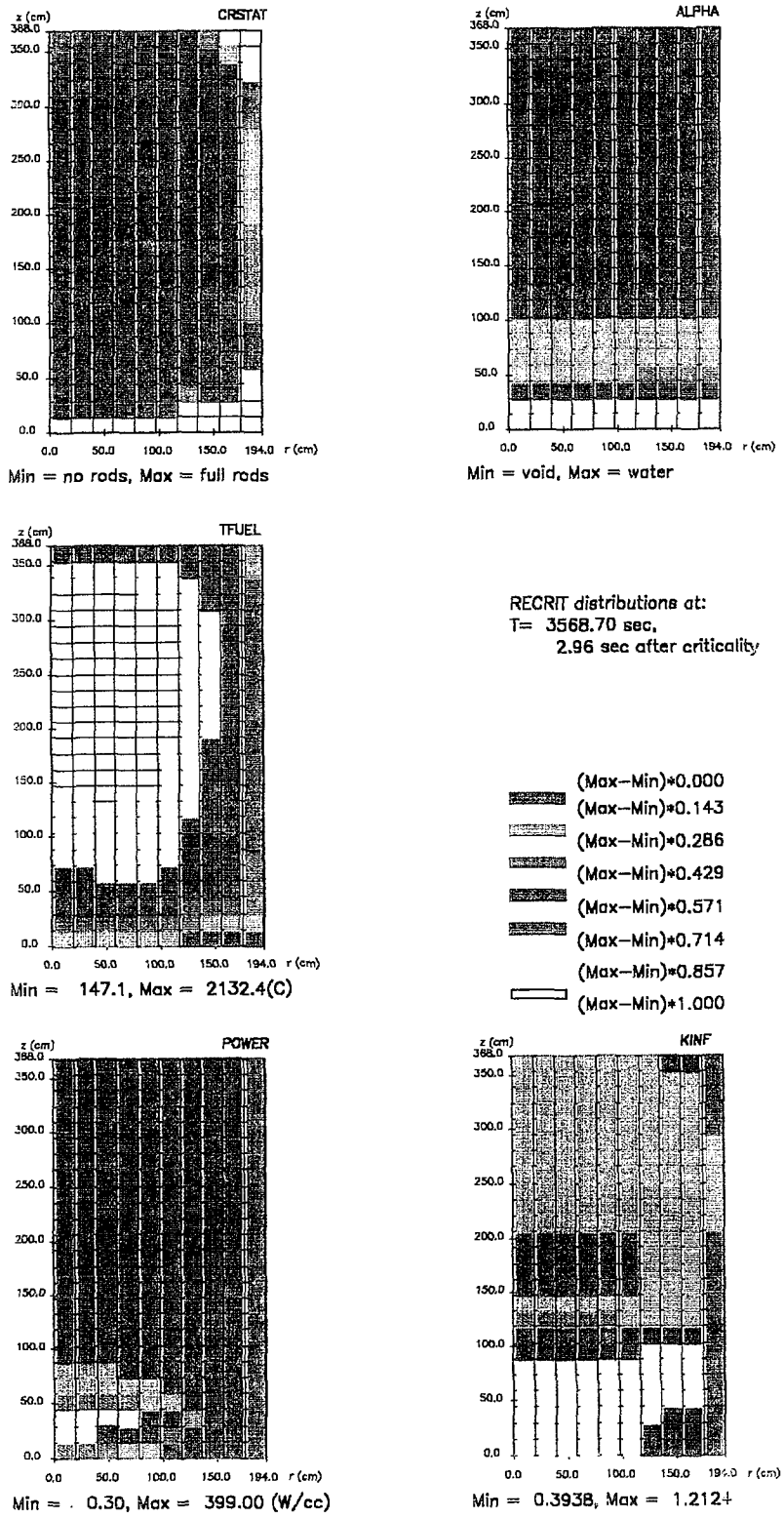

Figure 5.32 Case 1. Normal ADS. Spatial distributions by RECRIT at time of first recriticality. Control rod state, void, fuel temperatures, power density and reactivity (k_{inf}).

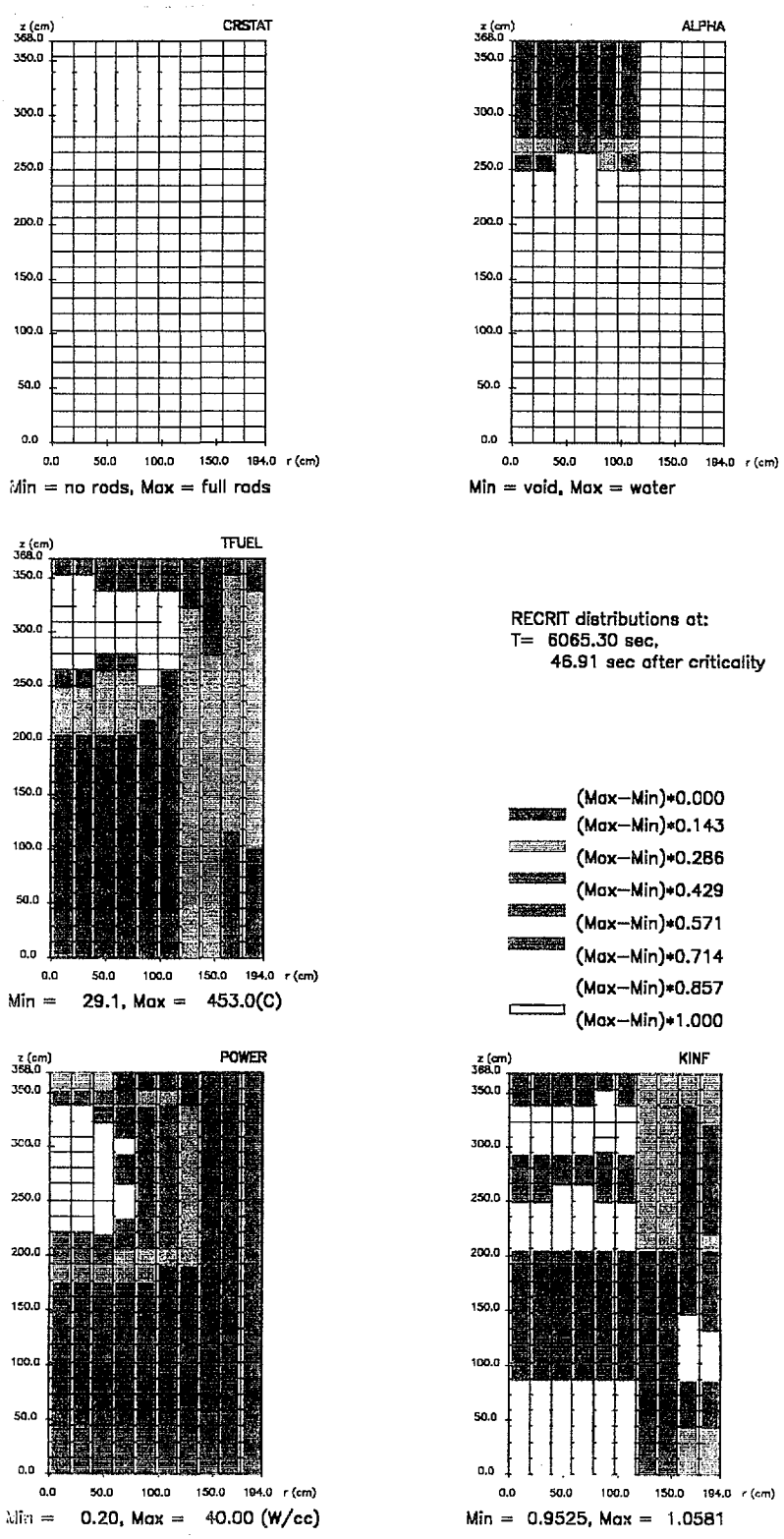

Figure 5.33 Case 2. Delayed ADS. Spatial distributions by RECRIT at time of first recriticality. Control rod state, void, fuel temperatures, power density and reactivity (k_{inf}).

The parameters in Figure 5.32 and Figure 5.33 have the following meaning and interpretation:

CRSTAT Shows the distribution of control rods. The difference between the two cases is significant. In Case 1, the rods are intact in a bottom layer. Then follows a layer with partly melted rods, and then a large part of the core, where all rods are melted away. Only at the very top of the core and in a thin peripheral zone the heat loss by radiation has been so large that some fraction of rods remain.

In Case 2 the control rods are melted (partly) only in a small fraction of the core near the top.

ALPHA The void fraction is zero in the bottom part and unity in the top.

TFUEL The maximum fuel temperature is found close to the top of the core. In Case 1 this is a result of the combination of the radiation heat and the time during which that part of the core has been without water cooling.

In case 2 the maximum fuel temperature is due to the fission heat from the power burst.

POWER The power distribution is very concentrated, especially in case 1. The major part of the power is generated in a small fraction of the core, resulting in quite large power densities (the numbers given are per cc of core, so per cc of fuel it is some 3 times larger).

KINF In the rodded and in the voided parts of the core k_{inf} is below 1.0.

In case 1 there is a layer of about ½ m thickness, in which k_{inf} is substantially above 1.0. In case 2 the layer is thicker, but because the control rods are only partially melted, k_{inf} is very close to unity.

Case 3

About 2.5% of the fission energy is carried away as kinetic energy of the fission neutrons. This energy is delivered to the moderator atoms in ~ 1 μs. If a steam volume corresponding to this energy and to the actual pressure in the reactor is generated in the same short time interval, it will represent a significant negative void reactivity during a power burst and thereby contribute to reducing the power peak. However, it is uncertain whether this is the case.

In RECRIT there is possibility of specifying the amount of the neutron slowing down energy, which is acting promptly in producing steam. In Table 5.6 the results of such a parametric study are presented.

The characteristics of the first power peak in the benchmark case with 160 kg/sec injection rate are given, when the prompt steam generation from the neutron slowing down corresponds to 0%, 0.1%, 1.0%, and 2.5% of the fission energy.

Table 5.6 Characteristics of first power peak

Fraction of fission energy for prompt steam generation (%)	Time after criti-lity for first peak (seconds)	Duration of peak (seconds)	Max. power (MW)	Energy in peak (MJ)
2.5	3.74	0.12	643	38
1.0	5.07	0.19	751	69
0.1	5.80	0.31	974	154
0.0	5.82	0.33	1653	255

It is seen, that the effect of the void formation on the magnitude of the power peak is considerable. It is therefore of great importance to determine the fraction of the neutron slowing down energy which might contribute to prompt void formation.

Note

At the very end of the SARA project additional RECRIT calculations were performed for the OL-1 reactor (Miettinen and Höjerup, 1999a). The assumed reflooding rates were 160 (as in Case 1), 540 and 1350 kg/s, i.e. the same as in the code comparison study described in section 5.4. According to these analyses the power after the first promp peak continued to oscillate showing several peaks. However, the average power increased with time, approaching about 50 % of nominal power for the highest reflooding rate, leading to fuel temperatures exceeding the melting point and termination of calculations. The power behaviour in these calculations was somewhat more stable than in the results described in the present report. Due to short calculation times, 70 - 180 seconds, it is of course hard to draw any certain conclusions about the long-term effects based on these RECRIT results.

5.4 Common Case Code Comparison for OL-1 plant

The three kinetics codes used in SARA have somewhat different modelling and simulation capability, because the codes were originally designed for different purposes. None of the codes includes complete modelling of the reactor systems combined with detailed physical models describing all phenomena involved in a reflooding/recriticality transient. However, the codes are to a large extent complementary to each other. S-3K has detailed fuel kinetics models, APROS an extensive system description, while RECRIT combines good kinetics with, after the upgrading, considerably improved thermal-hydraulics including reflood and quench models. In order to investigate the effect on results by use of different codes and to assess the uncertainties in the recriticality predictions, as well as to identify the shortcomings of the codes, a code comparison analysis was carried out. For this purpose three common cases for the Olkiluoto 1 plant were defined with the same accident sequence, the only difference between the three being the water injection mass flow rate (Höjerup, 1998, Puska, 1998b and Nilsson, 1999).

5.4.1 Assumptions and initial conditions

It was decided to introduce certain simplifications for fuel data and other boundary conditions in order to account for various modelling differences in the three codes. Three cases were defined for the calculations with the following conditions set up as a target :

- Constant steam dome pressure = 0.5 MPa (because no power – pressure feedback was modelled in S-3K).
- Injection ECCS mass flow rates to downcomer = 160, 540 and 1350 kg/s (Case 1, Case 2 and Case 3, respectively), chosen to reflect possible flow rates in OL-1.
- Temperature of injected water as function of time (around 48 °C) based on MELCOR results [Lindholm, 1998].
- Control rod configuration according to MELCOR results [Lindholm, 1998], shown in Table 5.7 below.
- Initial fuel temperature distribution based on MELCOR and MAAP4 results (Table 5.8).
- Water level in the vessel should be at the core lower boundary at start of water injection, i.e. when the reflooding transient is defined to begin (time zero).

The node numbers in Table 5.7 and Table 5.8 refer to a nodalisation of the core region used in MELCOR with 25 and 8 axial nodes of equal length, respectively. The division in the radial direction was made into 5 rings with equal flow areas. (In MAAP calculations 7 radial rings with varying widths were used). The radial division in RECRIT had 10 rings with equal width, but for APROS and S-3K, where each fuel assembly could be modelled individually, the distribution of B_4C and fuel temperatures for each assembly channel were interpreted directly from the MELCOR ringwise data.

Table 5.7 Status of control rod absorber material in the core prior to recriticality based on MELCOR predictions.

Fraction of B_4C from original inventory left in a node 5 radial · 25 axial nodes										
	From MELCOR Radial Ring					Specified for Common Cases Radial Ring				
Axial node	1	2	3	4	5	1	2	3	4	5
25	0	0	0	0	1.0	0	0	0	0	1.0
24	0	0	0	0	1.0	0	0	0	0	1.0
23	0	0	0	0	1.0	0	0	0	0	1.0
22	0	0	0	0	1.0	0	0	0	0	1.0
21	0	0	0	0	0.92	0	0	0	0	1.0
20	0	0	0	0	0	0	0	0	0	1.0
19	0	0	0	0	0	0	0	0	0	1.0
18	0	0	0	0	0	0	0	0	0	1.0
17	0	0	0	0	0	0	0	0	0	1.0
16	0	0	0	0	0	0	0	0	0	1.0
15	0	0	0	0	0	0	0	0	0	1.0
14	0	0	0	0	0	0	0	0	0	1.0
13	0	0	0	0	0	0	0	0	0	1.0
12	0	0	0	0	0	0	0	0	0	1.0
11	0	0	0	0	0	0	0	0	0	1.0
10	0	0	0	0	0	0	0	0	0	1.0
9	0	0	0	0	0.12	0	0	0	0	1.0
8	0	0	0	0	0.68	0	0	0	0	1.0
7	0	0	0	0.01	1.02	0	0	0	0	1.0
6	0.02	0.02	0.02	0.02	1.53	0	0	0	1.0	1.0
5	0.03	0.03	0.03	0.04	1.88	1.0	1.0	1.0	1.0	1.0
4	0.04	0.04	0.05	0.09	2.13	1.0	1.0	1.0	1.0	1.0
3	0.02	0.03	0.08	0.22	2.40	1.0	1.0	1.0	1.0	1.0
2	0.08	0.10	0.16	0.29	2.29	1.0	1.0	1.0	1.0	1.0
1	1.55	1.55	2.13	3.60	5.46	1.0	1.0	1.0	1.0	1.0

Table 5.8 Initial nodal fuel temperatures based on MELCOR and MAAP results.

Axial node/ radial ring	1	2	3	4	5
8	1000	1000	1000	1000	1000
7	1700	1700	1700	1700	1500
6	2100	2100	2100	2100	1600
5	2000	2000	2000	2000	1600
4	1950	1950	1950	1950	1500
3	1900	1900	1900	1900	1500
2	1800	1800	1800	1800	1300
1	1600	1600	1600	1600	1200

OL-1 plant data included recent plant upgradings for the increased operating power to 2500 MW_{th}. By courtesy of the TVO utility these plant data were made available. The real fuel data were, however, replaced by simplified data using only two fuel types with a few, fixed burnup histories, as agreed for the common case calculations in order to facilitate the code comparison. The two fuel types were of Siemens-KWU Atrium design, 10x10 pin geometry with 1.7% to 4.1% enrichment and some 3.5% Gd rods.

The following data for the fuel type 1 and 2 were specified:

- Fuel type No. 1: 91 fuelled pins, 10 of which are Gd rods, and 9 water rods.
- Fuel type No. 2: 83 fuelled pins, 9 with Gd, and 17 water rods.

Information to produce accompanying neutron cross sectional data was obtained from Anttila [1998]. Six different fuel segments were defined, according to Figure 5.34:

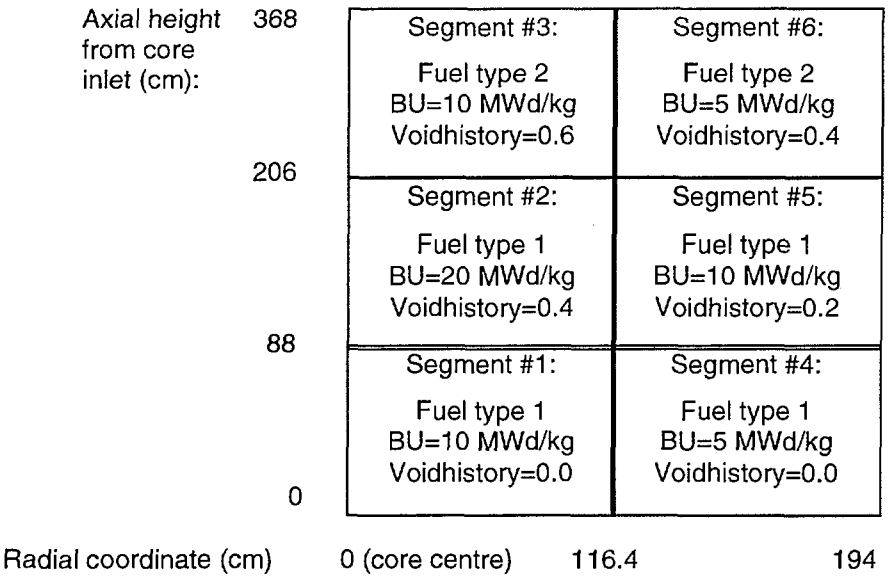

Figure 5.34 Fuel segment data for OL-1 common cases

The fuel data above were used to establish core initial conditions by means of steady-state runs with SIMULATE-3, APROS and RECRIT, from which the transient runs could be started. The steady-state runs were made with initial condition data given by TVO for full 2500 MW_{th} power operation of OL-1.

The initial conditions, primarily the fuel rod temperatures, prior to the recriticality transient were established by a transient run with S-3K and APROS through simulation of depressurisation to 0.5 MPa dome pressure and core uncovery and heat-up by stopping RC pumps and the feedwater flow. This part of the transient was completed when core maximum temperatures agreed with the specified maximum temperature based on MELCOR results. Due to differences in the simulation of the heat-up phase between the various codes, relatively large deviations in the temperature distributions compared with the specified temperature values were obtained. For S-3K this resulted in a shift of the temperature peak towards the upper part of the core compared to specification, as shown in Figure 5.35. In RECRIT the initial core temperatures could be implemented directly.

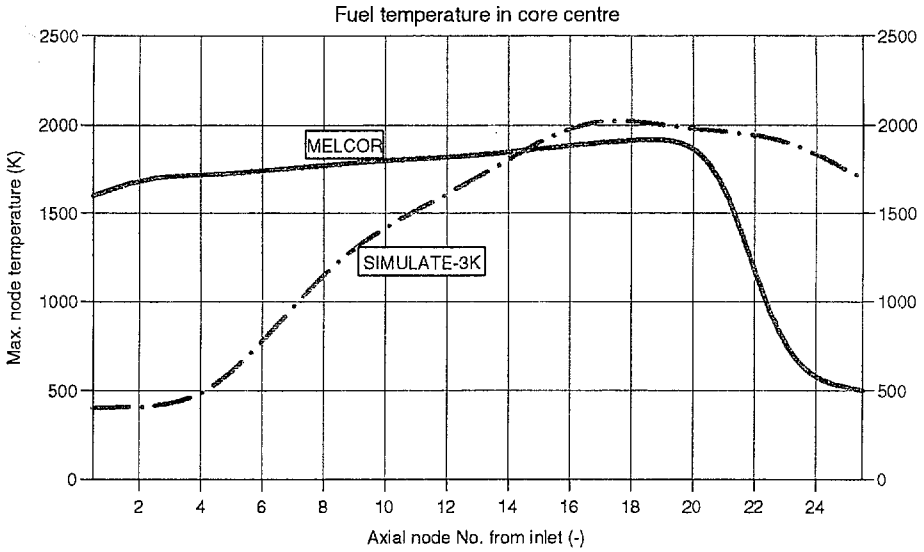

Figure 5.35 Axial temperature distributions after heat-up phase before reflooding.

The control rod configuration which should be applied to simulate the core state prior to recriticality could be introduced by input into all three codes. Minor deviations from the specified values were obtained since the nodalisation was different in the different codes. The MELCOR-based values were given for five radial core rings, while e.g. in S-3K all 500 fuel assemblies and the 121 control rods are modelled as individual flow channels and components, respectively. The radial distribution could therefore not be copied exactly, but axially the same number of nodes, 25, was employed by all codes.

Simulation of the reflooding phase and the recriticality transient began with water injection applying the mass flow rates of 160, 540 and 1350 kg/s for the three chosen cases, respectively. This simulation was made differently in APROS compared to S-3K and RECRIT. In APROS the core model was separated from the outer systems and the boundary conditions were given at the core inlet and exit. This means that the water injection was directed into the core inlet and its mass flow kept at a constant value without feedback to the lower plenum and the downcomer. The reflooding then started without delay and the reflooding velocity became rather constant. For S-3K and RECRIT the reactor model comprised both core and an outer loop including lower and upper plenum, steam separators, steam dome and downcomer with RC pumps. The water was introduced with a constant mass flow rate into the downcomer and the core inlet flow was then controlled by the pressure head in the downcomer versus the core inlet pressure. This formed a complete parallel flow system with core pressure feedback on the inlet flow which facilitated coupled flow and power oscillations. In addition, it should be noted that, as an effect of the different injection points, the water reflooding the core had a lower temperature in the APROS than in the S-3K and RECRIT calculations. These simulation differences should be considered when comparing the results from the three codes.

5.4.2 Comparison of results

Outputs from the calculations comprise a large number of variables, of which the following were selected for comparison:

- Total core power. This includes power from fission and fission products decay, and for APROS and RECRIT also oxidation power before the first recriticality. Of special importance is the first super prompt recriticality peak and the long-term recriticality power at enduring reflooding.
- Maximum energy deposited in any fuel node during the largest recriticality peak with respect to risk for fuel fragmentation.
- Maximum nodal power peaking factor.
- Maximum fuel temperature.

In Figures 5.36 through 5.47 the predictions of the three codes for each case can be compared.

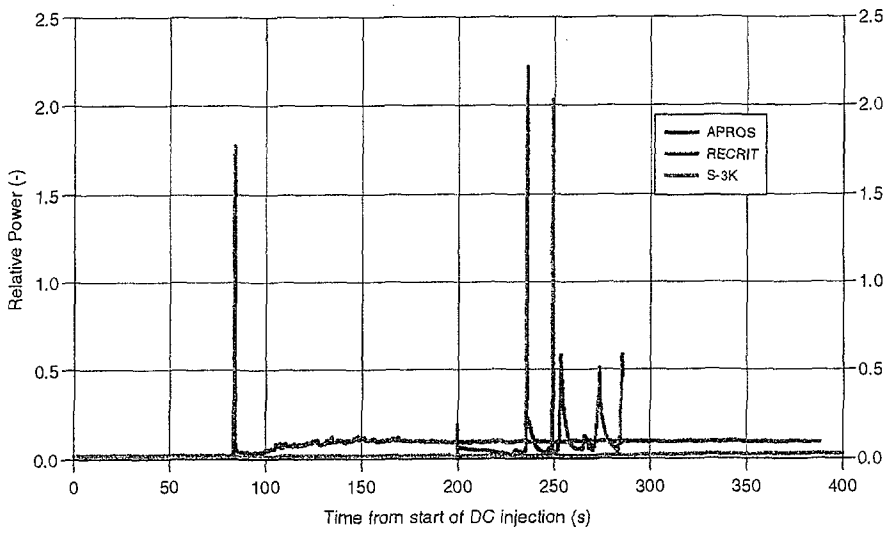

Figure 5.36 Relative core power in OL-1.Case 1: ECCS water mass flow rate = 160 kg/s.

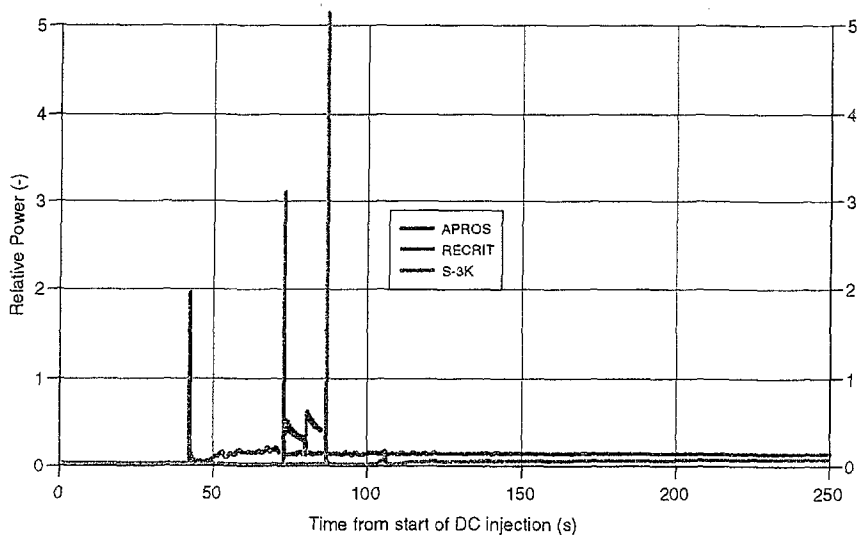

Figure 5.37 Relative core power in OL-1. Case 2: ECCS water mass flow rate = 540 kg/s.

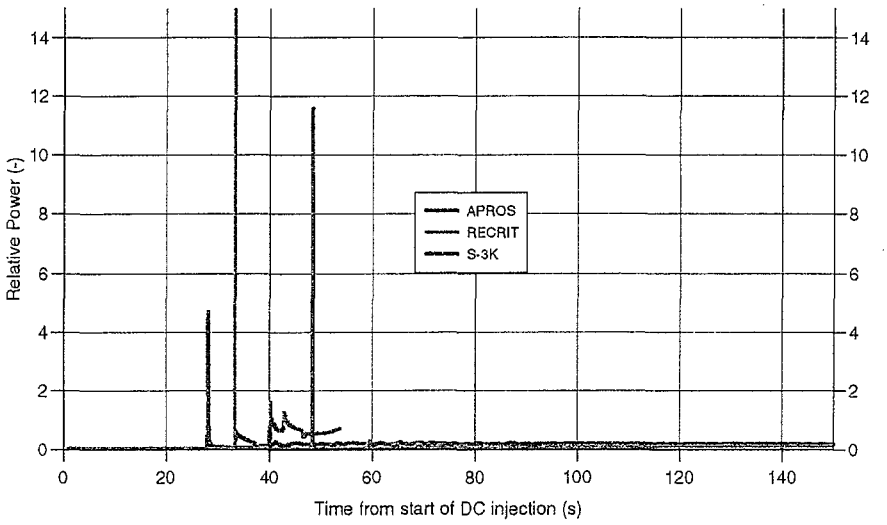

Figure 5.38 Relative core power in OL-1. Case 3: ECCS water mass flow rate = 1350 kg/s.

All three codes predicted recriticality with a first super prompt power peak and then a more or less stabilised power level for the applied range of ECCS injection flow rate from 160 to 1350 kg/s. The time of the first power peak, however, was different. S-3K and RECRIT were rather close in time, but APROS predicted the first peak to arrive much earlier. The difference is mainly due to the fact that in the APROS calculations water injection was made directly to the core inlet, starting at the same time as the water injection to the downcomer in S-3K and RECRIT. In S-3K and RECRIT the core inlet flow was driven by the gravity head in the downcomer, which first had to be filled to a certain level from an initially empty state. The core inlet flow and water level then steadily increased, but were oscillating due to the hydraulic coupling with the parallel channels in the core. This damping seems to be less for RECRIT than for S-3K. In APROS a constant core inlet flow was applied equal to the downcomer flow in S-3K and RECRIT.

The initial reactivity peak was quickly reduced, first by the Doppler feedback as the fuel temperatures increased, and eventually by increased void as the heat was transported to the surrounding water. These phenomena were predicted in a similar way by all three codes, but in the longer term the course was different. With S-3K and RECRIT the power oscillated because of the hydraulic coupling, so that increased inflow of water resulted in new power peaks, which for S-3K showed decreasing amplitudes. The choice of hydraulic damping, i.e. pressure loss coefficients in the downcomer, through the recirculation pumps and in the core inlet, had a substantial effect on the amplitudes. The average power predicted by S-3K seemed to increase slowly after the first peak to an asymptotic power level corresponding to the power needed to boil off the mass of reflood water entering the core.

Also APROS results showed an oscillating power after the first peak and increasing power, but the power rather quickly reached a constant level with only slight ripples on the power curve. The reason why the power so soon stabilised at a constant level is most likely that the core inlet flow was constant.

The RECRIT calculations resulted in a number of relatively high power peaks after the first recriticality. Inlet flow and power oscillated like in S-3K calculations, but with

larger amplitudes, which probably depended on lower pressure losses, i.e. the hydraulic damping, in RECRIT compared to S-3K. The repeated large power peaks made the maximum temperatures in RECRIT increase steadily. The calculations were therefore intentionally aborted when the maximum nodal temperature exceeded 3000 °C, which was before any actual long-term stabilised conditions were reached.

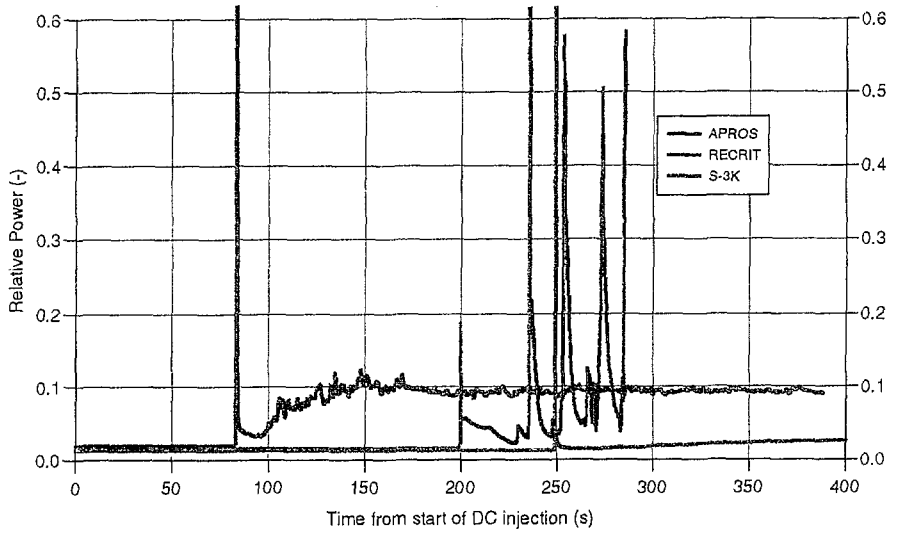

Figure 5.39 Longer term relative core power in OL-1. Case 1: ECCS water mass flow rate = 160 kg/s.

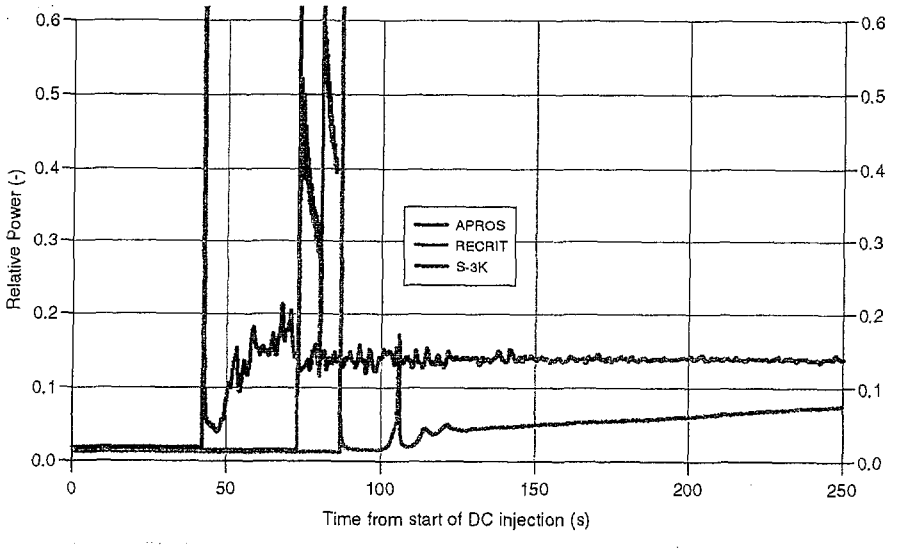

Figure 5.40 Longer term relative core power in OL-1.Case 2: ECCS water mass flow rate = 540 kg/s.

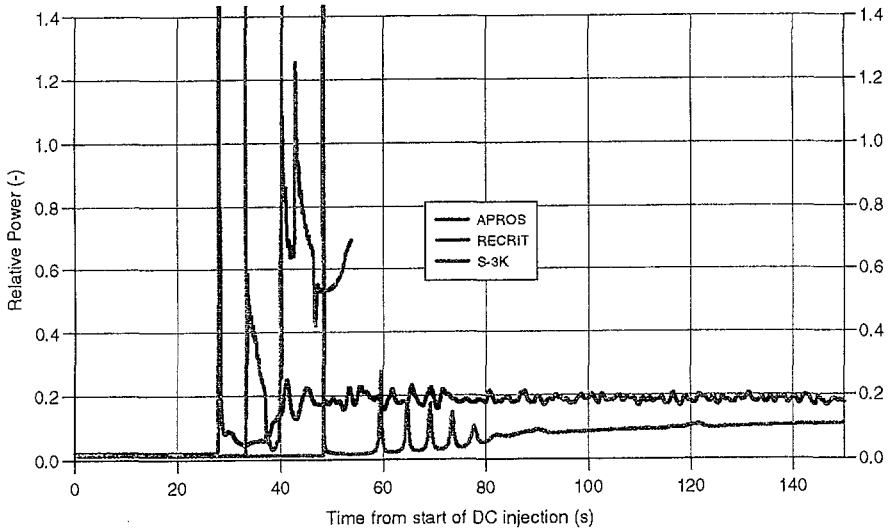

Figure 5.41 Longer term relative core power in OL-1. Case 3: ECCS water mass flow rate = 1350 kg/s.

The course of fuel temperatures was predicted to be quite different with the three codes. With S-3K the average initial temperatures were lower than with the two other codes, even if the maximum temperature in the centre was high and the same as in RECRIT and in agreement with specifications. In addition, S-3K predicted recooling in all core nodes, which was not the case in APROS and RECRIT. Rewetting was obtained at all levels and temperatures stabilised slightly above saturation temperature according to S-3K.

APROS predicted some recooling of the core, but fuel temperatures remained at about 1500 K, a much higher level than that given by S-3K. One reason can be that oxidation power was taken into account in APROS in the first phase of the reflooding.

The repeated power excursions obtained in RECRIT contributed to steadily increasing maximum fuel temperatures. Evidently the energy transport to the coolant was not able to keep up with the power being repeatedly generated in the fuel. The calculations were therefore halted when temperatures exceeded the fuel melting temperature, at about 3300 K. After that the fuel configuration could not be considered intact.

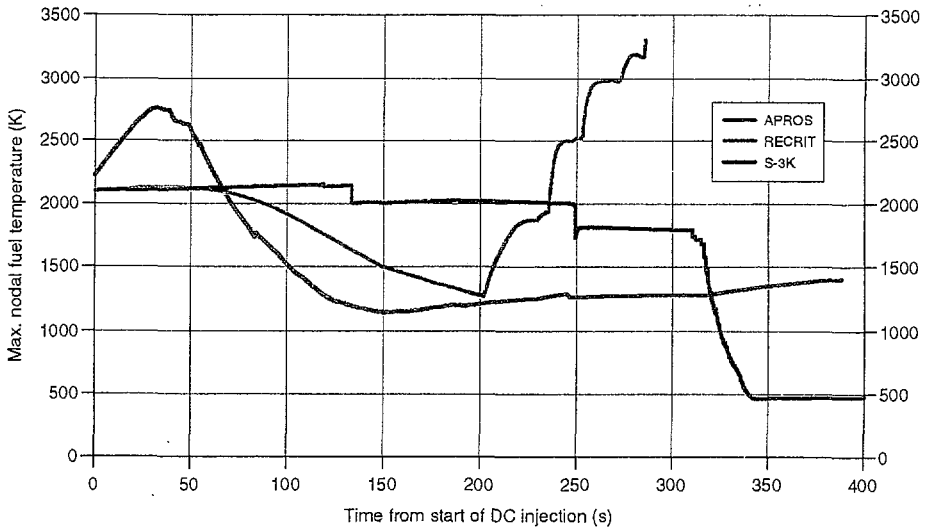

Figure 5.42 Maximum fuel temperatures in OL-1. Case 1: ECCS flow = 160 kg/s.

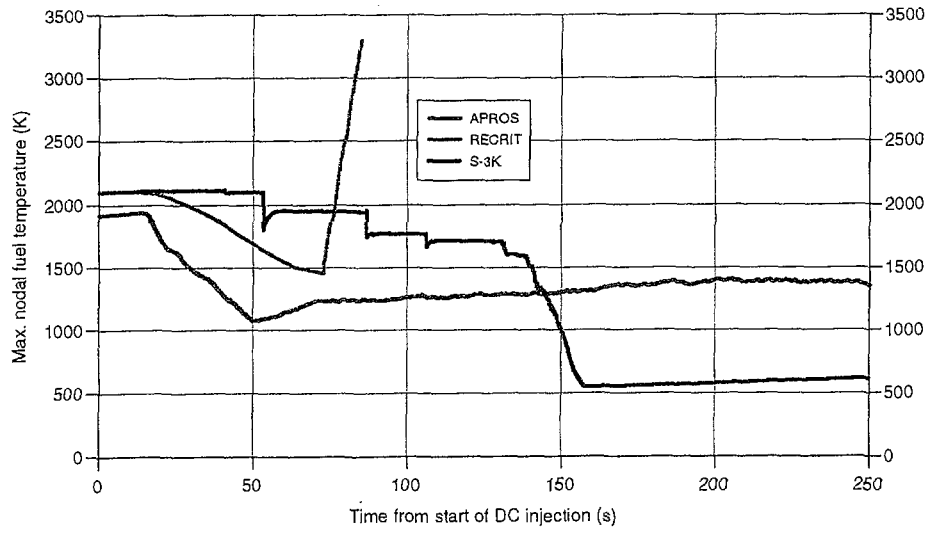

Figure 5.43 Maximum fuel temperatures in OL-1. Case 2: ECCS flow = 540 kg/s.

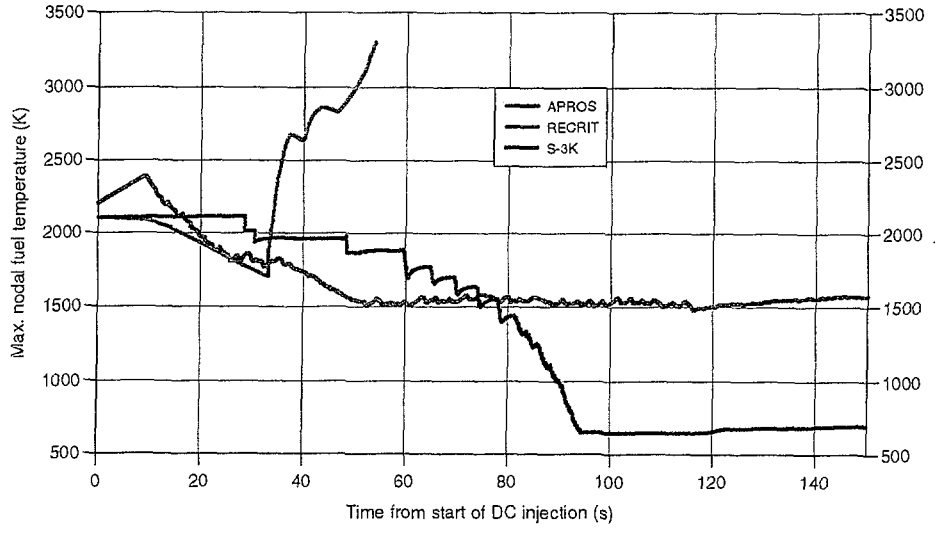

Figure 5.44 Maximum fuel temperatures in OL-1. Case 2: ECCS flow = 1350 kg/s.

All codes predicted the recriticality to take place in a relatively small fraction of the core, just below the rising water surface, in the same way as in the individual calculations. The power density there became extremely large, especially during the first prompt power peak, which gave high power form factors. The maximum nodal power factors are compared in Figures 5.45 through 5.47.

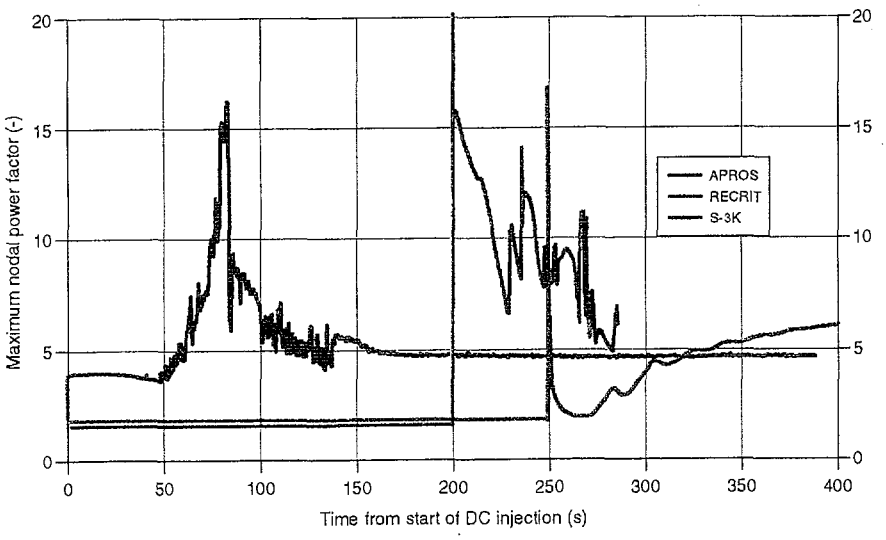

Figure 5.45 Maximum nodal power factor in OL-1. Case 1: ECCS flow = 160 kg/s.

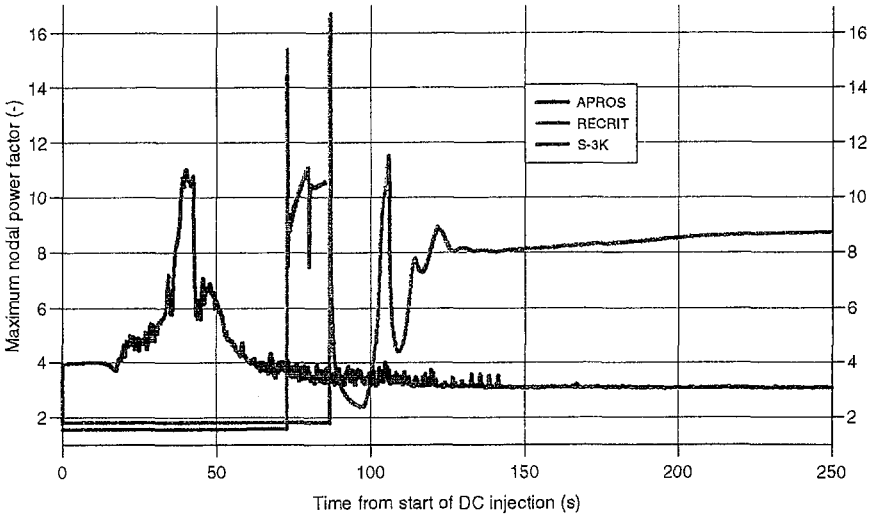

Figure 5.46 Maximum nodal power factor in OL-1. Case 2: ECCS flow = 540 kg/s.

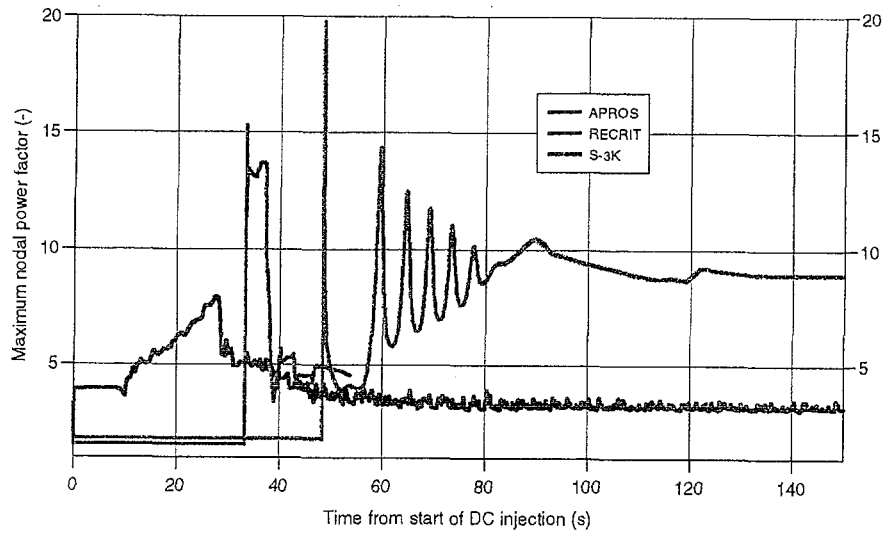

Figure 5.47 Maximum nodal power factor in OL-1. Case 3: ECCS flow = 1350 kg/s.

The local nature of the recriticality power, and the high maximum nodal power factor of the first peak, result in a large energy deposition in the fuel within a short period of time in a small critical fraction of the core. The energy density could then approach the limit for fuel fragmentation. Several factors have influence on this limit, which still is rather uncertain and subject to experimental studies. It is among other things depending on fuel burnup. For moderate burnups in BWRs, as in the studied OL-1 cases, a damage limit of 200 to 280 cal/g of fuel is used as a regulatory limit (OECD, 1996). This provided that the power is developed in such a short time that most of the generated heat energy stays in the fuel and is not dissipated to the coolant. It should be noted that much lower damage threshold values, about 70 cal/gUO_2, have recently been observed in experiments with high burnup fuel, above 50 MWd/kgU (Fuketa et al., 1995). The threshold for fragmentation and dispersion of fuel under severe accident conditions is unknown but it is reasonable to assume that it is lower than for fuel under normal operating conditions.

A rough estimation of the energy deposition based on the shape of the largest power peak and the nodal power factors was made for the different cases. Table 5.10 below summarises some of the results of the code comparison for the OL-1 common cases.

Table 5.10 Common case comparison of results from S-3K, APROS and RECRIT

Case No:	Case 1, 160 kg/s			Case 2, 540 kg/s			Case 3, 1350 kg/s		
Code:	S-3K	APROS	RECRIT	S-3K	APROS	RECRIT	S-3K	APROS	RECRIT
Time at max. power peak (s)	249.0	83.4	235.3	86.7	42.3	72.7	48.4	28.1	33.2
Peak amplitude, relative (Times nominal power)	2.03	1.77	2.22	5.18	1.95	3.09	11.6	4.69	14.9
Nodal power factor (-)*	16.8	12.4	13.0	16.7	10.2	14.7	19.7	7.65	13.5
Duration of max. peak (s)	0.40	0.80	0.17	0.17	0.29	0.08	0.11	0.33	0.03
Energy deposition in fuel during max. peak (cal/g)	39	70	15	39	26	27	64	38	51
Power at end of simulation, relative	0.032	0.090	0.458	0.108	0.14	0.399	0.118	0.187	0.690
Time at end of simulation (s)	400	388	285	400	257	85.0	365	230	53.7
Max. fuel temperature (K)	2146	2757	3299	2115	1937	3293	2109	2384	3297
Max. fuel temperature at end of simulation (K)	490	1402	3299	728	1350	3293	717	1602	3297

* at maximum power peak (which in all cases is equal to first prompt power peak except for RECRIT case 1, where 2nd peak was the largest)

5.4.3 Discussion of code comparison results

Differences in the results between the three codes are evident and inevitable due to different modelling and simulation capability of the individual codes, because they originally were designed for different purposes. None of the codes includes complete modelling of the reactor systems combined with detailed physical models describing all phenomena involved in a reflooding/recriticality transient. However, the codes are to a large extent complementary to each other. S-3K has detailed fuel kinetics models, APROS has good neutronics and thermal-hydraulics and an extensive system description, while RECRIT combines good kinetics and thermal-hydraulics including reflood and quench models. Unfortunately, the comparison of the results from the common cases has been complicated by problems to implement the targeted initial and boundary conditions which

should be identical for all codes. This can partially explain the differences in the code comparison results.

Below follows a discussion of the possible effects on the results caused by deviations from the aimed initial and boundary conditions for certain parameters.

- **Different initial fuel temperatures**

The specified temperature distribution for the common cases was based mainly on the preparatory MELCOR calculations (MAAP4 results were also used) which had a maximum of 2100 K in four of the five radial zones about 1 m above core inlet. The temperature distribution could be implemented directly by input only in RECRIT, whereas in S-3K and APROS it was obtained by simulation of the heat-up phase. None of these codes could exactly reproduce the specified temperature profile, and especially S-3K showed a deviation giving a temperature maximum shifted towards the core exit. However, sensitivity studies with S-3K, varying the initial fuel temperature, indicated only a small effect of initial temperature (3 % increase in recriticality power for a change in maximum temperature from 1800 to 2100 K). High initial temperatures for RECRIT in nodes where recriticality took place might, however, have contributed to the fact that the maximum nodal temperatures there became higher than those predicted by S-3K and APROS.

- **Only core model in APROS**

In the APROS calculations only the core model was applied. This means that the outer systems with the recirculation loop comprising upper plenum, steam separator downcomer, RC pumps and lower plenum were decoupled. The core inlet flow was specified to be constant, i.e. the reflooding mass flow rate was equal to the feed water injection mass flow rate. No coupled flow oscillation with the downcomer could then take place and the flow and water level in the core was controlled by the injection flow rate and the boiling rate. With RECRIT and S-3K the water injection was directed into the downcomer and the core inlet flow was driven by the static pressure difference between downcomer and core which then controlled the reflooding flow rate. The coupling between parallel channels in fuel channels, bypass and downcomer then gave rise to coupled flow and power oscillations, which for RECRIT became quite violent. With injection into the downcomer a certain water level had to be reached there in order to give enough driving pressure to start the core inlet flow. This caused a time delay for the reflooding and a considerable delay until the first recriticality, which was not the case with APROS.

- **Lower flow resistance in recirculation loop in RECRIT than in S-3K**

The S-3K calculations for O-3 showed, by varying the loss coefficient in the RC pumps, that the hydraulic damping had a significant effect on the coupled power - flow oscillations. With low loss coefficients the inlet mass flow experienced oscillations in phase with recriticality power and slowly increasing frequency, about 0.2 Hz. The average value of the core inlet flow increased almost linearly, but the power mean value seemed to remain at a low value in the long-term. Using what was estimated to be realistic, larger loss coefficients for the RC pumps in S-3K gave more damped oscillations with only a few initial waves after which both flow and power increased very slowly.

The RECRIT results showed a different behaviour. The initial recriticality power peak was followed by several high peaks, which in the 160 kg/s case were higher than the first one. The repeated power excursions made the maximum fuel temperature to rise to very high values. When the temperature exceeded 3000 °C the calculations were stopped since it was assumed that the core integrity could no longer be maintained as the melting temperature was reached. One explanation to the larger oscillations in the RECRIT calculations is that the loop pressure losses there were smaller than in S-3K.

- **Power - pressure feedback**

In all code comparison calculations presented here the dome pressure was kept at 0.5 MPa, as specified. RECRIT has, however, possibility to calculate the power–pressure interaction, which was utilized in some additional parameter studies. The effect of the recriticality power on pressure turned out to be rather small, with an increase less than 0.3 bar for the 160 kg/s and 540 kg/s cases. For the first recriticality peak no noticeable pressure increase could be seen in any case since the energy content was small due to the short duration of the peak, although the amplitude was large.

- **Void in bypass**

At the beginning of the transient there is 100 per cent void in both fuel channels and bypass channel as the water level is at the core inlet level. During the reflooding phase, when liquid water enters the core, the void decreases more rapidly in the bypass than within the fuel channels, since the latter comprise the main energy sources. This was taken into account by the thermal-hydraulic models in all three codes, although in somewhat various ways. The effect of the bypass void on the kinetics was, however, treated differently in the codes. In the S-3K and the APROS calculations the bypass void could be either 0 or 1.0, and variation between these extremes was neglected. Inside the fuel channels, however, the real variations of the void were taken into account. A weighting of the void outside (bypass) and inside the fuel channels was then applied for the reactivity calculation for each fuel assembly. Concerning RECRIT, the neutronic cross sections calculation is based on the assumption that the void fractions inside and outside fuel channels are equal. In one set of RECRIT calculations weighting of the void between channel and bypass was applied. This weighting was done in relation to the flow areas of fuel channels and bypass channels in each radial ring. There is in RECRIT, however, only one common bypass channel in the core so the bypass void is the same in all radial rings.

Different approximations were thus applied for the effect of bypass void in the codes. It is therefore difficult to tell how large its effect on the recriticality would be in general. A parameter study was made only with RECRIT. This was done for the 160 kg/s case with the core void weighted as described above and without taking the bypass void into account. The results showed that if the bypass void was taken into account the recriticality power increased noticeably, more than a factor of two both in for the first peak and the long-term power. The influence of the bypass void in this RECRIT study is probably exaggerated since the weighting by areas reduces the average void too much inside the channel. A large fraction of the bypass area is located outside the outermost fuel channels towards the core barrel in which the void is expected to be lower than in the middle of the core.

- **Oxidation models**

It was decided to exclude the effect of oxidation due to exothermic metal-water reactions at high temperatures in the code comparison calculations. However, both APROS and RECRIT were updated to include oxidation models, which was not the case for S-3K. In the APROS calculations for the code comparison this model was active only for the heat-up phase and until the first recriticality. A parameter study was later performed with RECRIT with and without the oxidation model for Case 1 with 160 kg/s. The oxidation model had, however, almost no effect on the long-term behaviour of the reflooding/recriticality. In cases where the fuel was recooled by the reflooding water, which was the case at an early stage with S-3K and APROS, the cladding temperatures were so low that there would be no cladding oxidation.

6. CONTAINMENT RESPONSE TO RECRITICALITY: MELCOR ANALYSIS FOR OL-1 PLANT (TASK 2)

6.1 Assumptions

The effects of recriticality event on the containment response were assessed with the MELCOR code for Olkiluoto 1 and 2 BWR (Lindholm, 1998). The accident was initiated with a total station blackout followed by recovery of power at 4000 seconds from the beginning of accident, when the maximum cladding temperature had reached 2100 K.

The reactor coolant system was depressurised at 1800 seconds into the accident and at the time of power recovery all low and high-pressure injection system pumps were assumed to start. The full capacity of ECCS injection in Olkiluoto BWR is 540 kg/s. The capacity of the low-pressure injection system is counter-pressure dependent with zero net flow above 1.0 MPa. Furthermore, the low-pressure system sucks water from the suppression pool, which brings in another limitation to the operation of this ECCS system. It is the temperature of suppression pool water, which cannot exceed saturation temperature with regard to the risk of pump cavitation.

The total reactor power after the first recriticality was taken from RECRIT and APROS calculations and was given as a tabular function of time in the MELCOR input. Locally the power generation was distributed according to the initial axial and radial peaking factors, since MELCOR cannot take into account local changes in power distribution during calculation. This simplification can be allowed, since the containment response in this case is mainly defined by the net energy input from the reactor coolant system.

According to RECRIT and APROS predictions the total energy of the first power peak is small (less than one full-power second) and has a negligible effect on containment response. The RECRIT results indicate that the power would stabilise to level of 10 to 20% of the full power. APROS calculations resulted in stabilised power level of about 14 %. Due to the uncertainties in the stabilised power level, four different sensitivity cases were calculated with MELCOR, and the stabilised power level was assumed to be 8 %, 10 %, 14 % and 19 % of the nominal power.

The reactor coolant system pressure increases rapidly after start of reflooding, see Figure 6.1. In cases with power level remaining at the levels of 14 % to19 %, the reactor pressure remains at about 2.0 MPa. In cases of 8 % and 10 % stabilised power level, the reactor pressure first decreases after the first peak of reflooding due to quenching and steam cooling, and then increases again.

The high pressure injection system has piston driven pumps producing a constant flow rate of 4 x 22.5 kg/s. The capacity of the low pressure injection system is counter-pressure dependent and is strongly related to reactor power, as shown in Figure 6.2. In the cases with stabilised reactor power being 14 % to 19 %, the low pressure injection system is capable of injecting water only for about 4 minutes. In the case of 10 % nominal power, the injection phase lasts longer but reduces with increasing counter-pressure, ceasing after about 1 hour from the start of reflooding. In case of 8 % nominal reactor power, the low

pressure system is capable of injecting water with relatively high capacity, but in this case the injection ceases after about 2 h 20 min due to assumed cavitation of pumps (suppression pool reaches saturation temperature).

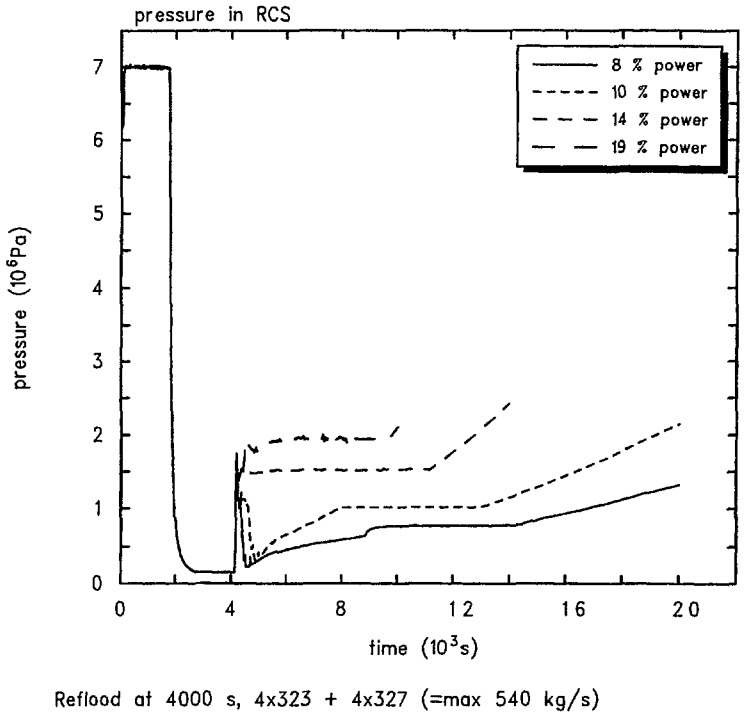

Figure 6.1. Reactor coolant pressure in assumed recriticality event, where semi-stabilised power is assumed to be 8, 10, 14 or 19 per cent of the nominal power.

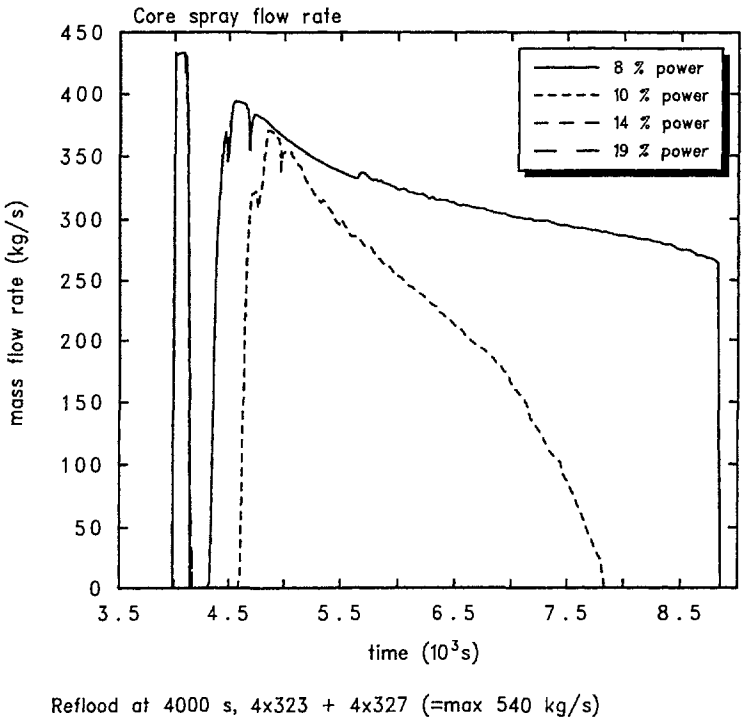

Figure 6.2. Low pressure system injection rate in case of recriticality event with stabilised power being 8, 10, 14 or 19 % of full power.

The maximum cladding temperature decreases rapidly and stabilises around 1200-1400 K after start of reflooding in the three lowest reactor power cases, but in the case of reactor power being 19 % of full power, the core is not coolable and the maximum cladding temperature oscillates around 2000 K, slowly increasing. This temperature increase is affected by continuous Zircaloy oxidation. In the other three recriticality power variations oxidation stops soon after reflooding.

6.2 Containment Response

The containment of Olkiluoto 1 and 2 nuclear power plants is of pressure suppression type (Figure 6.3). It is inerted, i. e filled with nitrogen under normal operation. The containment of each plant unit has been backfitted in order to mitigate the severe accidents. The necessary plant modifications were carried out during 1989 - 1990.

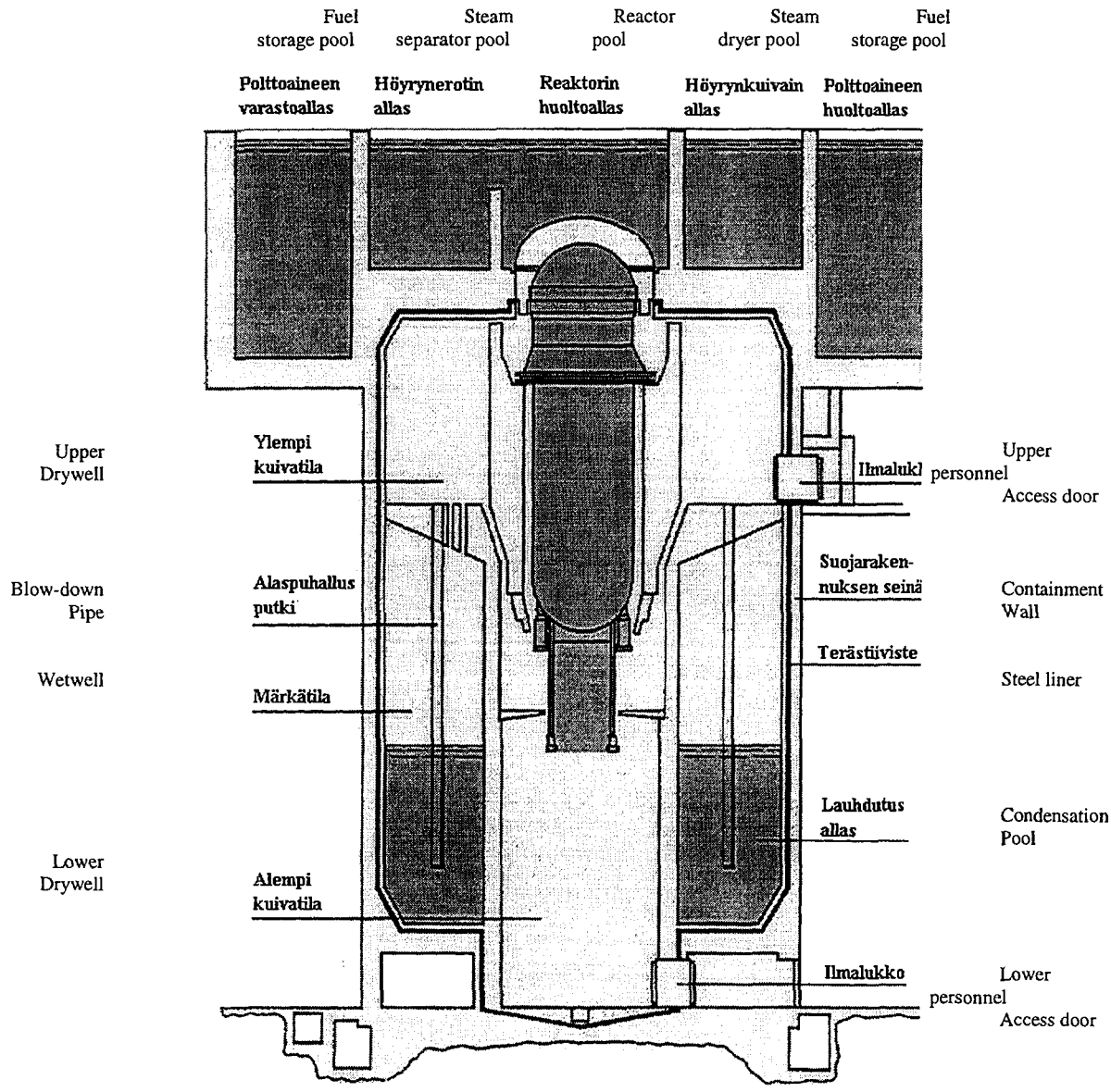

Figure 6.3 The containment of Olkiluoto 1 and 2.

The major containment heat sink is the suppression pool. Both low pressure core spray and containment spray take suction from the suppression pool. A heat exchanger is aligned to each of the four spray lines. Each heat exchanger is capable of cooling the water with a capacity of $1.72 \cdot 10^5$ W/°C (at the sea water temperature of 18 °C). When power is restored, the containment sprays will start. The temperature of suppression pool is 320 K at the start of reflooding transient. Elevated power level and hot core material produces superheated steam that is blown to the suppression pool through ADS valves. The amount of energy dumped into the suppression pool exceeds the capacity of heat exchangers and the temperature of the pool starts to increase rapidly, as illustrated in Figure 6.4. The capacity of heat exchangers corresponds roughly to the core power of 2.4 % of nominal reactor power. The water mass of the pool increases due to high pressure safety injection,

which takes water from two tanks, each having a water volume of 820 m^3. This water reservoir will last for 4.5 hours with full capacity of high pressure system injection. According to the present calculations, the tanks are not exhausted before containment failure. The containment would fail at absolute pressure of approximately 0.8 - 0.9 MPa and the containment failure location would be the containment vessel cover flange. The release would go through the reactor service pool, which would act as a scrubbing device. The time from first recriticality to the start of suppression pool boiling is 34 min - 1.3 h depending on the recriticality power. The drywell pressure increases rapidly when suppression pool reaches saturation, as depicted in Figure 6.5. The timing of key containment phenomena for the studied cases is shown in Table 6.1.

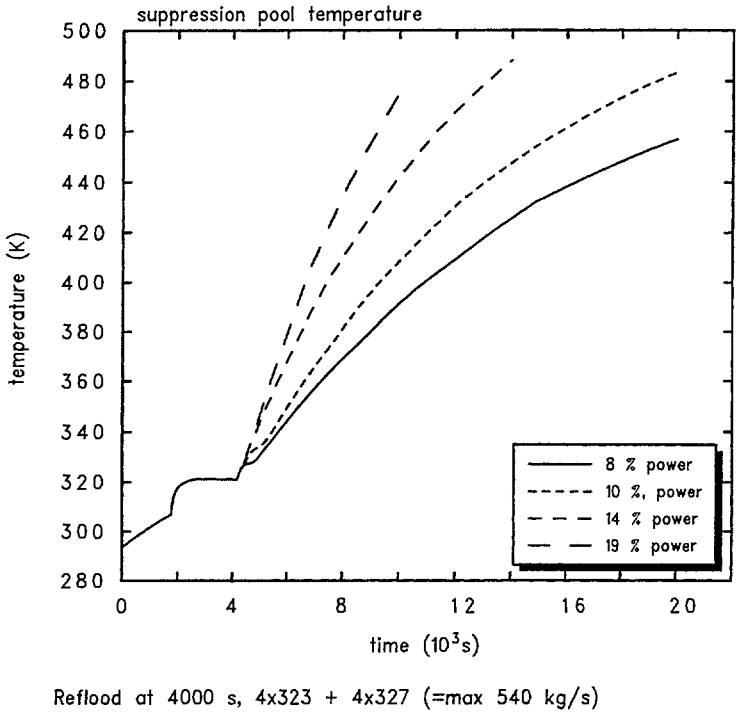

Figure 6.4 Suppression pool temperature.

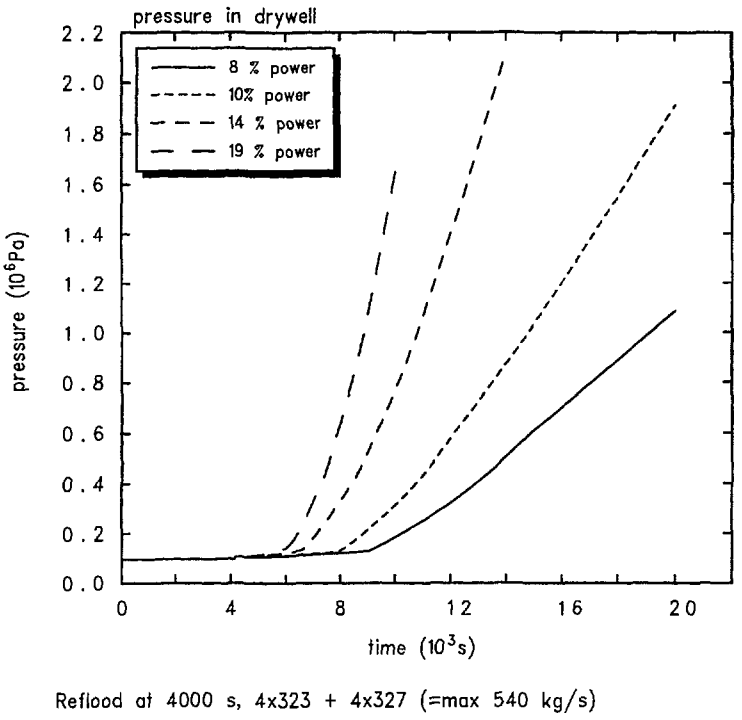

Figure 6.5 Drywell pressure in case of assumed recriticality event at Olkiluoto 1.

Table 6.1. Timing of containment events in case of assumed recriticality.

Time from first recriticality to:	Stabilised power relative to nominal power due to recriticality			
	8 %	10 %	14 %	19 %
Suppression pool starts to boil	1.3 h	1.0 h	38 min	34 min
Containment venting begins	3.0 h	2.2 h	1.4 h	1.0 h
Containment failure (at 10 bar)	4.2 h	3.0 h	1.8 h	1.3 h

When suppression pool starts to boil the containment spray system is lost due to pump cavitation. The energy dump into the suppression pool is higher than could be controlled, in a short-term, by filling the containment with cold water via enhanced containment spray system which uses back-up sources of water and has connections to diesel-driven pumps in the fire water system or mobile pumps. The pool vaporisation rate also exceeds the containment venting capacity leading eventually to containment failure. The capacity of the containment vent lines is designed for removing energy equivalent of 1 % full power.

The gas temperature in the containment increases rapidly in the cases of 14 % and 19 % nominal power, as illustrated Figure 6.6. When the suppression pool starts to boil, it is assumed that steam passes through the pool into the atmosphere without change in specific energy.

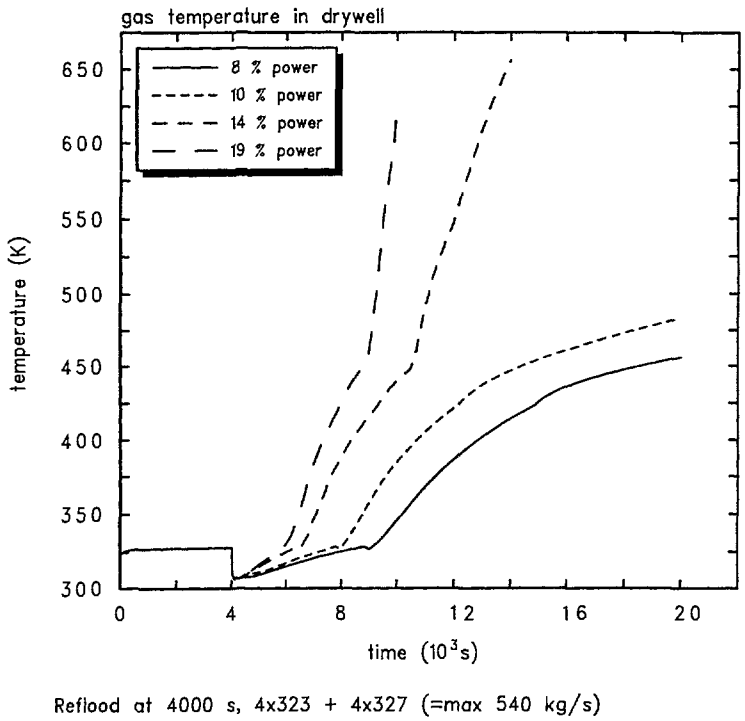

Figure 6.6 Gas temperature in the drywell in case of assumed recriticality event at Olkiluoto.

6.3 Discussion

The initial high but short duration power peaks due to recriticality have minor effect on the containment, since the total energy in the peaks is small. The possible risk related to the power peaks is solely due to consequences of possible the fuel fragmentation. The stabilised power level is the key contributor to fast containment loading. The heat removal through containment spray heat exchangers is designed for about 2.4 % of full power and is not capable maintaining the suppression pool under saturation temperature and the containment heat sink is lost in 34 min -1.3 h after first recriticality. Furthermore, once the suppression pool reaches saturation, the steaming rate is higher than can be controlled by filtered containment venting, or containment water filling systems, thus leading to continuous pressurisation of the containment and eventual uncontrolled containment leakage.

The performed studies indicate that if a recriticality event occurred with the sustained power generation being around 10 %, the containment failure would occur in a few hours. Thus the prevention of conditions for and mitigation of recriticality, should it occur, is crucial in accident management.

Olkiluoto reactors have a boron injection system, which has been recently modified to secure fast shutdown of the reactor. The system will start automatically if the reactor power exceeds 8 % of full power ten seconds after the low reactor water level signal. The

boron system can be started also manually. In addition, the system has also been upgraded by adding enriched boron (B^{10}) to the reservoir tank. Boron concentration in reactor pressure vessel will be 120 ppm enriched boron (580 ppm natural boron). These upgradings have increased the shutdown capacity of the boron system by 500 % and the current system is capable of shutting down the reactor from full power in a few minutes.

7. CONCLUSIONS AND RECOMMENDATIONS

Qualitatively, the results of the SARA project confirm the conclusions from other recriticality studies. Recriticality is possible during reflooding with unborated water of a partly degraded core, and can lead to sharp power peaks of large amplitudes – including super-prompt power excursions – followed by quasi steady-state power generation at a level significantly higher than the decay power. Concerning the quasi steady-state power levels, the SARA results are largely in agreement with earlier studies, i.e. the stabilised power seems to be below 20% of the nominal power for reflooding rates in the range of 90 - 1350 kg/s. However, in some cases higher power levels, approaching 50% of the nominal power, were predicted leading to fuel temperatures exceeding the melting point as a result of insufficient cooling of the fuel. It is important to mention that these quasi steady-state power levels were calculated during rather short periods of time, up to 500 seconds, following the recriticality. It is likely that in the longer time perspective the reactor power would adjust itself to a level corresponding to the power necessary to evaporate all water entering the core.

Concerning the energy deposition in the fuel during power excursions, the results of SARA analyses differ from other studies. While these studies found that the energy deposition in the fuel due to super-prompt power excursion would be below the threshold for fuel fragmentation and dispersion, the SARA results indicate that for reflooding rates higher than about 500 kg/s these threshold values are approached or exceeded, in some cases with large margin. The threshold values referred to here are in the 200 – 280 cal/g range for low burn-up fuel, and down to about 70 cal/g for high burn-up fuel as observed experimentally. In this context it is important to consider that these threshold values have been obtained in tests with "normal" fuel rods, and are therefore likely to be lower for strongly overheated fuel rods under severe accident conditions. Thus, SARA results suggest that there might be a risk for fuel fragmentation and dispersal during a reflooding transient. The consequences of such a scenario were not investigated in the SARA project.

MELCOR calculations of long-term containment response to predicted quasi steady-state recriticality powers have shown that the containment would fail within a few hours after recriticality if the accident is not mitigated. This result and the risk for fuel fragmentation point out the importance of adequate accident management strategies to be used by reactor operators and emergency staff during recovery actions. Based on the results obtained in the SARA project, the following measures can be proposed:

- Upgrading of the boron shut-down system with the introduction of automatic initiation trigged by e.g. high neutron flux signal after shut down. This will prevent long-term recriticality for a considerable time (except for the first power peak), assuming that the boron concentration will not be diluted by the emergency cooling water in the containment pool.

- Limitation of the reflooding flow rate whenever control rod melting might be expected:

  - Limitation of the maximum injection mass flow rate to less than 500 kg/s in order to avoid the risk of fuel fragmentation and melting. (This recommendation is based on fuel fragmentation and dispersion thresholds obtained for "normal" fuel).

  - The normal feed water should not be started. The flow rate of the low pressure injection system will be automatically limited, in the short-term due to reactor pressure increase during quenching, and in the long-term due to pressure increase from elevated recriticality power. The minimum flow rate will then be equal to that of the high-pressure system (90 kg/s in both O-3 and OL-1), which is sufficient to cool the core, if water injection is initiated at maximum core temperatures up to 1800 K. In this case the recriticality power will be low, thus providing more time for countermeasures.

- Delaying depressurization of the primary system, if possible, in order to limit relocation of control rods.

The SARA studies have clearly shown the sensitivity of recriticality phenomena to thermal-hydraulic modelling, the specifics of accident scenario, such as system pressure and distribution of boron-carbide in the core, and the importance of multi-dimensional neutron kinetics for the determination of local power distributions in the core. With regard to the predicted risk for fuel fragmentation and melting, and prevailing uncertainties, it is recommended that systematic studies of reflooding and recriticality continue. The improved reflooding models should be validated against data from high temperature reflooding experiments. Equally important is the further improvement and testing of the codes capabilities to model the entire BWR primary system as realistically as possible in order to capture the reactor power – primary system behaviour feedback effects.

REFERENCES

Analytis G.Th., Yadigaroglu G. Analytical modelling of inverted annular film boiling. Nuclear Engineering and Design, 99, pp. 201-212, (1987).

Analytis, G, TH. A developmental assessment of RELAP5/MOD3.1 with separate effect and integral test experiments: model changes and options. Nuclear Engineering and Design, 163, pp. 125 – 148, (1996).

Anttila, M. CASMO-4 data for Atrium fuel types 114 and 116 with 10 and 11 Ba-rods as absorbers for the lower end fuel and Atrium fuel type 115 with 9 Ba-rods as absorbers in OL-1/2 fuel, VTT Energy, Finland, unpublished, (1998).

Bandurski, Th., Cabezudo, C., Mathews, D., Knoglinger, E. Recriticality of a BWR core during reflood after control blade meltdown. ANS Winter Meeting '94, Washington, D.C., November 13 – 17, (1994).

Borkowski, J., Rhodes, J. D., Esser, P., Smith, K. S. A three-dimensional transient analysis capability for SIMULATE-3. Trans. Am. Nuc. Soc., 71, 456, (1994).

Cronin, J.T., Smith, K.S., Ver Planck, D.M. SIMULATE-3 methodology. STUDSVIK/SOA-95/18, (1995).

Elias E., Sanchez V., Hering W. Development and validation of a transition boiling model for RELAP5/MOD3 reflood simulation. Nuclear Engineering and Design, 183, pp. 269-286, (1998).

Fuketa, T., et al. NSRR Experiment with 50 MWd/kgU PWR fuel under an RIA condition. IAEA Technical Committee Meeting on "Behaviour of LWR core materials under accident conditions, Dimitrovgrad, Russian Federation, 9-13 October, 1995. Proceedings, IAEA-TECDOC-921, pp 265-279, (1995).

Hochreiter, L.E. Aspects of reflood heat transfer modeling. 25th Water Reactor Safety Information Meeting. Bethesda, MD, USA, October 22-27, (1997).

Hofmann, P., Markiewicz, M., Spino, J. Reasons for the low-temperature failure of BWR absorber elements. Severe Accident Research Program Partners Meeting, Idaho Falls, Idaho, April 10 - 14, (1989).

Hofmann, P. et al. Physic-chemical behaviour of zircaloy fuel rod cladding tubes during LWR severe accident reflood; Part II: Modelling of quench phenomena. Forschungszentrum Karlsruhe, FZKA 5846, (1997).

Höjerup, F. et al. On recriticality during reflooding of a degraded boiling water reactor core. Nordic nuclear safety research. NKS/RAK-2(97)TR-A3, (1997a).

Höjerup, F. Use of steady-state neutron flux code, TWODIM, for dynamic calculations: A New Approach. Working. document, INV-SARA (97)-D003, (1997b).

Höjerup, F. RECRIT calculations of the SARA benchmark problem. Working document, Risö-I-1349, INV-SARA(98)-D015, (1998).

Höjerup, F. What happens when high neutron densities slow down in water. Working document, Risö-I-1295 (EN), INV-SARA(98)-D008, (1998a).

Höjerup, F. How fast is steam and gas formed from neutron slowing down in water. Working document, Risö-I-1304 (EN), INV-SARA(98)-D009, (1998b).

Kropaczek, D. J., Smith, K. S., Borkòwski, J. A. A fully-implicit, five equation channel hydraulics model for SIMULATE-3K. Proc. Joint Intl. Conf. on Math. Methods and Supercomputing for Nuclear Applications, Vol. 2, 1401 (1997).

Kropaczek, D..J. Documentation of tasks performed for the European Community Severe Accident and Recriticality Analysis Project in support of Studsvik EcoSafe. Studsvik Scandpower, Incorporated, (1999).

Lindholm, I. Calculations of core state prior to anticipated reflooding/recriticality with MELCOR 1.8.3 Code. INV-SARA (97)-D004, VTT Technical Report, ROIMA-7/97, (1997).

Lindholm, I. Studies on BWR containment response to a postulated recriticality event. VTT Technical report, ROIMA-14/98, INV-SARA(98)-D012, (1998).

Lindström, K. E. Development and Verification of Nuclear Calculation Methods for Light-Water Reactors. Risö Report No. 235. Danish Atomic Energy Commission Research Establishment Risö, (1970).

MacDonald, P. E. et al. Assessment of light-water-reactor fuel damage during a reactivity-initiated accident. Nuclear Safety, 21, 582. (1980).

Miettinen J., Höjerup F. Recriticality analyses with RECRIT for the Olkiluoto-plant. VTT Technical Report, MOSES-12/99, (1999a).

Miettinen J. Validation of thermohydraulics in the RECRIT BWR-recriticality code. VTT Technical Report, MOSES-08/99, (1999b).

Miettinen J., Höjerup F. Numerical solutions, constitutive correlations and system models of the RECRIT BWR-recriticality code, VTT Technical Report, MOSES-07/99, (1999c).

Mosteller, R.D. and Rahn, F.J. Monte Carlo calculations for recriticality during the reflood phase of a severe accident in a BWR. Trans. Am. Nucl. Soc. , 63, 254. (1991).

Nilsson, L. SARA Project: Reflooding calculations for Oskarshamn 3 BWR with SCDAP/RELAP5. Studsvik EcoSafe, Studsvik/ES-98/23, INV-SARA(98)-D010, (1998).

Nilsson, L. SARA Project: Recriticality calculations for Oskarshamn 3 and Olkiluoto 1 BWRs with SIMULATE-3K during reflooding of a partly degraded core. Studsvik EcoSafe, Studsvik/ES-99/2, INV-SARA(98)-D011, (1999).

OECD/CSNI Status Report. Transient behaviour of high burnup fuel, OECD/GD(96)196, NEA/CSNI/R(96)23, (1996).

Okkonen, T., Hyvärinen, J. and Haule, K. Safety issues related to fuel-coolant interactions in BWRs. Proc. of CSNI Specialist Meeting on Fuel-Coolant Interactions. Jan. 5-8, 1993, Santa Barbara, USA. NUREG/CP-0127, NEA/CSNI/R(93)8, pp. 296-307, (1993).

Puska, E. K., et al. APROS simulation system for nuclear power plant analysis. Proceedings of ICONE-3, The 3rd JSME/ASME Joint International Conference on Nuclear Engineering, April 23-27, 1995, Kyoto, Japan, The Japan Society of Mechanical Engineers, Tokyo, 1995, Vol. 1, pp.83-88, (1995a).

Puska E. K., Kontio, H. Three-dimensional core in APROS plant analyser. Proceedings of the International Conference on Mathematics and Computations, Reactor Physics and Environmental Analyses, April 30-May 4, 195, Portland, Oregon, USA, IBSN 0-89448-198-3, American Nuclear Society Inc., 1995, Vol. I, pp. 264-273, (1995b).

Puska, E. K. Recriticality calculations with APROS-3D core model. VTT Technical report, ROIMA-1/98, INV-SARA(98)-D014, (1998a).

Puska, E. K. Calculation of the SARA reflooding cases 160 kg/s, 540 kg/s and 1350 kg/s with APROS code. VTT Technical report, ROIMA-20/98, INV-SARA(98)-D013, (1998b).

Sandervåg, O. Reflood of a partially degraded core. Studsvik-Technical Note NP-88/34. Studsvik Nuclear, (1988).

Scott, W.B., et al. Recriticality in a BWR following a core damage event. Pacific Northwest Laboratory, Battelle Memorial Institute. NUREG/CR-5653, PNL-7476. (1990).

Shamoun, B.I and Witt, R.J. Parametric study of recriticality in a boiling water reactor severe accident. Nuclear Technology, Vol. 107, (1994).

Silvennoinen, E., et al. The APROS software for process simulation and model development. Technical Research Centre of Finland, Research Report 618, ISBN-951-38-3463-8, Espoo, (1989).

Sjövall, H. SARA-project: Reflooding calculations for Olkiluoto 1 and 2 with MAAP 4.0.2.computer code. INV-SARA(97)-D005, (1997).

www.ski.se

STATENS KÄRNKRAFTINSPEKTION
Swedish Nuclear Power Inspectorate

POST/POSTAL ADDRESS SE-106 58 Stockholm
BESÖK/OFFICE Klarabergsviadukten 90
TELEFON/TELEPHONE +46 (0)8 698 84 00
TELEFAX +46 (0)8 661 90 86
E-POST/E-MAIL ski@ski.se
WEBBPLATS/WEB SITE www.ski.se